Spin liquids
and
the phases of the cuprates

Perimeter Institute
May 17, 2023
Subir Sachdev

Maine Christos, Zhu-Xi Luo, Henry Shackleton, Ya-Hui Zhang,
Mathias Scheurer, and S. S., PNAS **120**, e2302701120 (2023)
Alexander Nikolaenko, Jonas v. Milczewski, Darshan G. Joshi,
and S.S., arXiv:2211.10452

Talk online: sachdev.physics.harvard.edu

Maine Christos

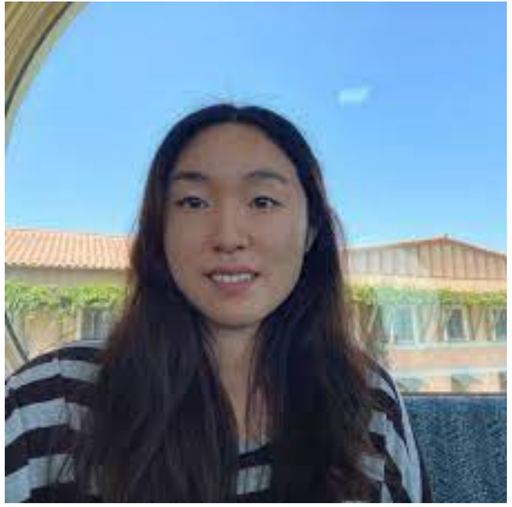

Zhu-Xi Luo
→GA Tech

Henry
Shackleton

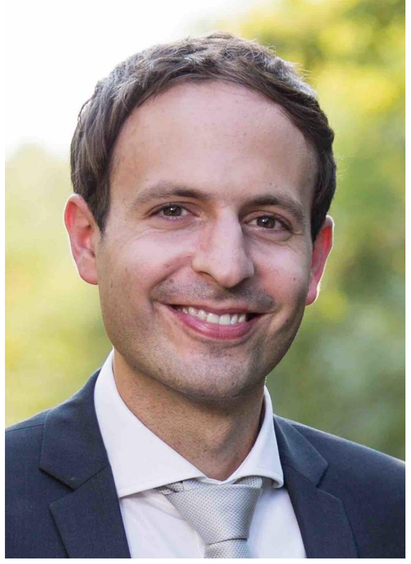

Mathias Scheurer
Innsbruck→Stuttgart

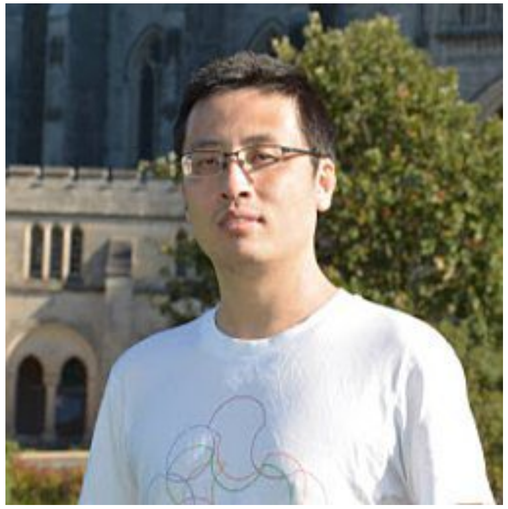

Ya-Hui Zhang
Johns Hopkins

Alexander
Nikolaenko

Darshan Joshi
TIFR Hyderabad

Jonas von Milczewski

B Keimer *et al. Nature* **518**, 179-186 (2015)

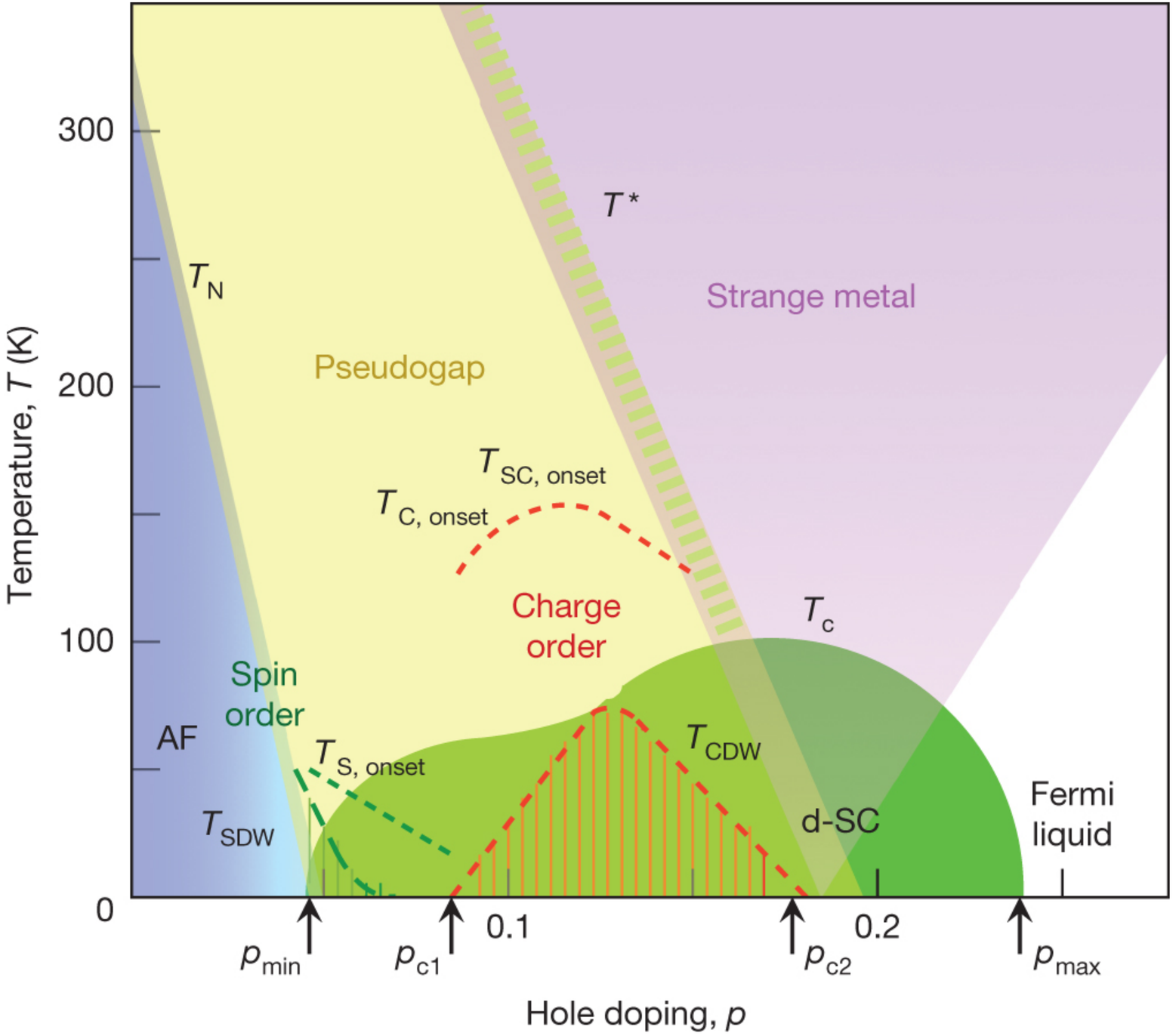

B Keimer *et al. Nature* **518**, 179-186 (2015)

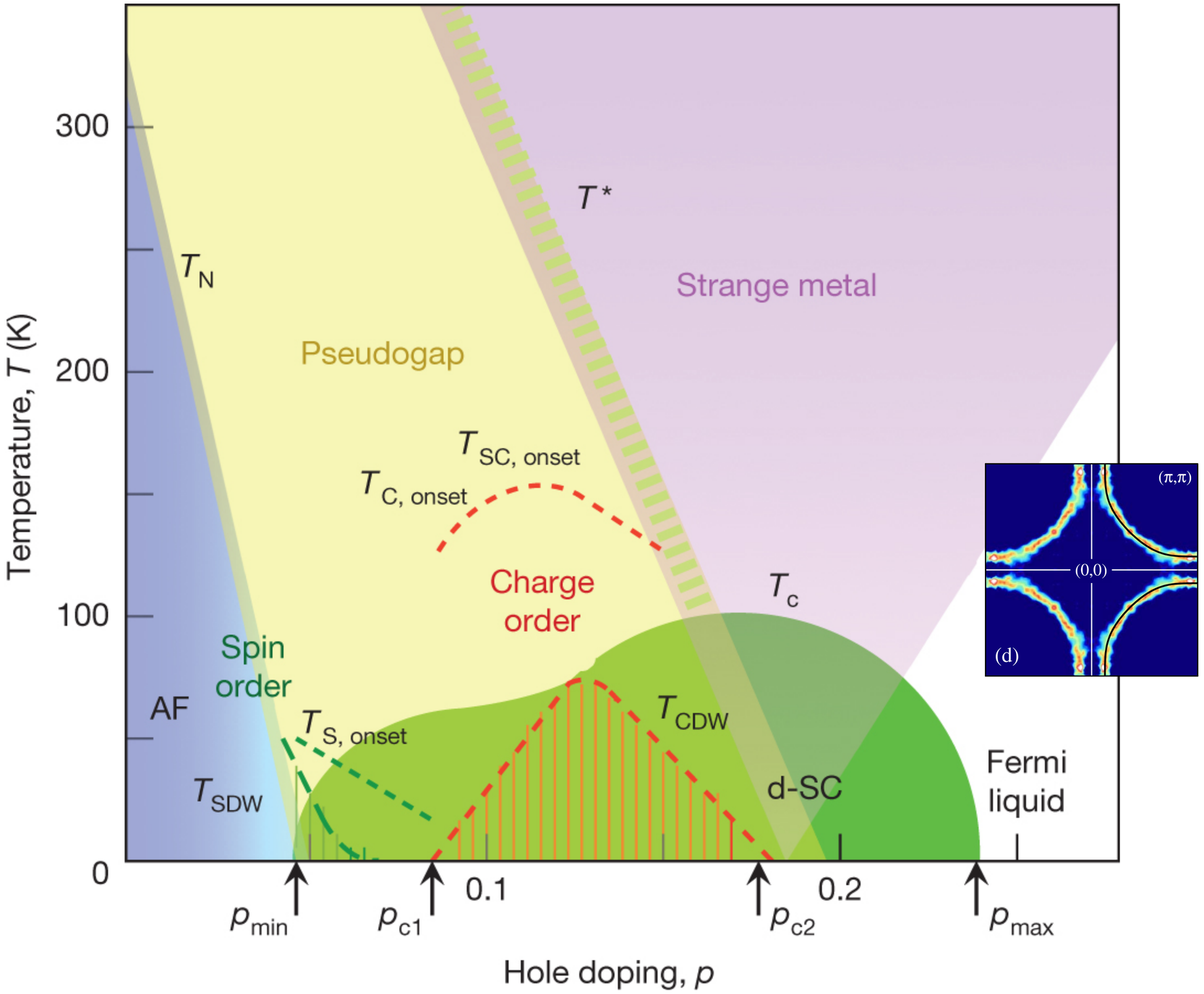

Fermi liquid
in the
overdoped metal

B Keimer *et al. Nature* **518**, 179-186 (2015)

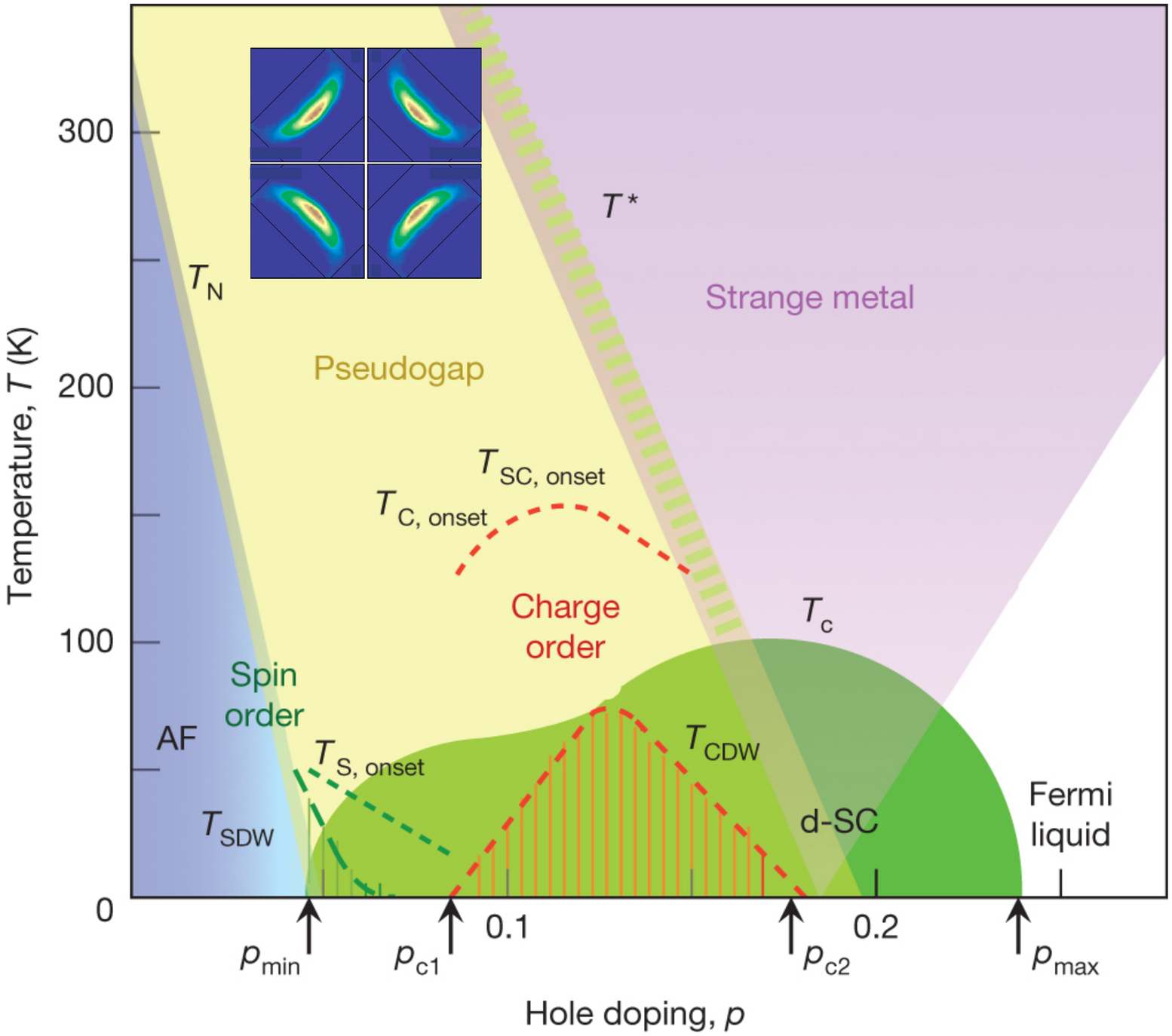

Theory for
"pseudogap metal"
with "Fermi arcs"?

B Keimer *et al. Nature* **518**, 179-186 (2015)

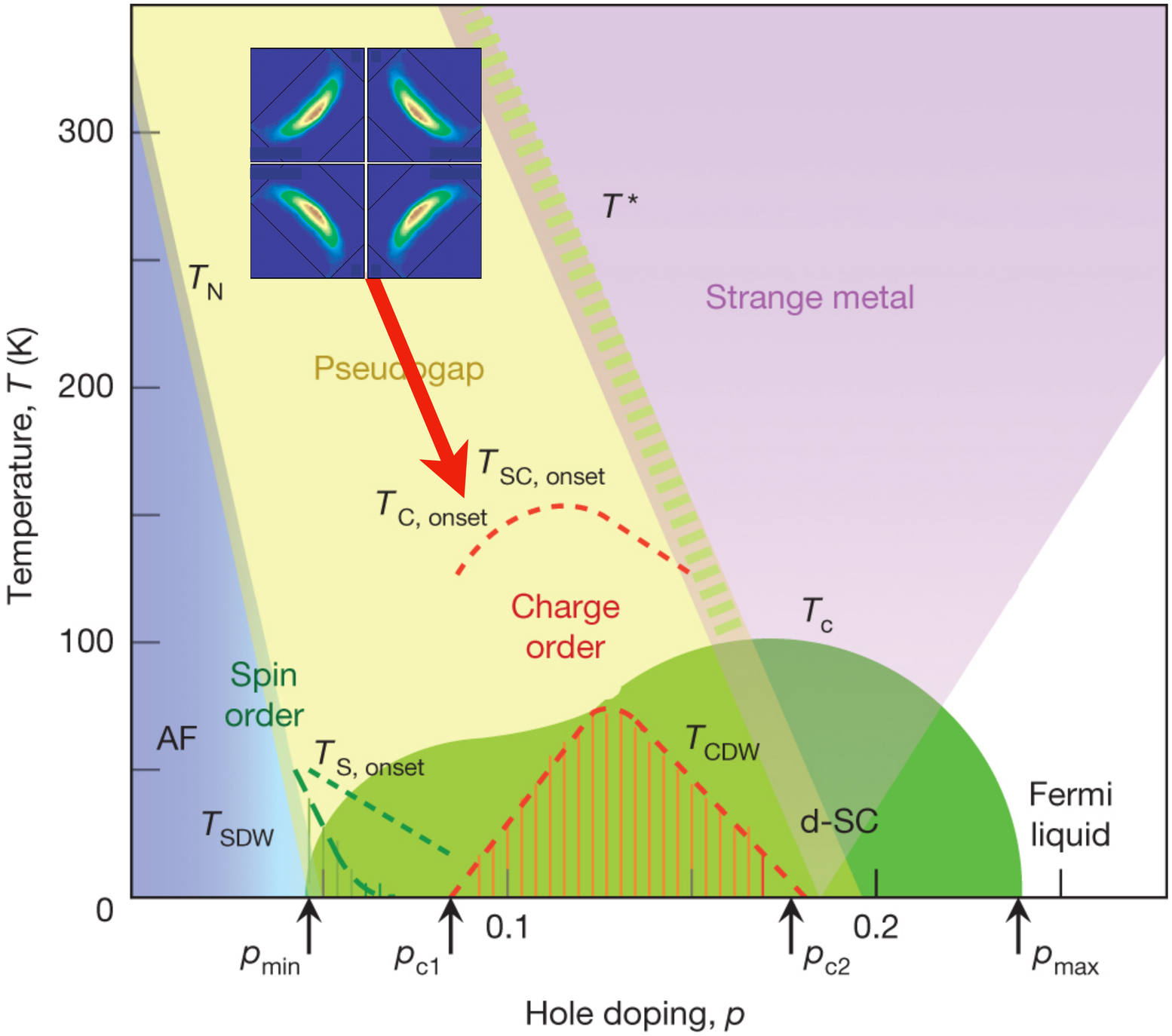

Needed: a theory for the onset of charge order and d-wave superconductivity from the pseudogap metal.

Why are T_c and $T_{\rm CDW}$ about the same?

B Keimer *et al. Nature* **518**, 179-186 (2015)

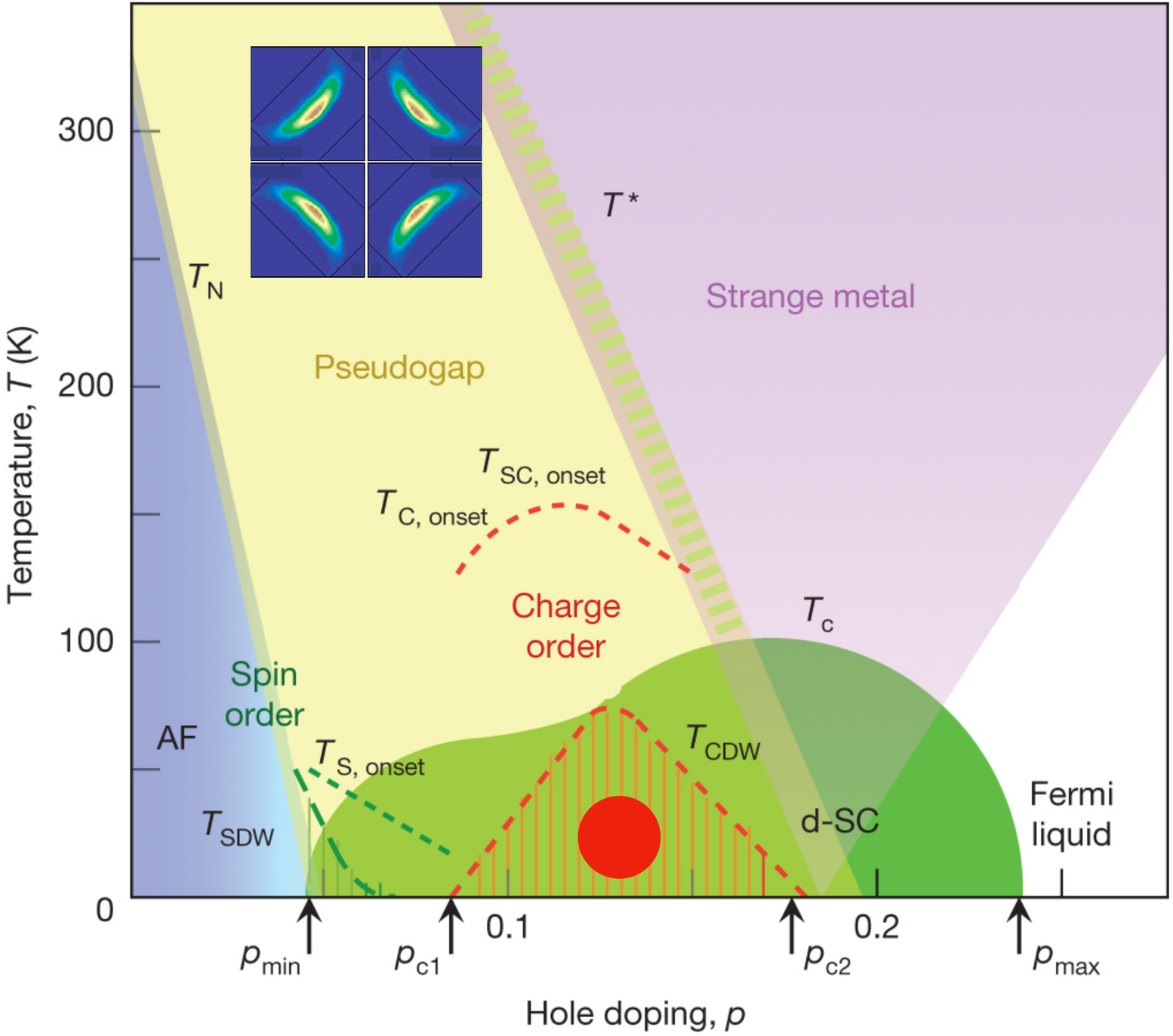

N. Doiron-Leyraud, C. Proust, D. LeBoeuf, J. Levallois, J.B. Bonnemaison, R. Liang, D.A. Bonn, W.N. Hardy, L. Taillefer, Nature **447**, 565 (2007)

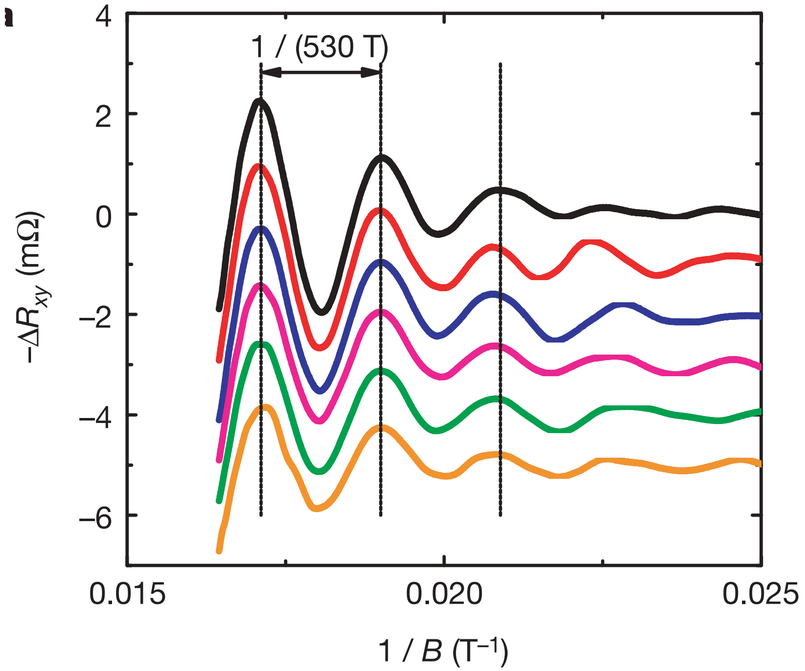

Quantum oscillations in the CDW phase at low T show only a single electron pocket of size p.

This cannot be obtained in the theory of CDWs in a Fermi liquid.

B Keimer *et al. Nature* **518**, 179-186 (2015)

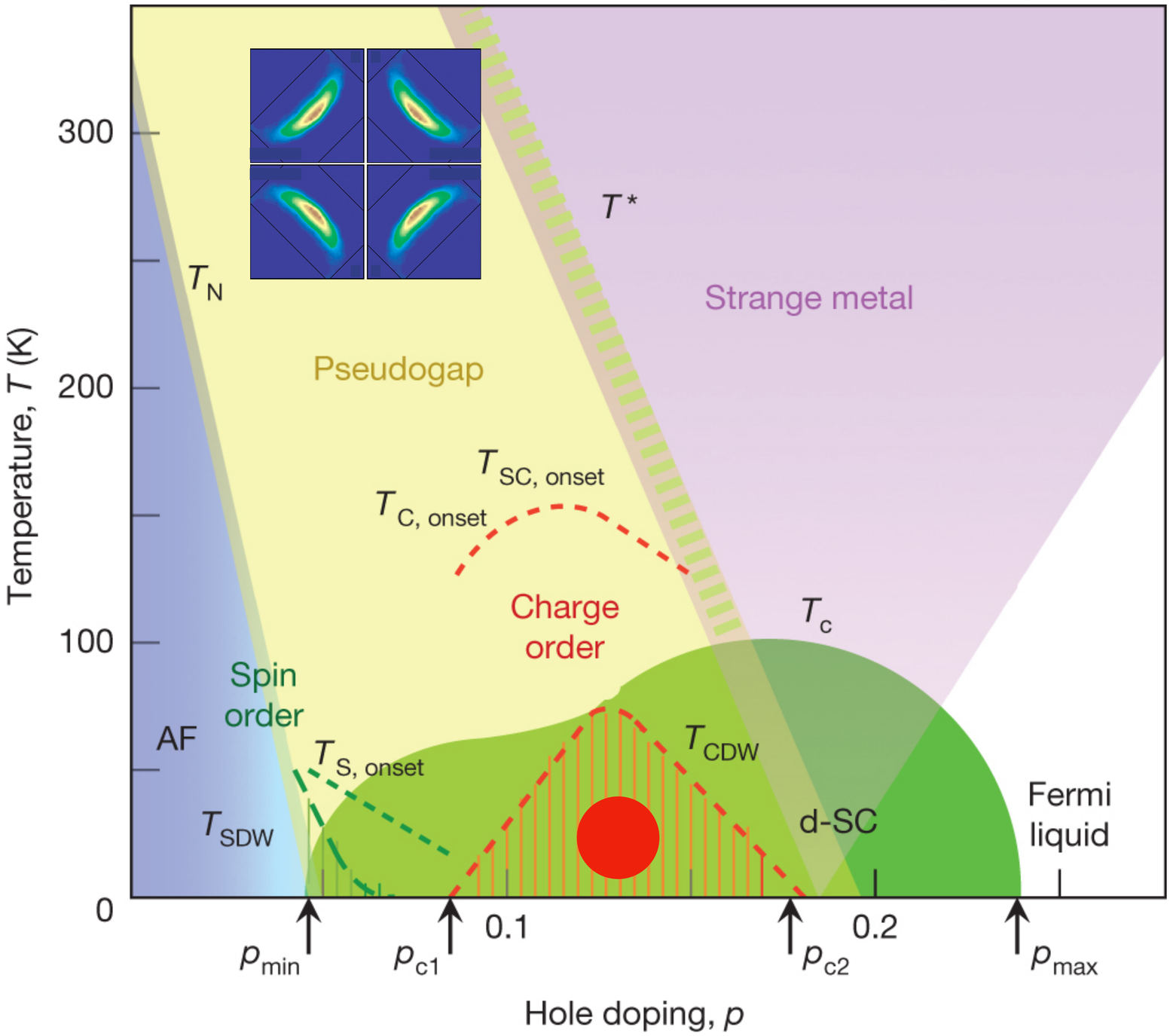

A. Allais, D. Chowdhury, and S. Sachdev,
Nature Communications **5**, 5771 (2014)

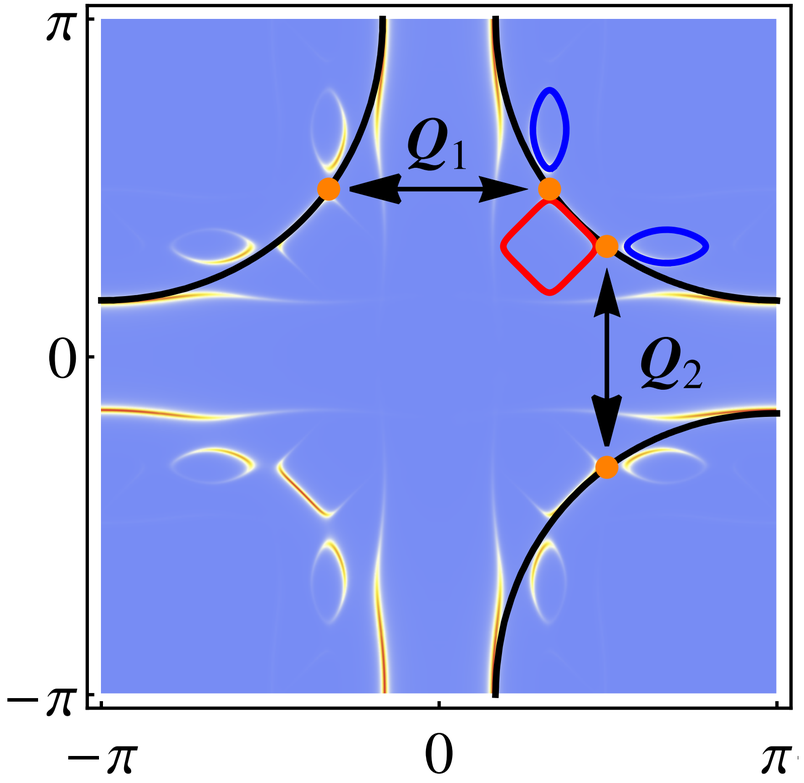

Quantum oscillations in the CDW phase at low T show only a single electron pocket of size p.

This cannot be obtained in the theory of CDWs in a Fermi liquid.

B Keimer *et al. Nature* **518**, 179-186 (2015)

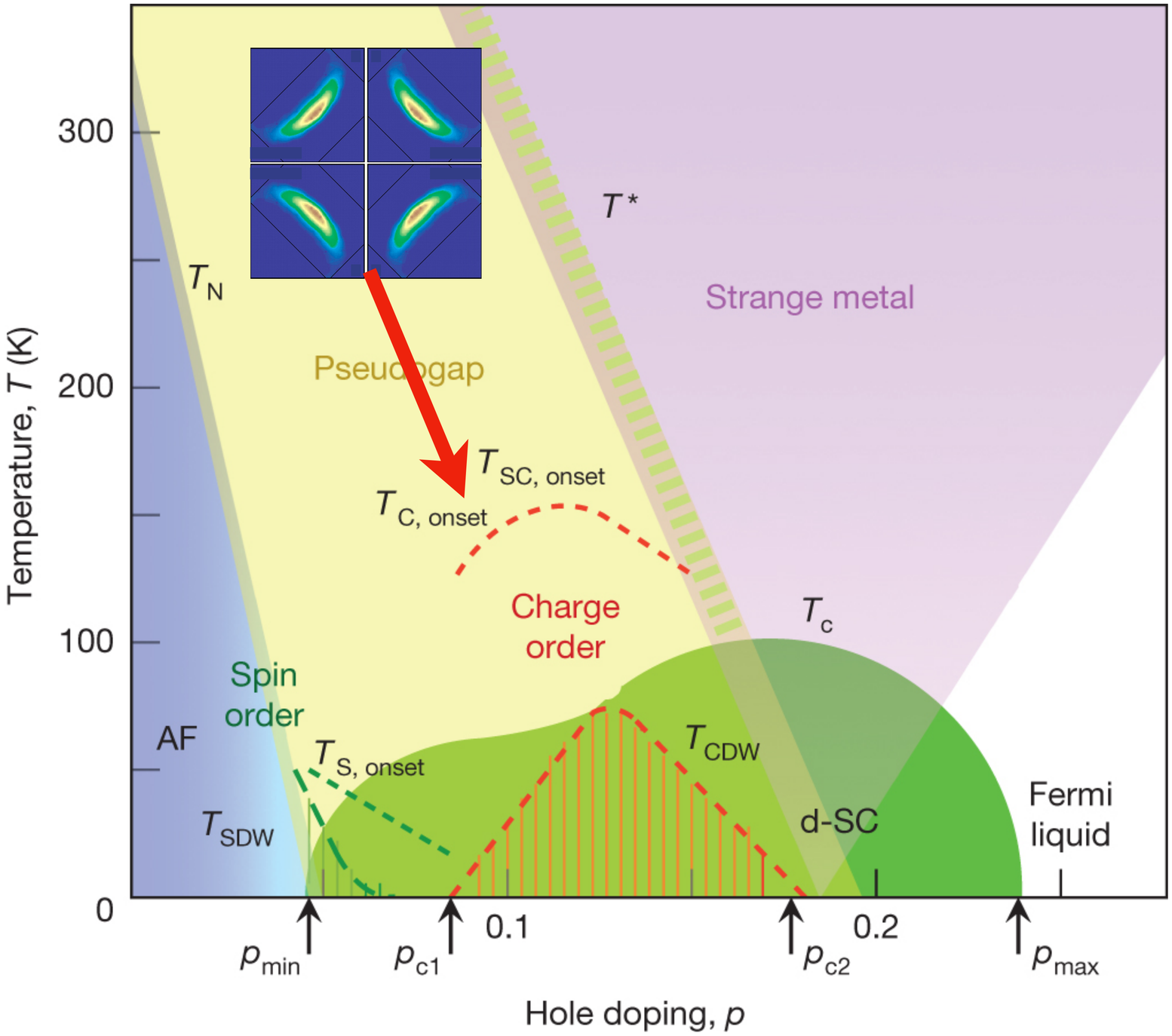

Theory for
"pseudogap metal"
with "Fermi arcs"?

Use the pseudogap metal
in place of the Fermi liquid
as the 'parent' to
conventional
d-wave superconductor,
charge density wave,
spin density wave,
pair density wave

...

B Keimer *et al. Nature* **518**, 179-186 (2015)

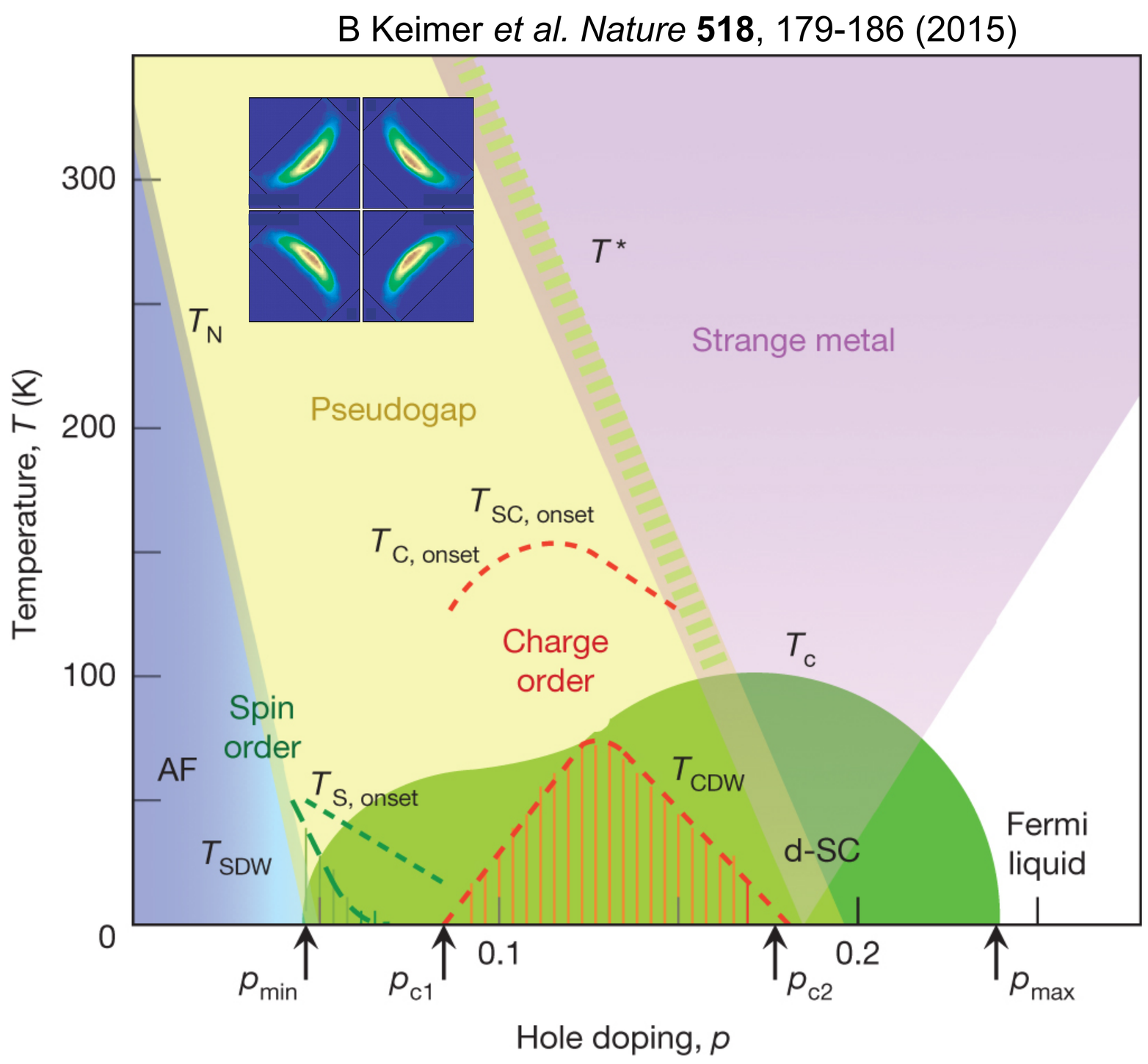

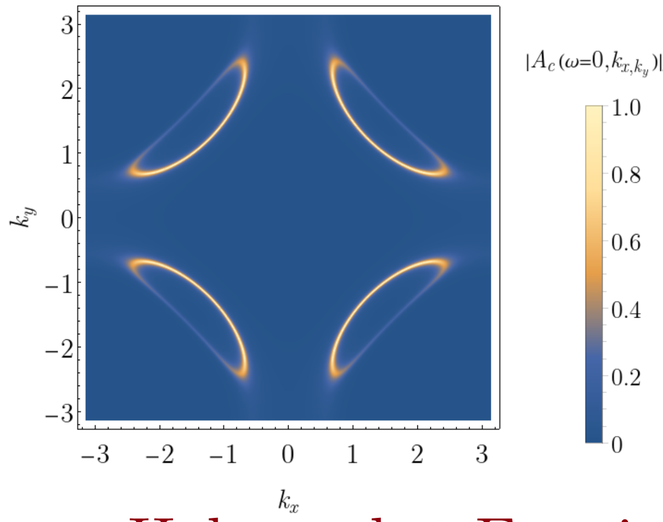

Ya-Hui Zhang and S. Sachdev, PRR **2**, 023172 (2020)

E. Mascot, A. Nikolaenko, M. Tikhanovskaya, Ya-Hui Zhang, D. K. Morr, and S. Sachdev, PRB **105**, 075146 (2022)

Hole pocket Fermi surfaces of size p with charge e, spin-1/2 quasiparticles

Kai-Yu Yang, T. M. Rice, Fu-Chun Zhang, PRB **73**, 174501 (2006).
T. D. Stanescu and G. Kotliar, PRB **74**, 125110 (2006).
C. Berthod, T. Giamarchi, S. Biermann, and A. Georges, PRL **97**, 136401 (2006).
S. Sakai, Y. Motome, M. Imada, PRL **102**, 056404 (2009).
J. Skolimowski and M. Fabrizio, PRB **106**, 045109 (2022).

Fermi surface transformation at the pseudogap critical point of a cuprate superconductor

Yawen Fang, Gaël Grissonnanche, Anaëlle Legros, Simon Verret, Francis Laliberté, Clément Collignon, Amirreza Ataei, Maxime Dion, Jianshi Zhou, David Graf, M. J. Lawler, Paul Goddard, Louis Taillefer, and B. J. Ramshaw, Nature Physics **18**, 558 (2022)

We use angle-dependent magnetoresistance (ADMR) to measure the Fermi surface of the cuprate Nd-LSCO. Above the critical doping $p^\star$ we extract a Fermi surface geometry that is in quantitative agreement with angle-resolved photoemission. Below $p^\star$ the ADMR is qualitatively different, revealing a clear transformation of the Fermi surface. We find that our data are most consistent with a reconstruction of the Fermi surface by a Q = (π, π) wavevector.

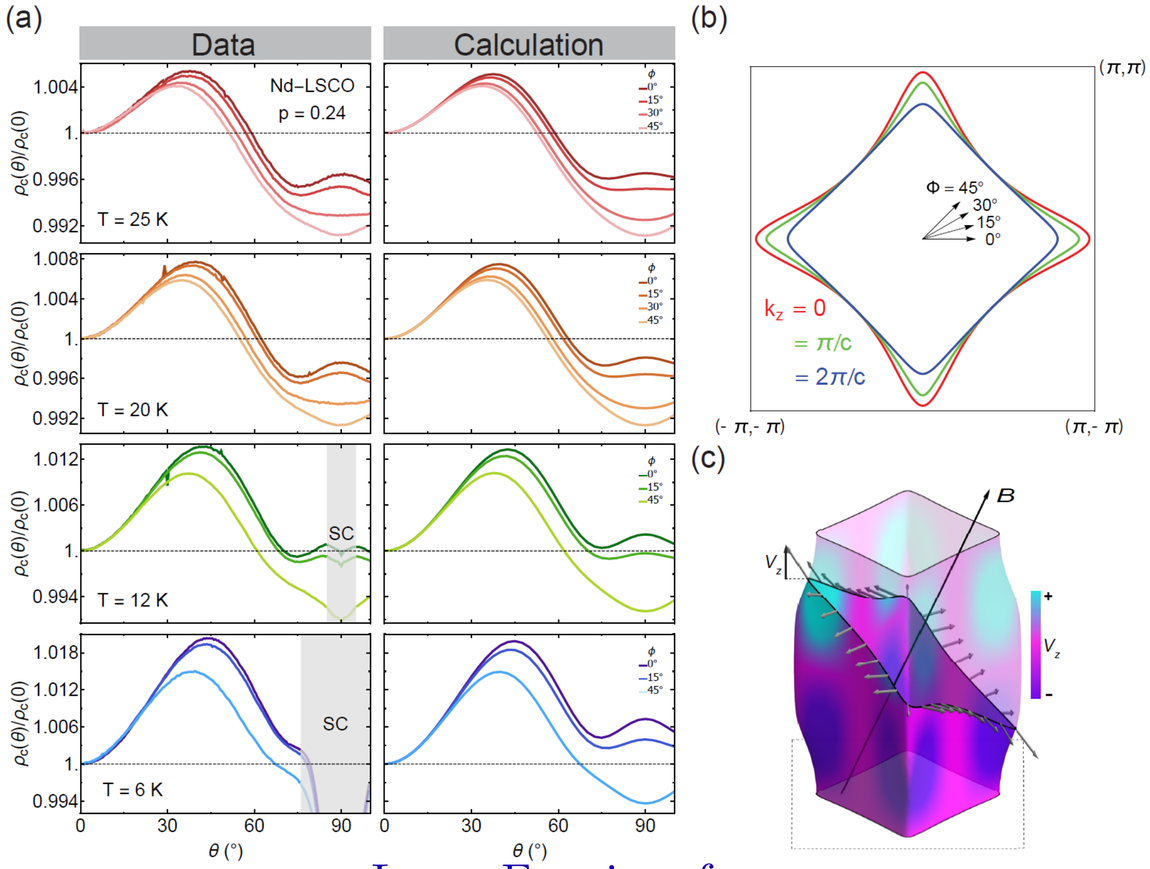

$p > p_c$ Large Fermi surface

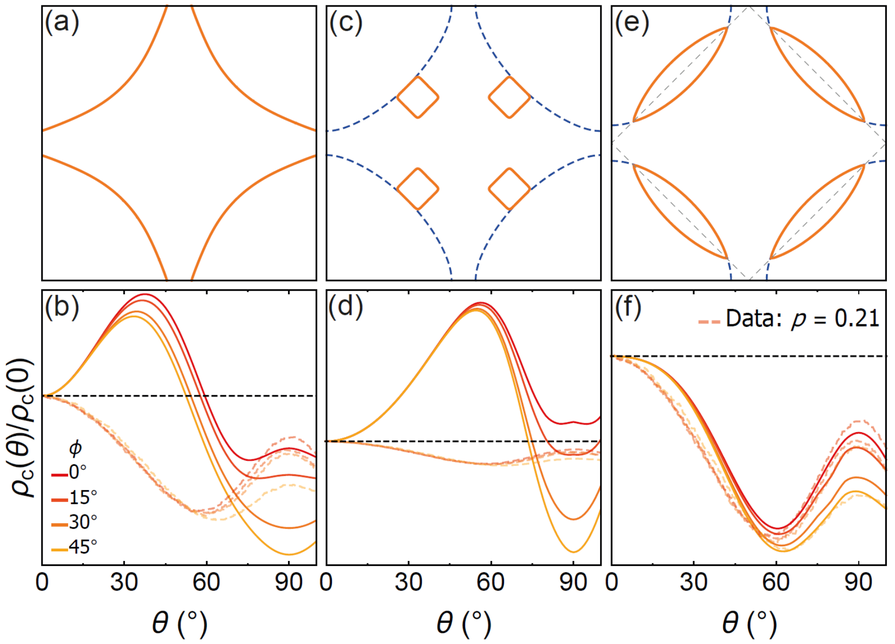

$p < p_c$ Reconstructed Fermi surface

B Keimer *et al. Nature* **518**, 179-186 (2015)

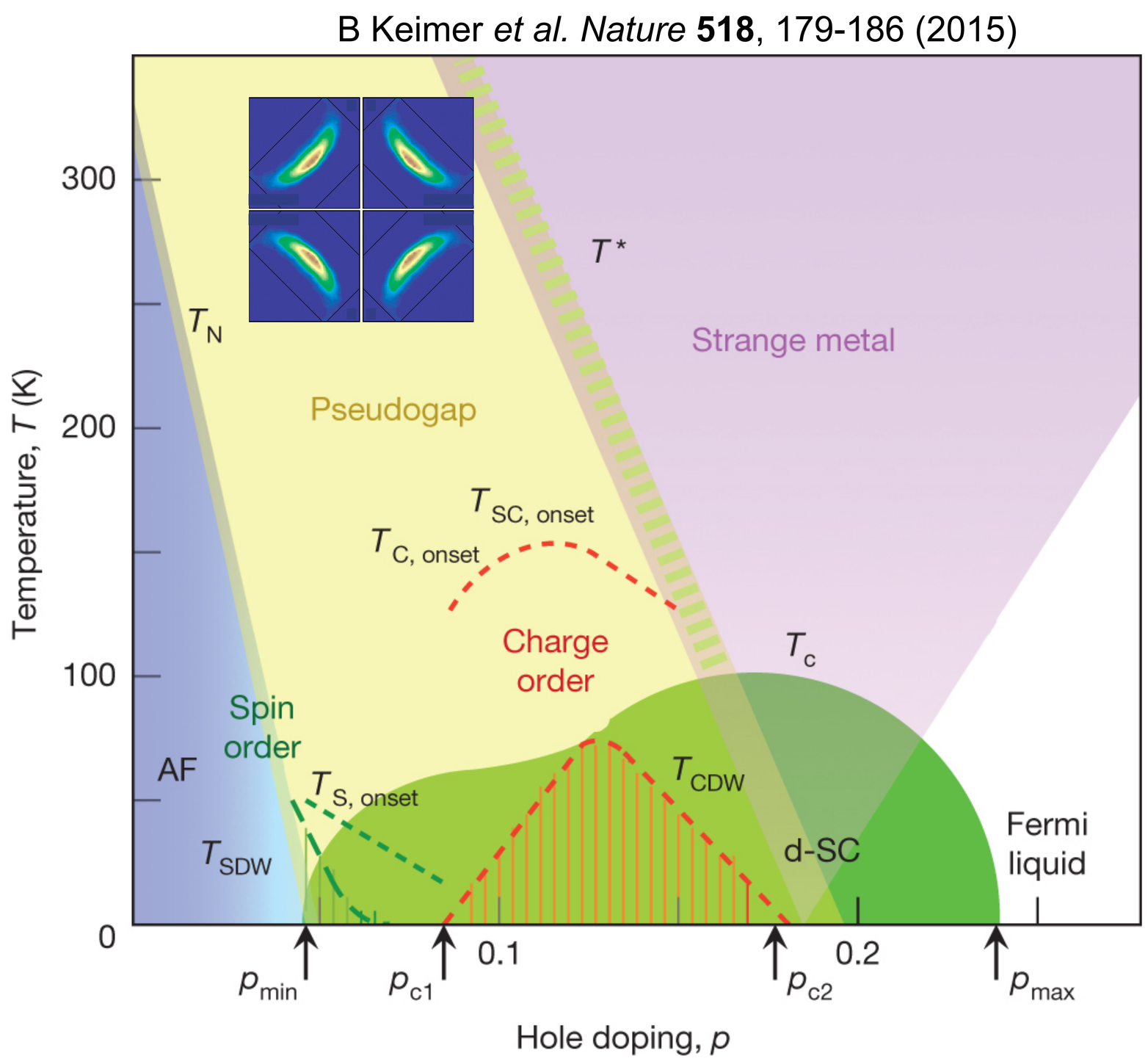

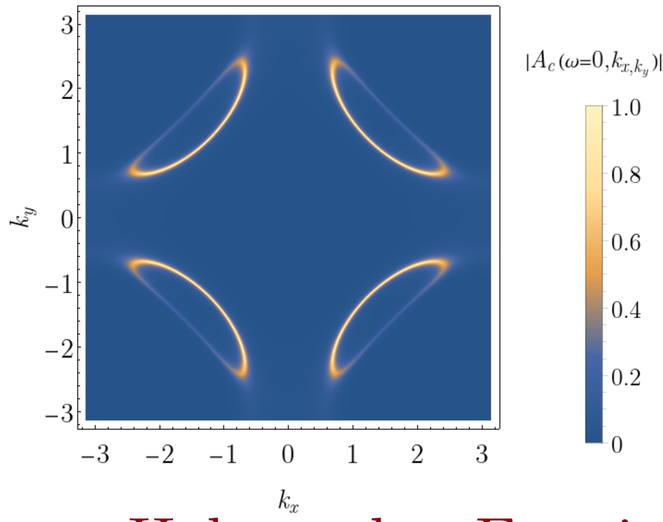

Ya-Hui Zhang and S. Sachdev, PRR **2**, 023172 (2020)

E. Mascot, A. Nikolaenko, M. Tikhanovskaya, Ya-Hui Zhang, D. K. Morr, and S. Sachdev, PRB **105**, 075146 (2022)

Hole pocket Fermi surfaces of size p with charge e, spin-1/2 quasiparticles

Kai-Yu Yang, T. M. Rice, Fu-Chun Zhang, PRB **73**, 174501 (2006).
T. D. Stanescu and G. Kotliar, PRB **74**, 125110 (2006).
C. Berthod, T. Giamarchi, S. Biermann, and A. Georges, PRL **97**, 136401 (2006).
S. Sakai, Y. Motome, M. Imada, PRL **102**, 056404 (2009).
J. Skolimowski and M. Fabrizio, PRB **106**, 045109 (2022).

B Keimer *et al. Nature* **518**, 179-186 (2015)

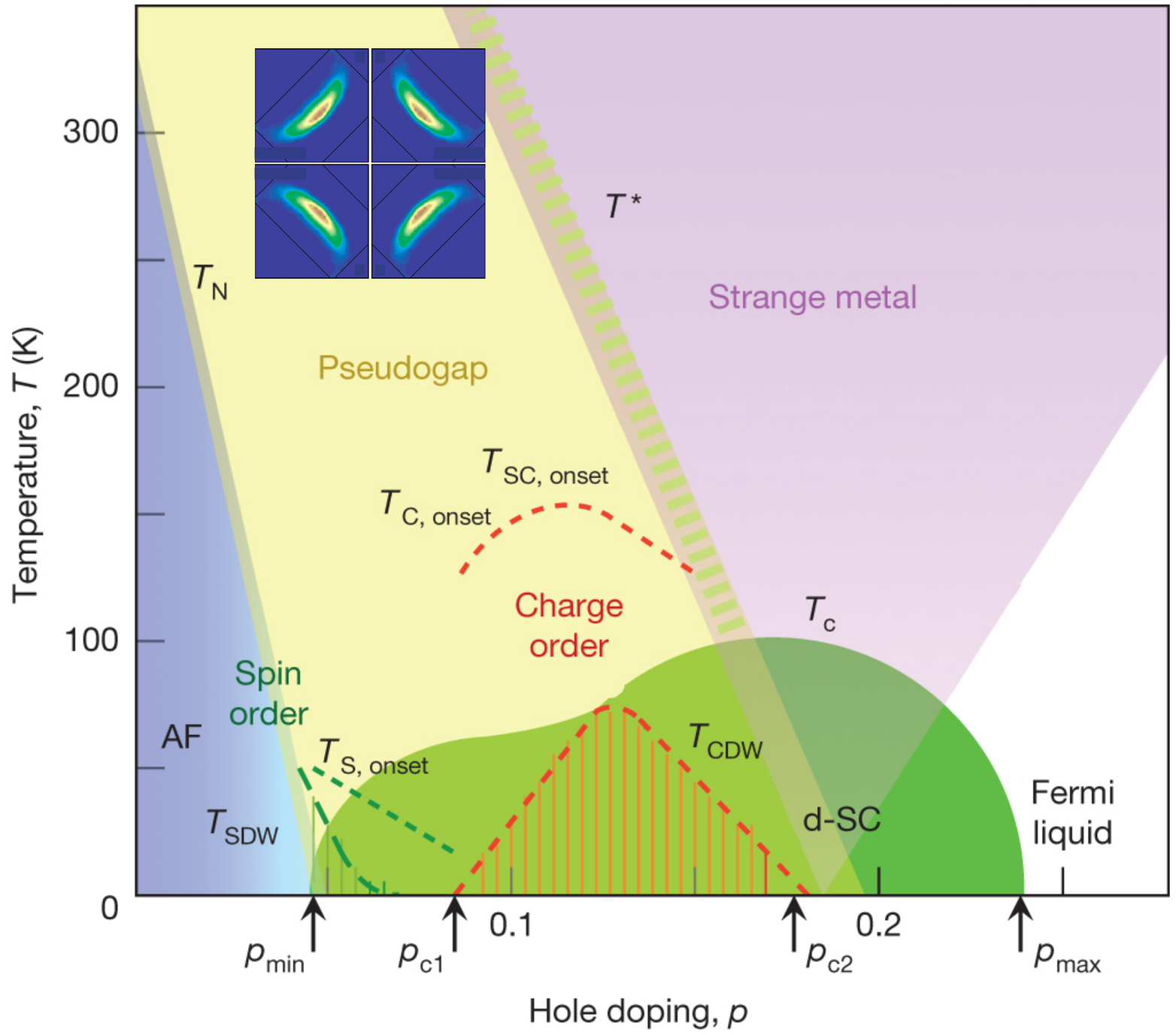

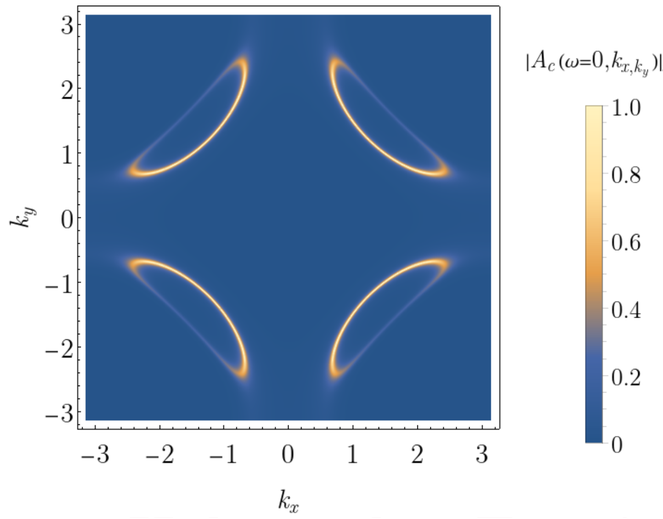

Ya-Hui Zhang and S. Sachdev, PRR **2**, 023172 (2020)

E. Mascot, A. Nikolaenko, M. Tikhanovskaya, Ya-Hui Zhang, D. K. Morr, and S. Sachdev, PRB **105**, 075146 (2022)

Hole pocket Fermi surfaces of size p with charge e, spin-1/2 quasiparticles
+
'spectator' square lattice spin liquid *at half-filling.*

FL*: Spin liquid is *required* because the Fermi surface does not enclose the Luttinger volume $(1+p)$.

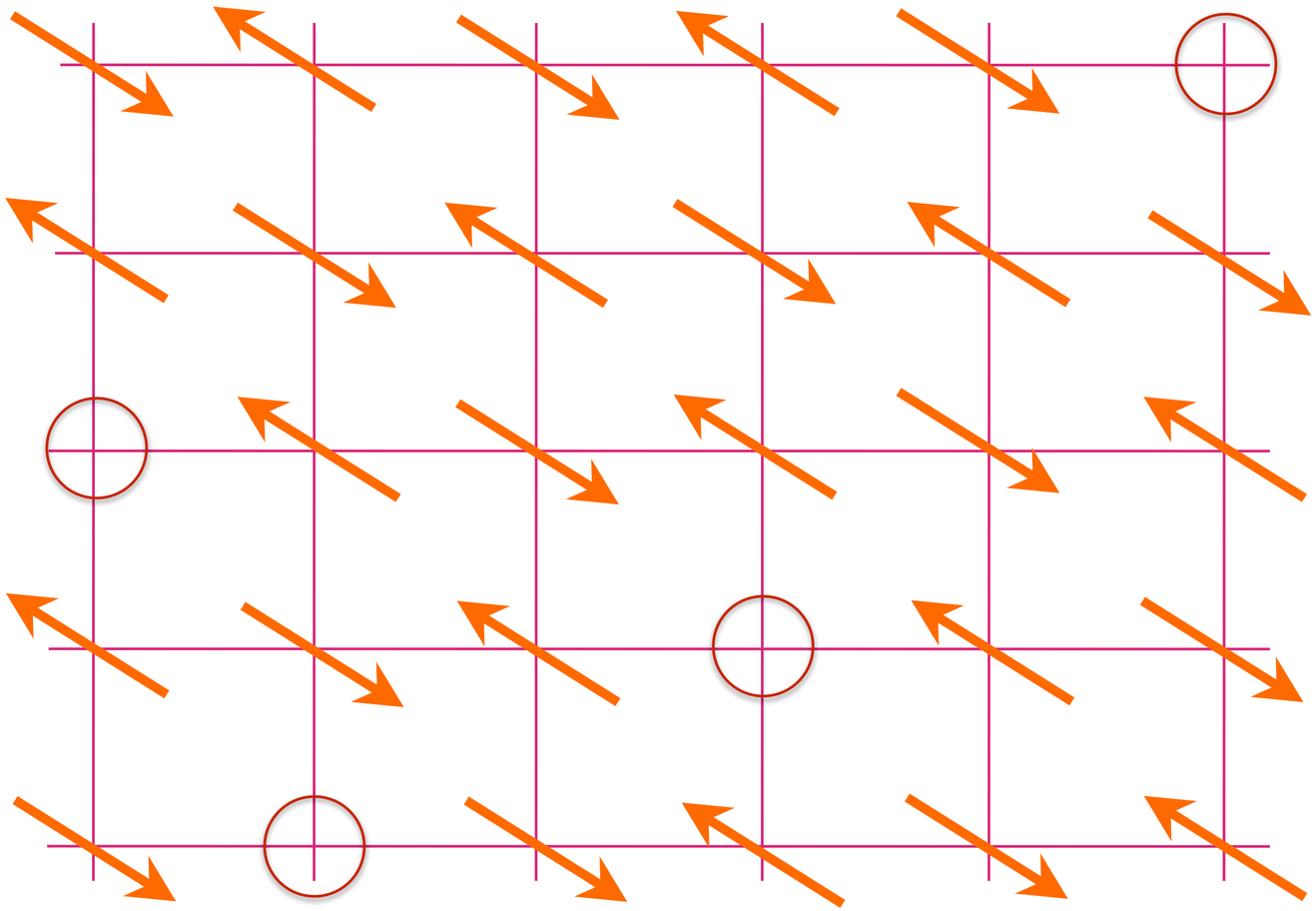

Anti-ferromagnet with p holes per square

Holon metal

G. Baskaran, Z. Zou, P.W. Anderson, Solid State Comm. **63**, 973 (1987)
S.A. Kivelson, D.S. Rokhsar and J.P. Sethna, PRB **35**, 8865 (1987)
D. Rokhsar and S.A. Kivelson, PRL **61**, 2376 (1988)

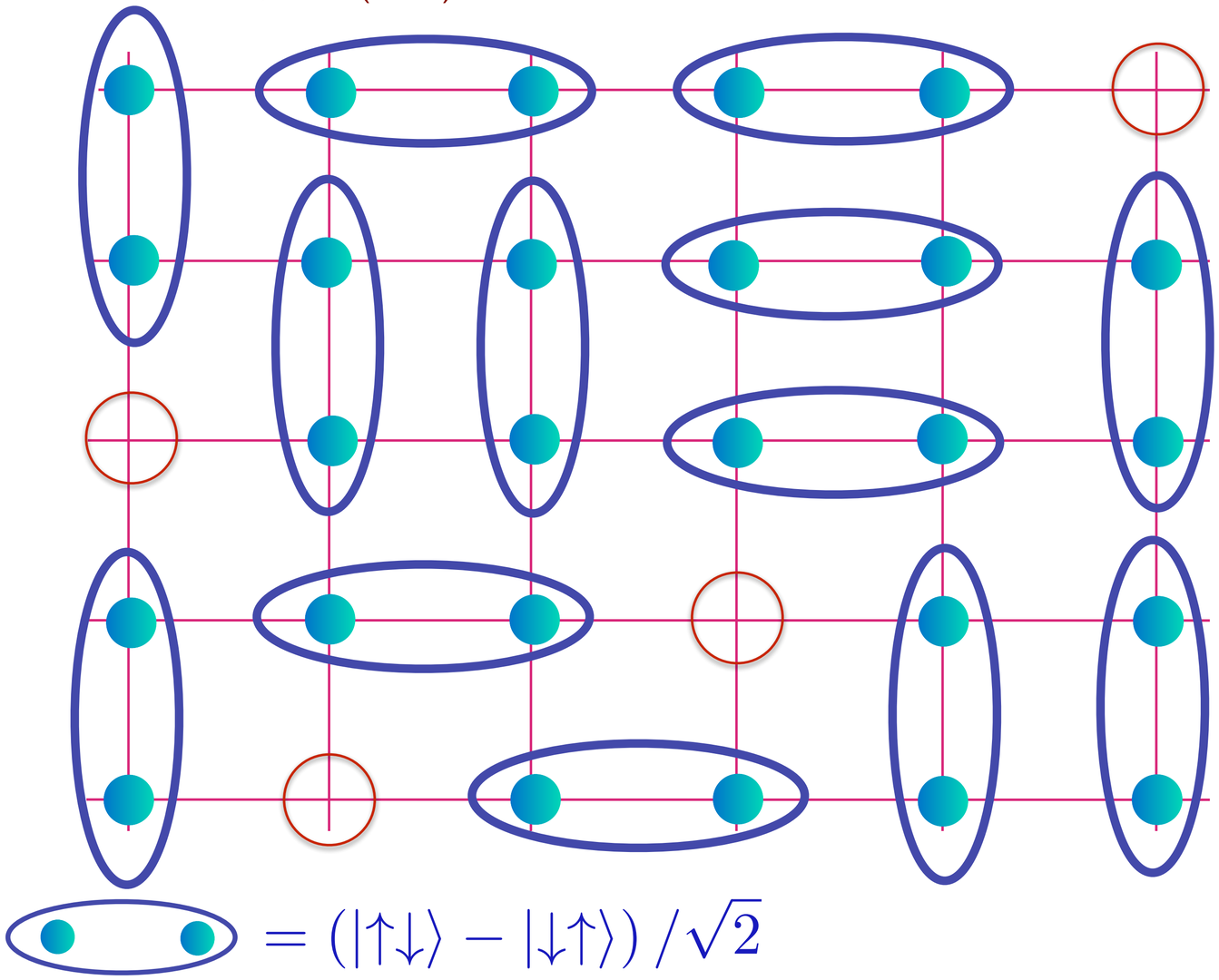

$$= \left(|\uparrow\downarrow\rangle - |\downarrow\uparrow\rangle\right)/\sqrt{2}$$

Spin liquid with density p of spinless, charge +e "holons".

Holon metal

G. Baskaran, Z. Zou, P.W. Anderson, Solid State Comm. **63**, 973 (1987)
S.A. Kivelson, D.S. Rokhsar and J.P. Sethna, PRB **35**, 8865 (1987)
D. Rokhsar and S.A. Kivelson, PRL **61**, 2376 (1988)

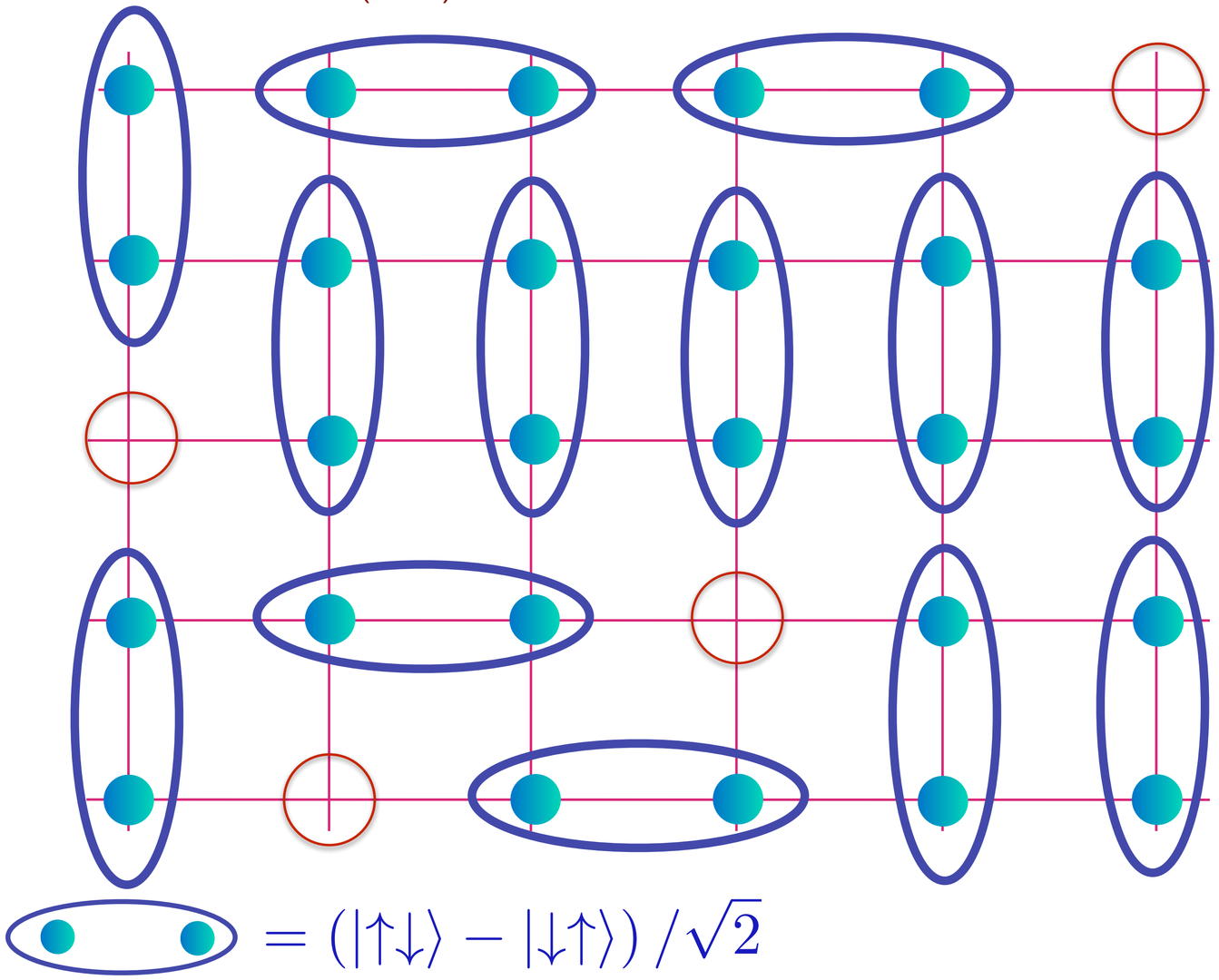

$$= \left(|\uparrow\downarrow\rangle - |\downarrow\uparrow\rangle\right)/\sqrt{2}$$

Spin liquid with density p of spinless, charge +e "holons".

Holon metal

G. Baskaran, Z. Zou, P.W. Anderson, Solid State Comm. **63**, 973 (1987)
S.A. Kivelson, D.S. Rokhsar and J.P. Sethna, PRB **35**, 8865 (1987)
D. Rokhsar and S.A. Kivelson, PRL **61**, 2376 (1988)

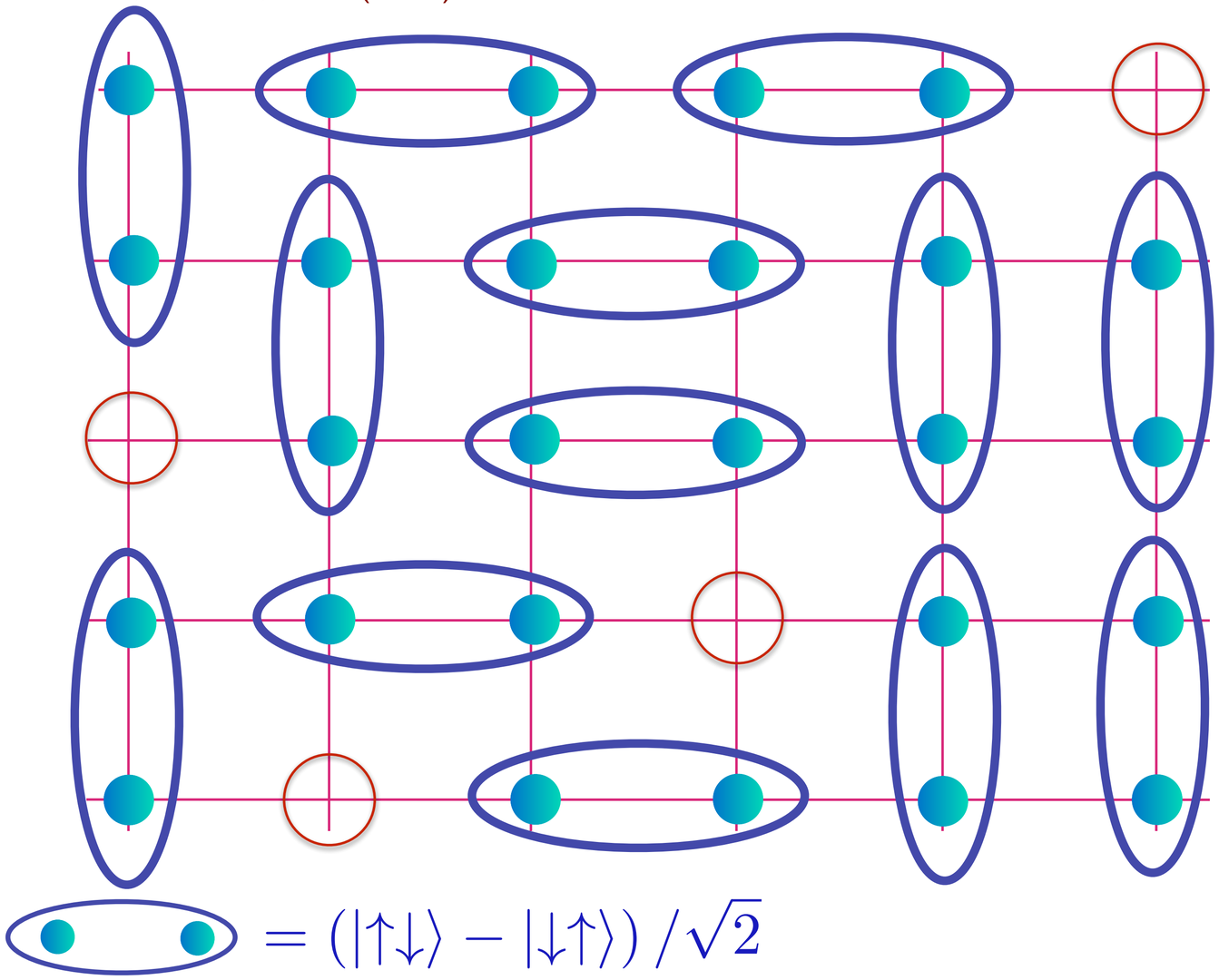

$$= \left(|\uparrow\downarrow\rangle - |\downarrow\uparrow\rangle\right)/\sqrt{2}$$

Spin liquid with density p of spinless, charge +e "holons".

Holon metal

G. Baskaran, Z. Zou, P.W. Anderson, Solid State Comm. **63**, 973 (1987)
S.A. Kivelson, D.S. Rokhsar and J.P. Sethna, PRB **35**, 8865 (1987)
D. Rokhsar and S.A. Kivelson, PRL **61**, 2376 (1988)

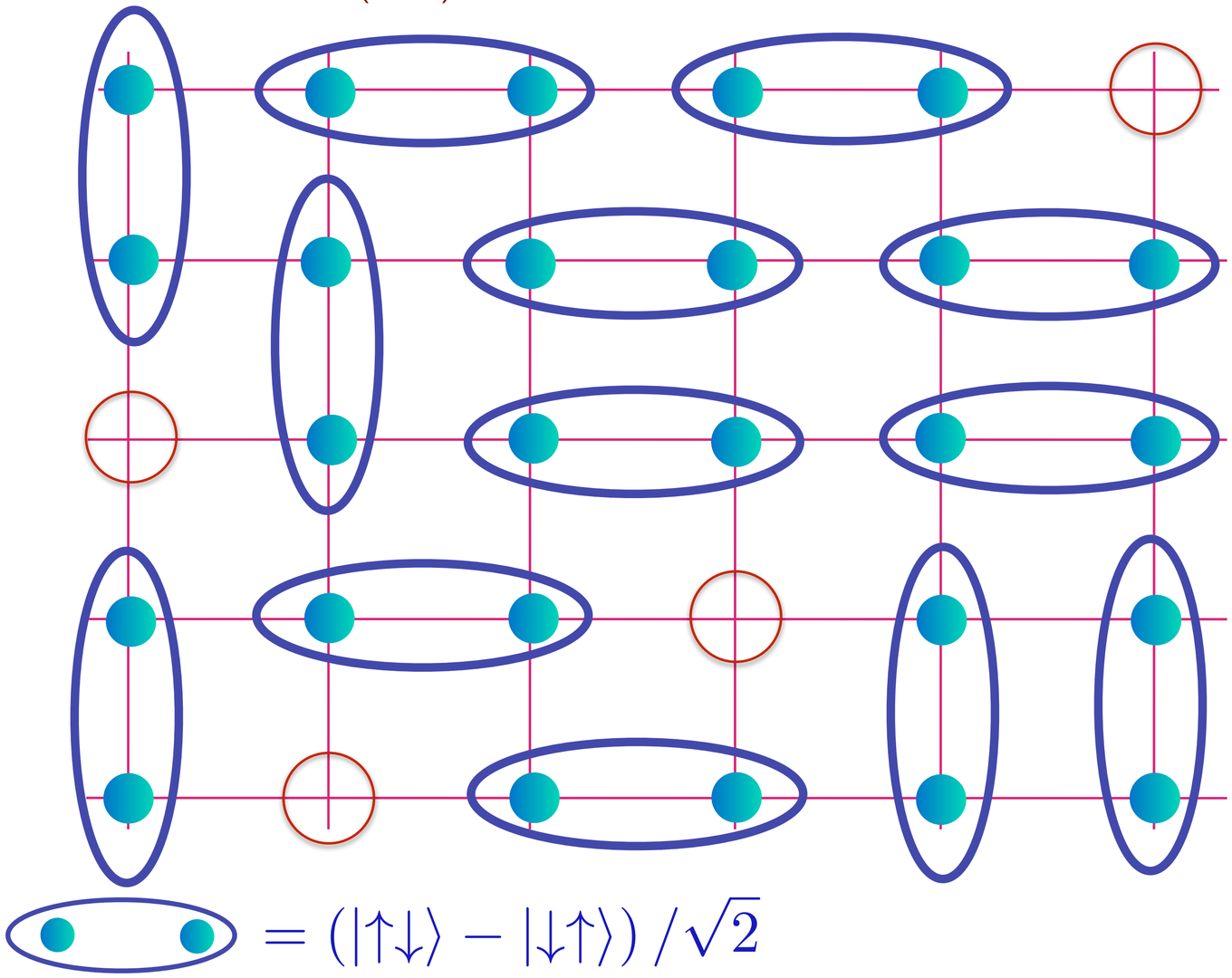

$$= \left(|\uparrow\downarrow\rangle - |\downarrow\uparrow\rangle\right)/\sqrt{2}$$

Spin liquid with density p of spinless, charge +e "holons".

Holon metal

G. Baskaran, Z. Zou, P.W. Anderson, Solid State Comm. **63**, 973 (1987)
S.A. Kivelson, D.S. Rokhsar and J.P. Sethna, PRB **35**, 8865 (1987)
D. Rokhsar and S.A. Kivelson, PRL **61**, 2376 (1988)

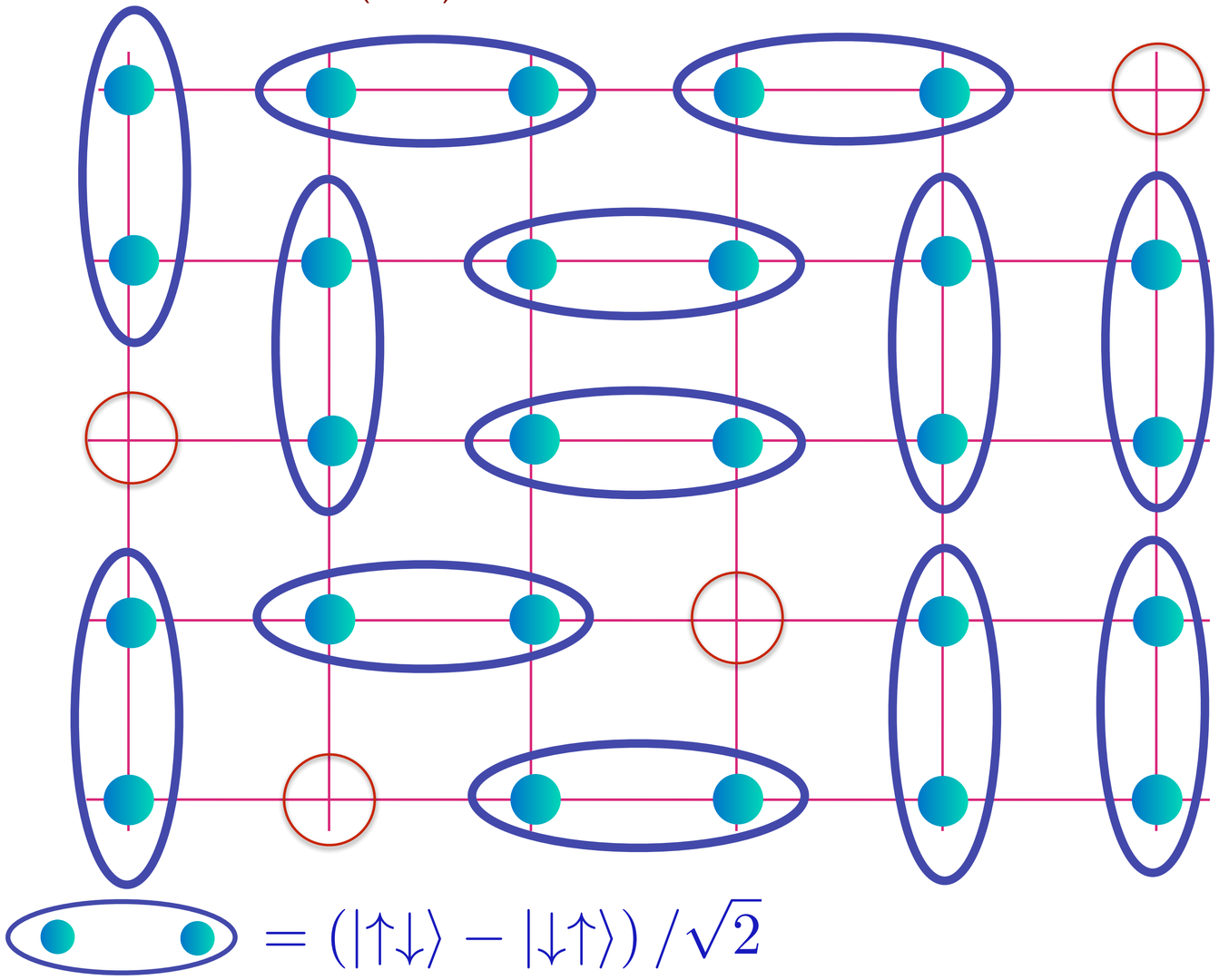

$$= \left(|\uparrow\downarrow\rangle - |\downarrow\uparrow\rangle\right)/\sqrt{2}$$

Spin liquid with density p of spinless, charge +e "holons".

Holon metal

G. Baskaran, Z. Zou, P.W. Anderson, Solid State Comm. **63**, 973 (1987)
S.A. Kivelson, D.S. Rokhsar and J.P. Sethna, PRB **35**, 8865 (1987)
D. Rokhsar and S.A. Kivelson, PRL **61**, 2376 (1988)

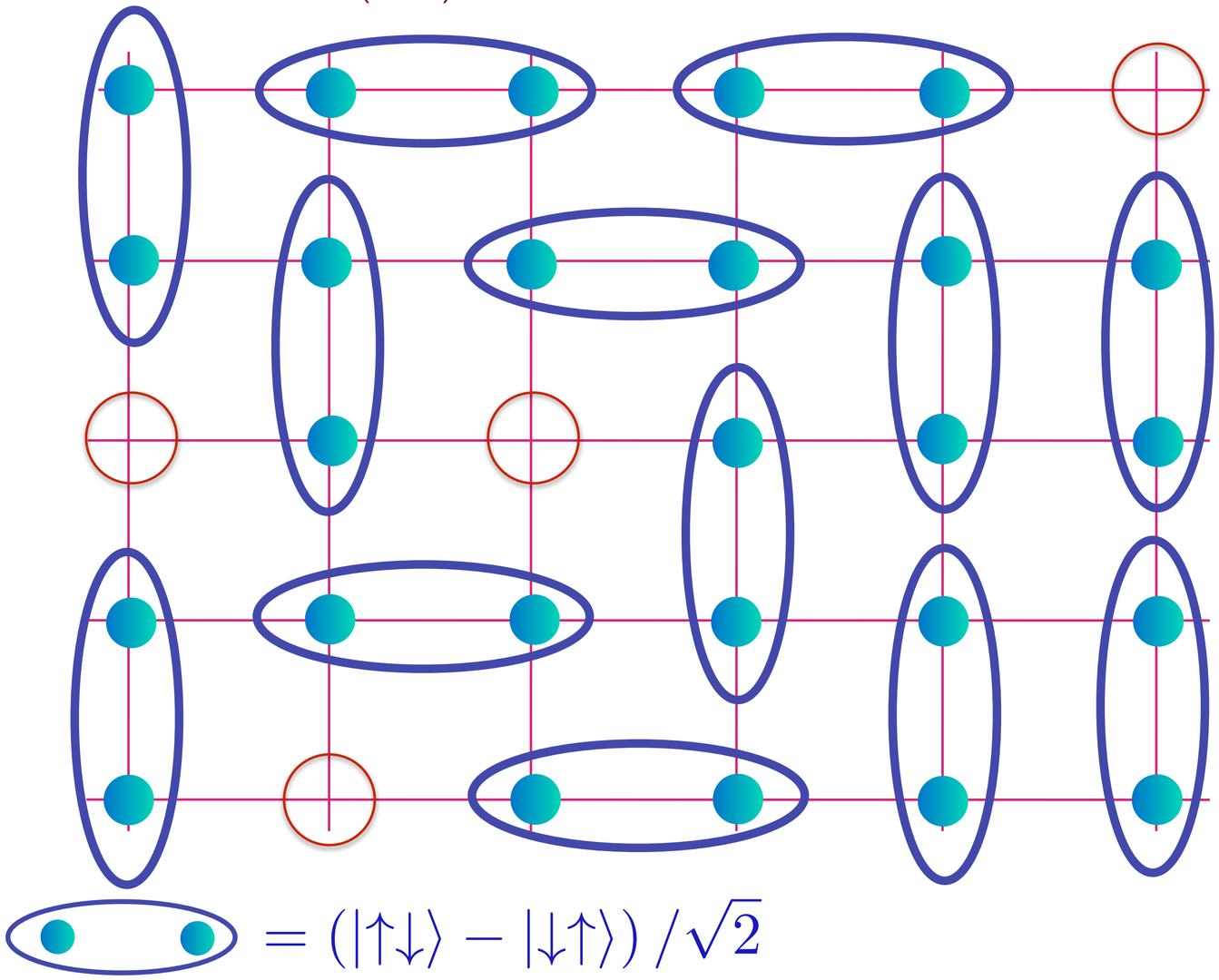

$$= \left(|\uparrow\downarrow\rangle - |\downarrow\uparrow\rangle\right)/\sqrt{2}$$

Spin liquid with density p of spinless, charge +e "holons".

Holon metal

G. Baskaran, Z. Zou, P.W. Anderson, Solid State Comm. **63**, 973 (1987)
S.A. Kivelson, D.S. Rokhsar and J.P. Sethna, PRB **35**, 8865 (1987)
D. Rokhsar and S.A. Kivelson, PRL **61**, 2376 (1988)

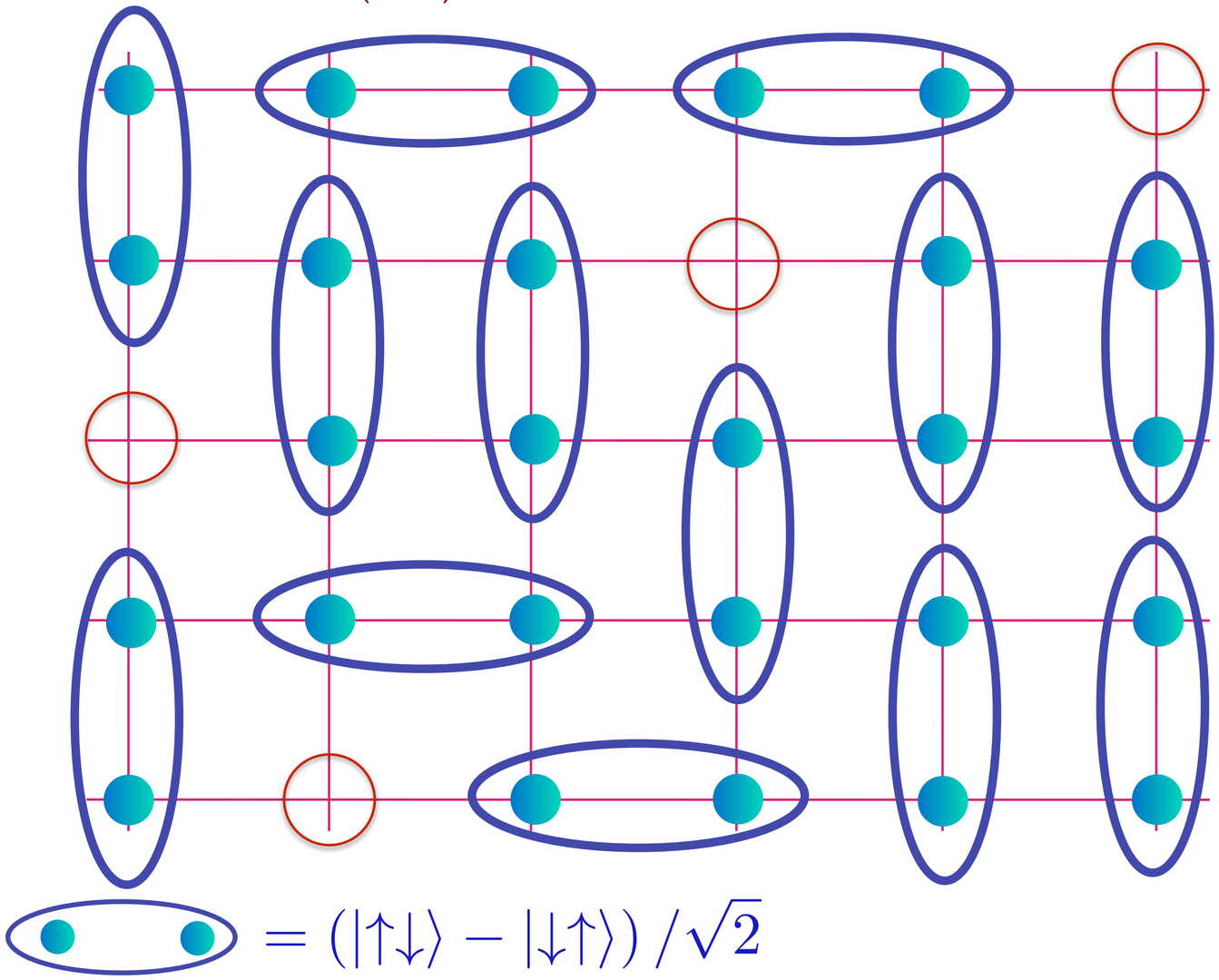

$$= \left(|\uparrow\downarrow\rangle - |\downarrow\uparrow\rangle\right)/\sqrt{2}$$

Spin liquid with density p of spinless, charge +e "holons".

Holon metal

G. Baskaran, Z. Zou, P.W. Anderson, Solid State Comm. **63**, 973 (1987)
S.A. Kivelson, D.S. Rokhsar and J.P. Sethna, PRB **35**, 8865 (1987)
D. Rokhsar and S.A. Kivelson, PRL **61**, 2376 (1988)

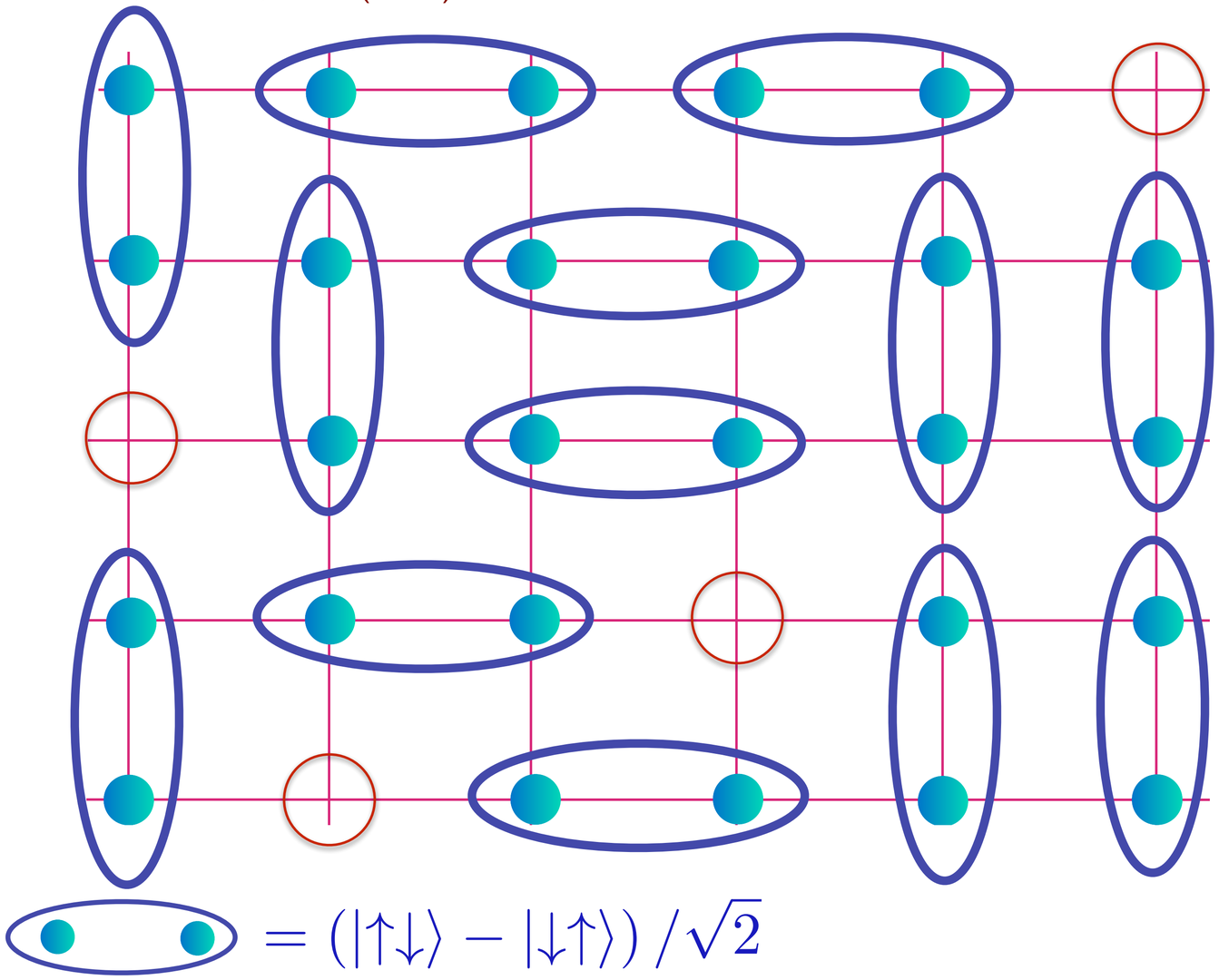

$$= \left(|\uparrow\downarrow\rangle - |\downarrow\uparrow\rangle\right)/\sqrt{2}$$

Spin liquid with density p of spinless, charge +e "holons".

Holon metal

G. Baskaran, Z. Zou, P.W. Anderson, Solid State Comm. **63**, 973 (1987)
S.A. Kivelson, D.S. Rokhsar and J.P. Sethna, PRB **35**, 8865 (1987)
D. Rokhsar and S.A. Kivelson, PRL **61**, 2376 (1988)

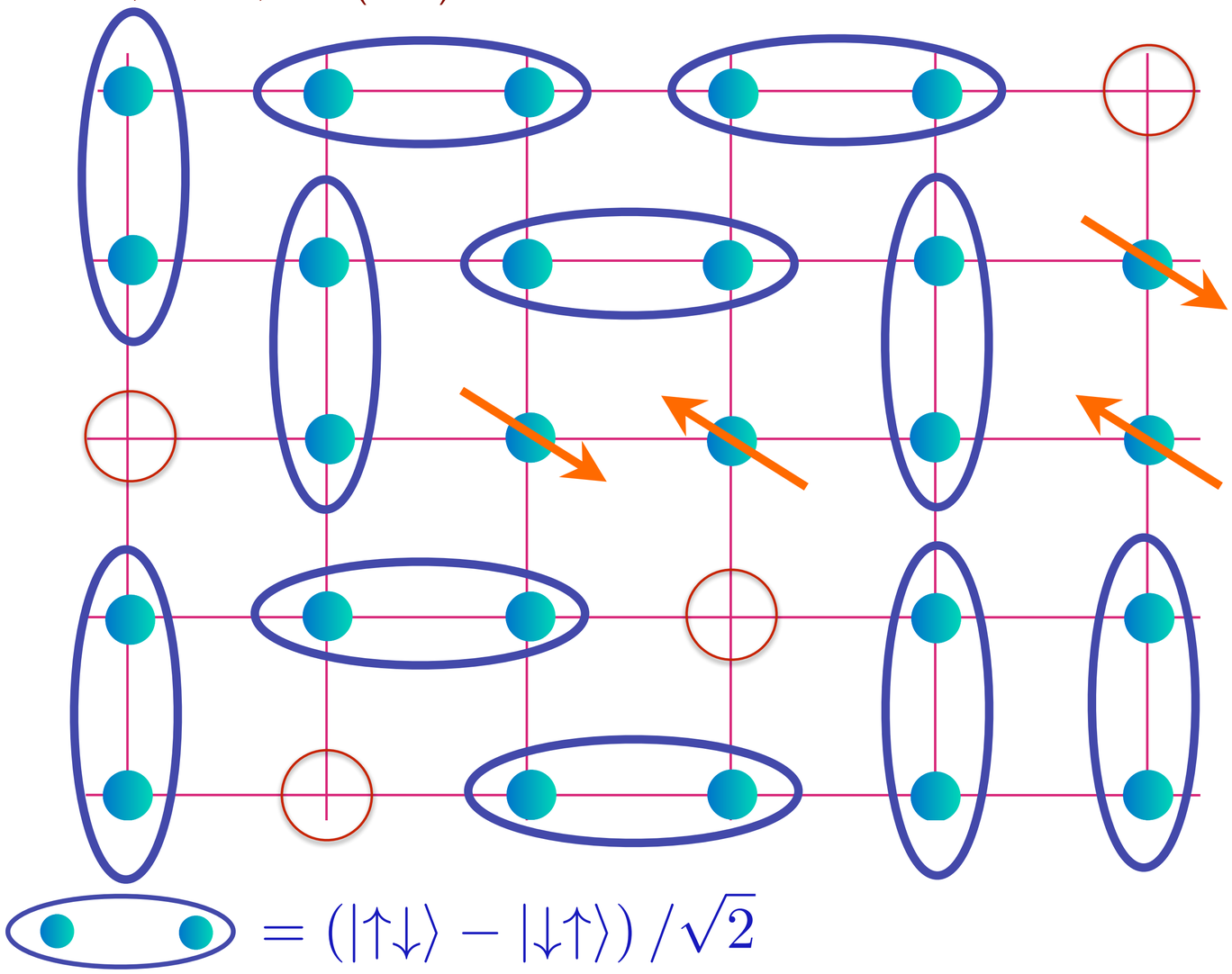

$$= \left(|\uparrow\downarrow\rangle - |\downarrow\uparrow\rangle\right)/\sqrt{2}$$

Spin liquid with density p of spinless, charge +e "holons" and charge 0, spin-1/2 "spinons".

Holon metal

G. Baskaran, Z. Zou, P.W. Anderson, Solid State Comm. **63**, 973 (1987)
S.A. Kivelson, D.S. Rokhsar and J.P. Sethna, PRB **35**, 8865 (1987)
D. Rokhsar and S.A. Kivelson, PRL **61**, 2376 (1988)

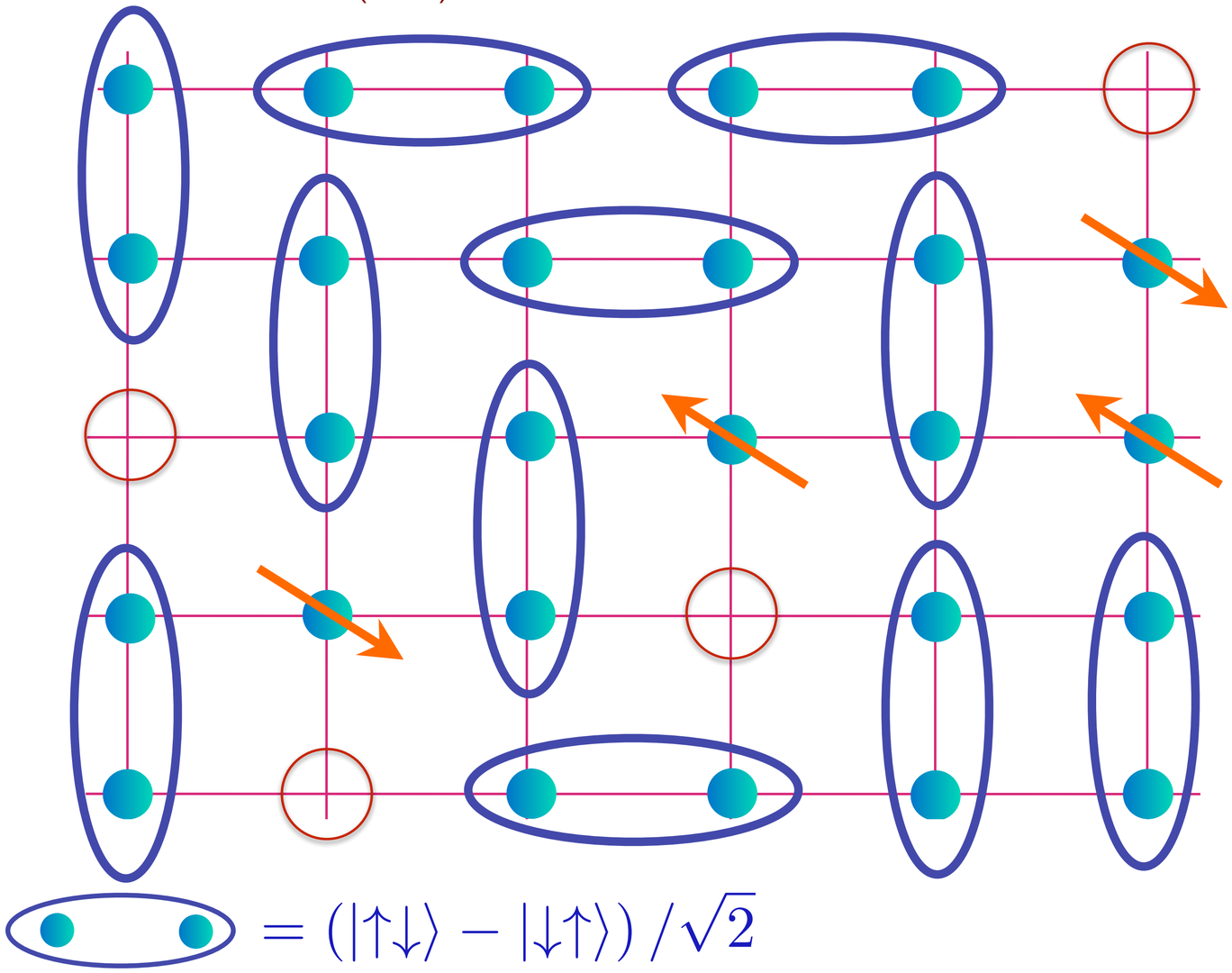

$$= \left(|\uparrow\downarrow\rangle - |\downarrow\uparrow\rangle\right)/\sqrt{2}$$

Spin liquid with density p of spinless, charge +e "holons" and charge 0, spin-1/2 "spinons".

Holon metal

G. Baskaran, Z. Zou, P.W. Anderson, Solid State Comm. **63**, 973 (1987)
S.A. Kivelson, D.S. Rokhsar and J.P. Sethna, PRB **35**, 8865 (1987)
D. Rokhsar and S.A. Kivelson, PRL **61**, 2376 (1988)

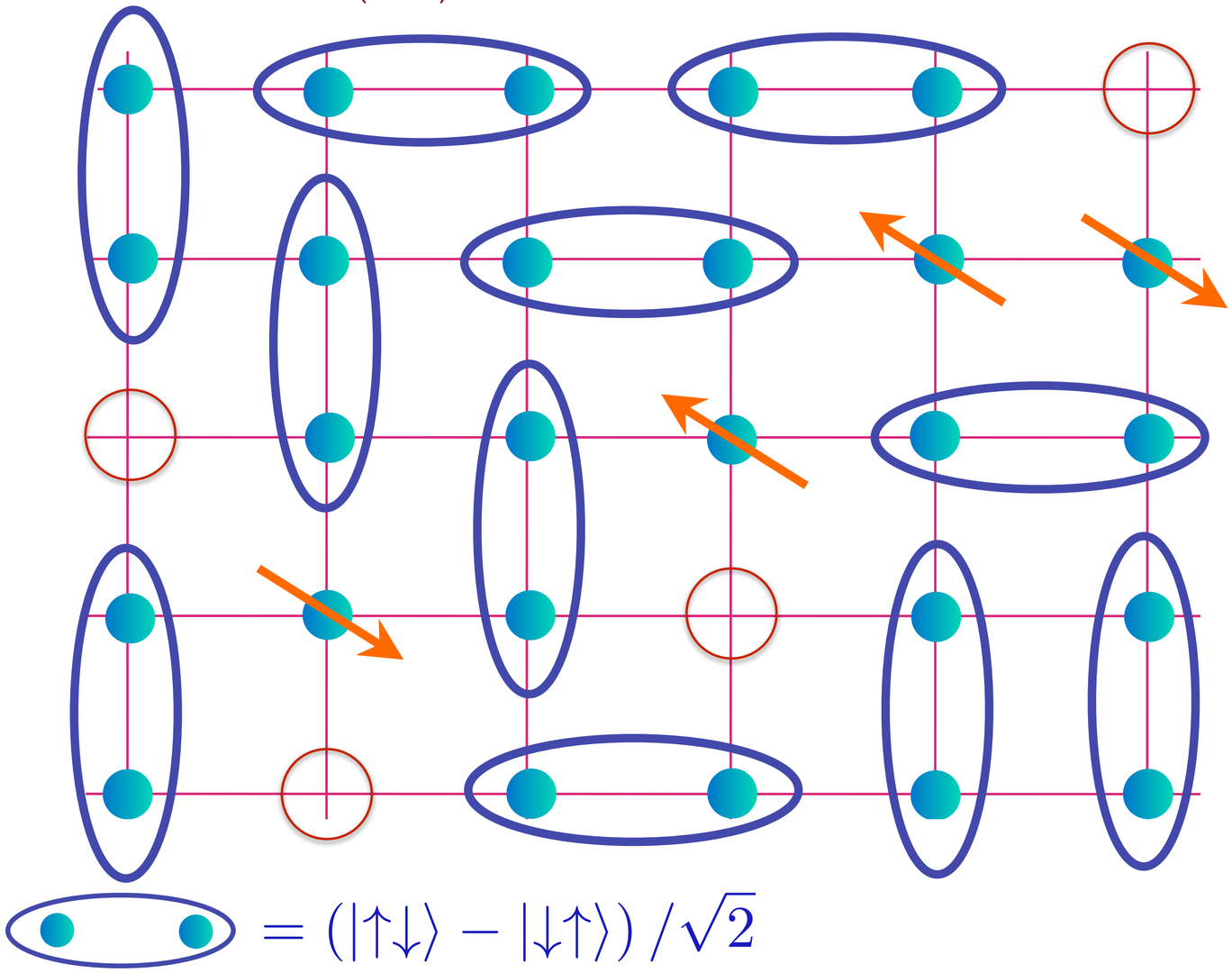

$$= \left(|\uparrow\downarrow\rangle - |\downarrow\uparrow\rangle\right)/\sqrt{2}$$

Spin liquid with density p of spinless, charge +e "holons" and charge 0, spin-1/2 "spinons".

Holon metal

G. Baskaran, Z. Zou, P.W. Anderson, Solid State Comm. **63**, 973 (1987)
S.A. Kivelson, D.S. Rokhsar and J.P. Sethna, PRB **35**, 8865 (1987)
D. Rokhsar and S.A. Kivelson, PRL **61**, 2376 (1988)

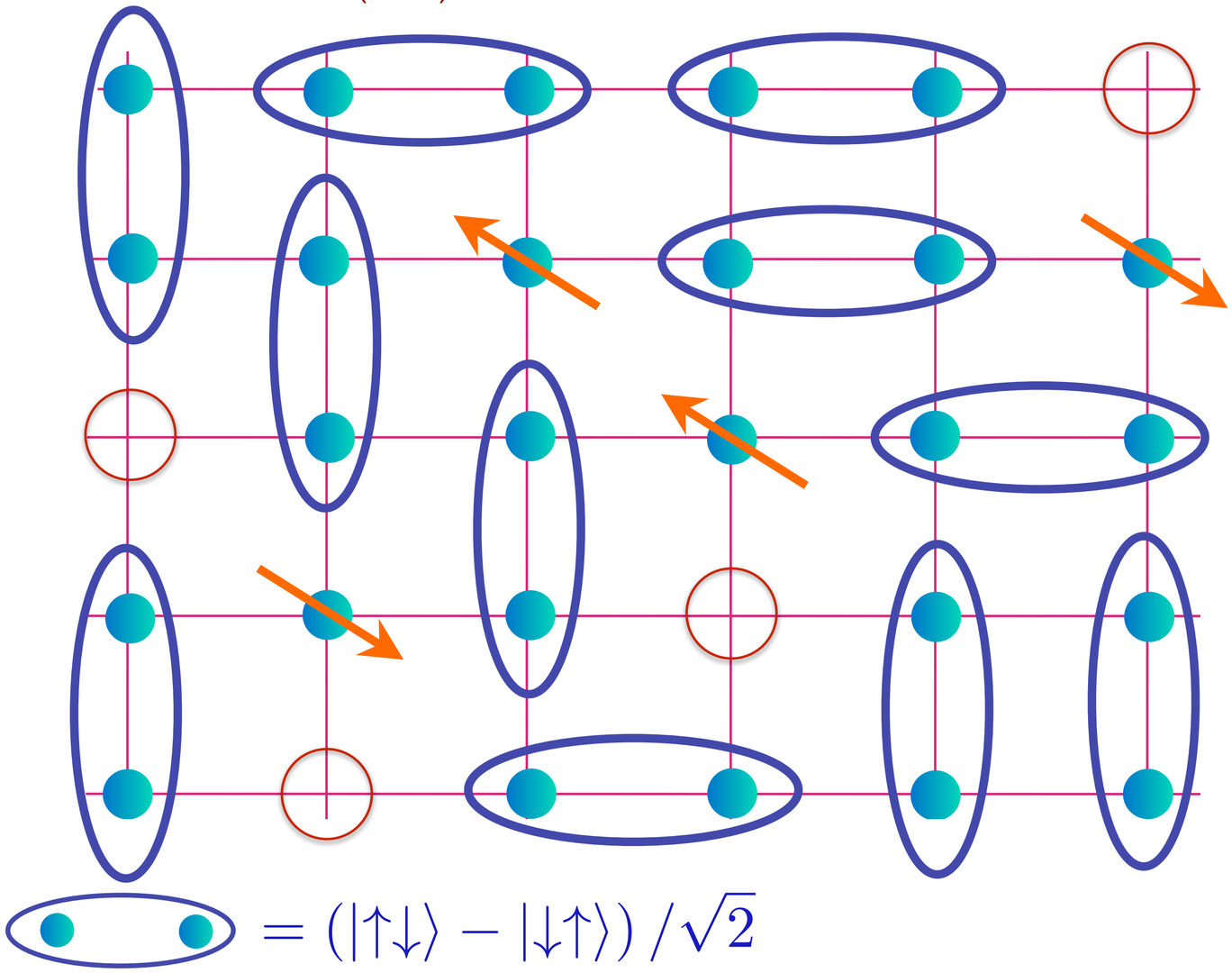

$$= \left(|\uparrow\downarrow\rangle - |\downarrow\uparrow\rangle\right)/\sqrt{2}$$

Spin liquid with density p of spinless, charge +e "holons" and charge 0, spin-1/2 "spinons".

Holon metal

G. Baskaran, Z. Zou, P.W. Anderson, Solid State Comm. **63**, 973 (1987)
S.A. Kivelson, D.S. Rokhsar and J.P. Sethna, PRB **35**, 8865 (1987)
D. Rokhsar and S.A. Kivelson, PRL **61**, 2376 (1988)

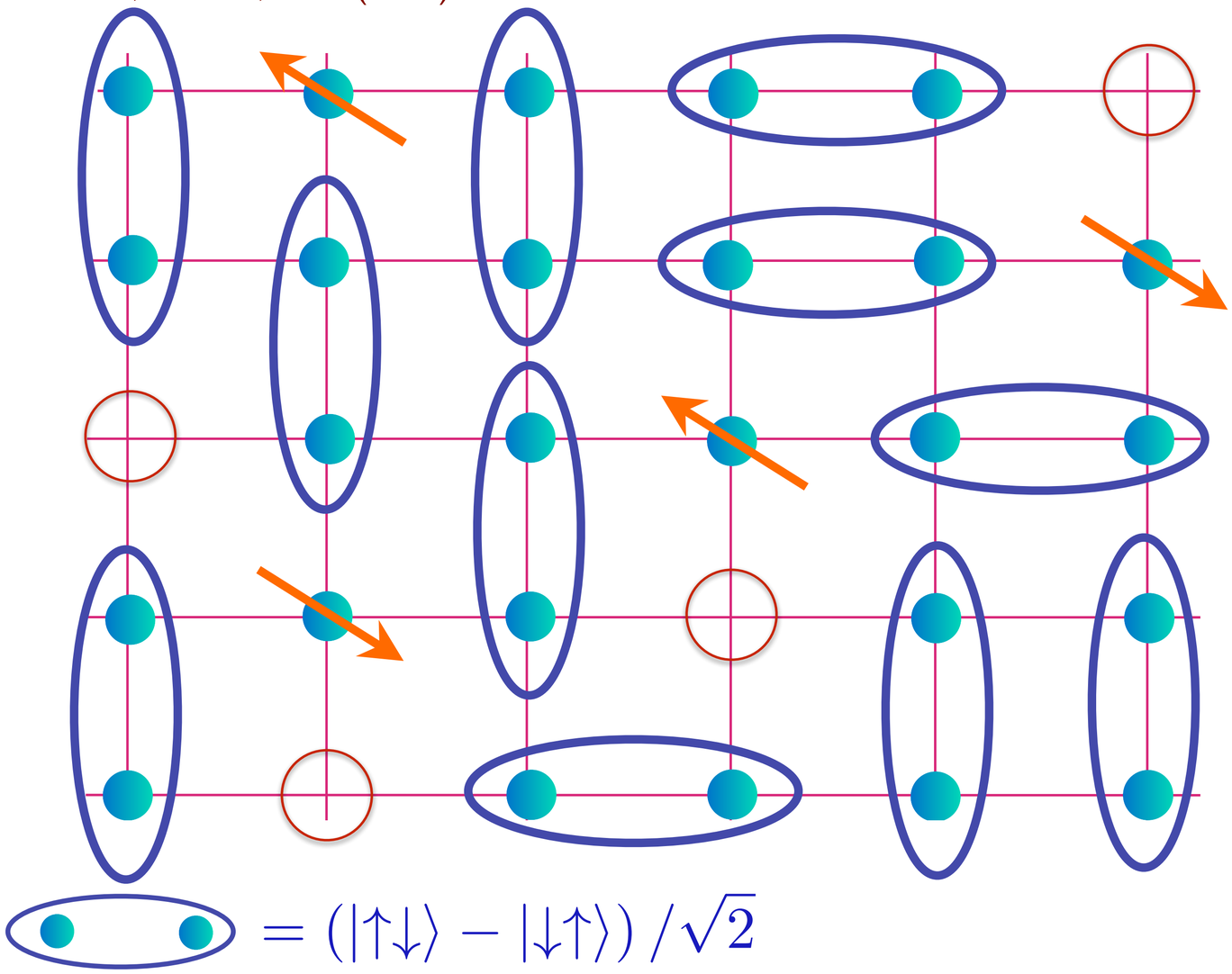

$$= \left(|\uparrow\downarrow\rangle - |\downarrow\uparrow\rangle\right)/\sqrt{2}$$

Spin liquid with density p of spinless, charge +e "holons" and charge 0, spin-1/2 "spinons".

Holon metal

G. Baskaran, Z. Zou, P.W. Anderson, Solid State Comm. **63**, 973 (1987)
S.A. Kivelson, D.S. Rokhsar and J.P. Sethna, PRB **35**, 8865 (1987)
D. Rokhsar and S.A. Kivelson, PRL **61**, 2376 (1988)

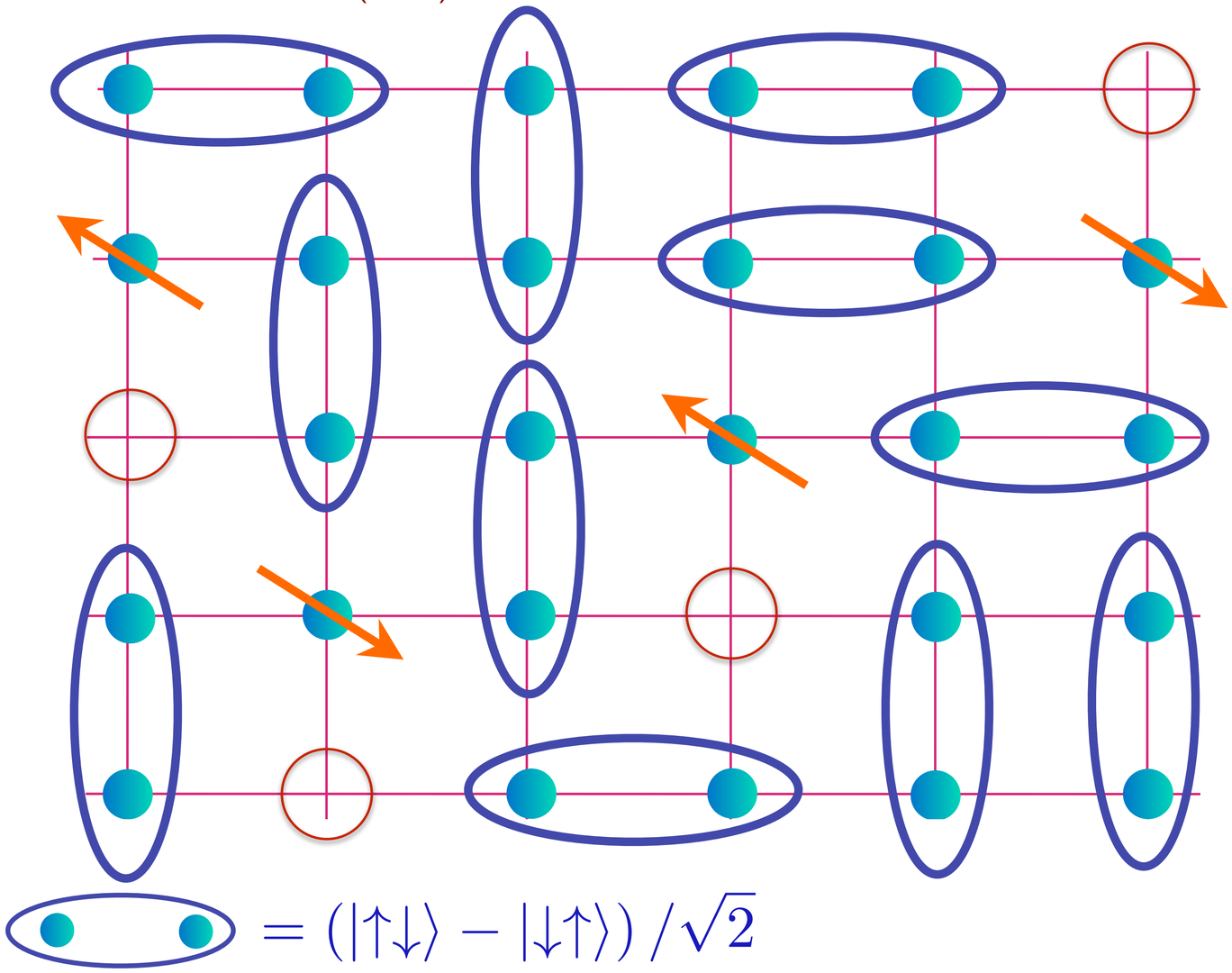

$$= \left(|\uparrow\downarrow\rangle - |\downarrow\uparrow\rangle\right)/\sqrt{2}$$

Spin liquid with density p of spinless, charge +e "holons" and charge 0, spin-1/2 "spinons".

Holon metal

G. Baskaran, Z. Zou, P.W. Anderson, Solid State Comm. **63**, 973 (1987)
S.A. Kivelson, D.S. Rokhsar and J.P. Sethna, PRB **35**, 8865 (1987)
D. Rokhsar and S.A. Kivelson, PRL **61**, 2376 (1988)

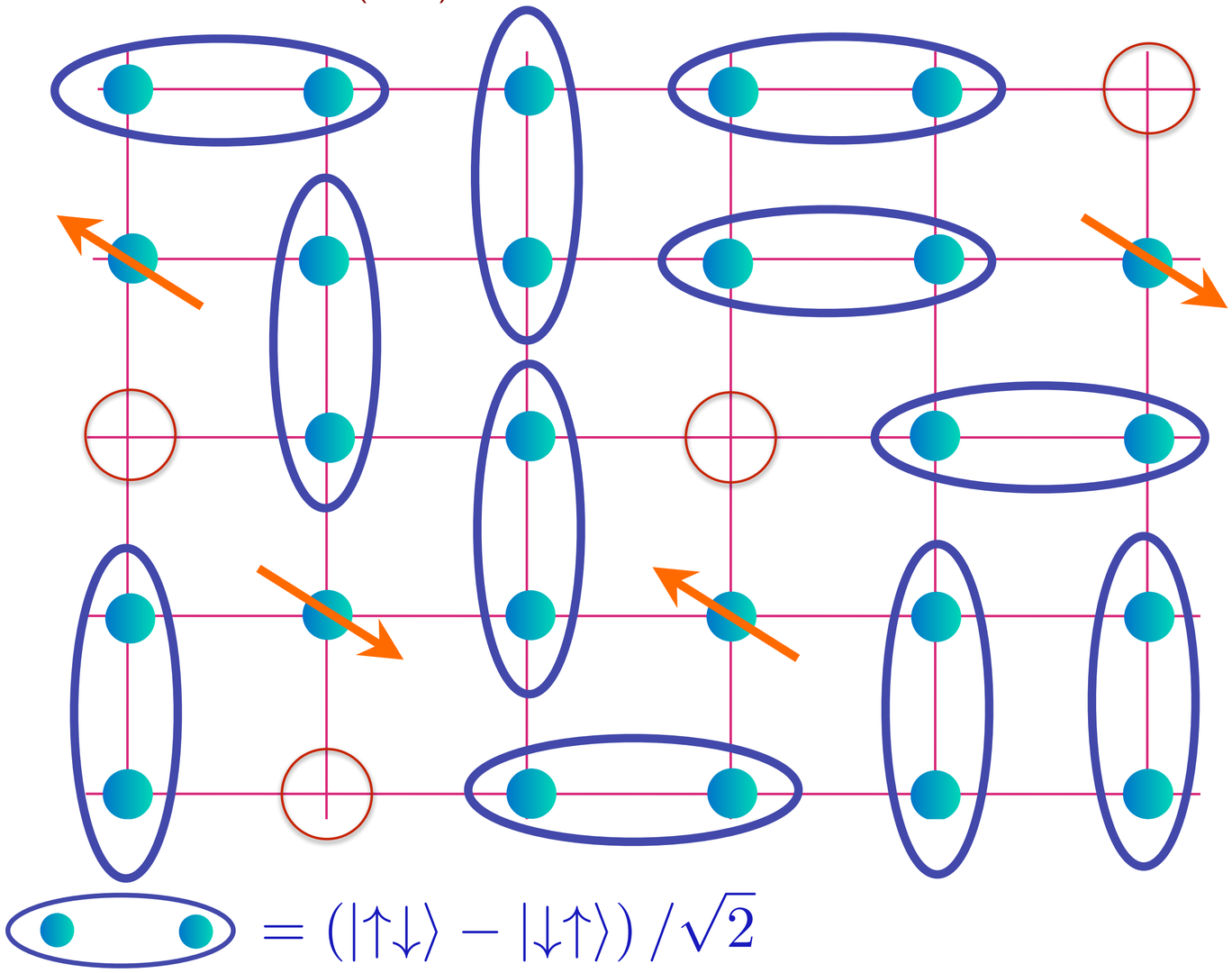

$$= \left(|\uparrow\downarrow\rangle - |\downarrow\uparrow\rangle\right)/\sqrt{2}$$

Spin liquid with density p of spinless, charge +e "holons" and charge 0, spin-1/2 "spinons".

Holon metal

G. Baskaran, Z. Zou, P.W. Anderson, Solid State Comm. **63**, 973 (1987)
S.A. Kivelson, D.S. Rokhsar and J.P. Sethna, PRB **35**, 8865 (1987)
D. Rokhsar and S.A. Kivelson, PRL **61**, 2376 (1988)

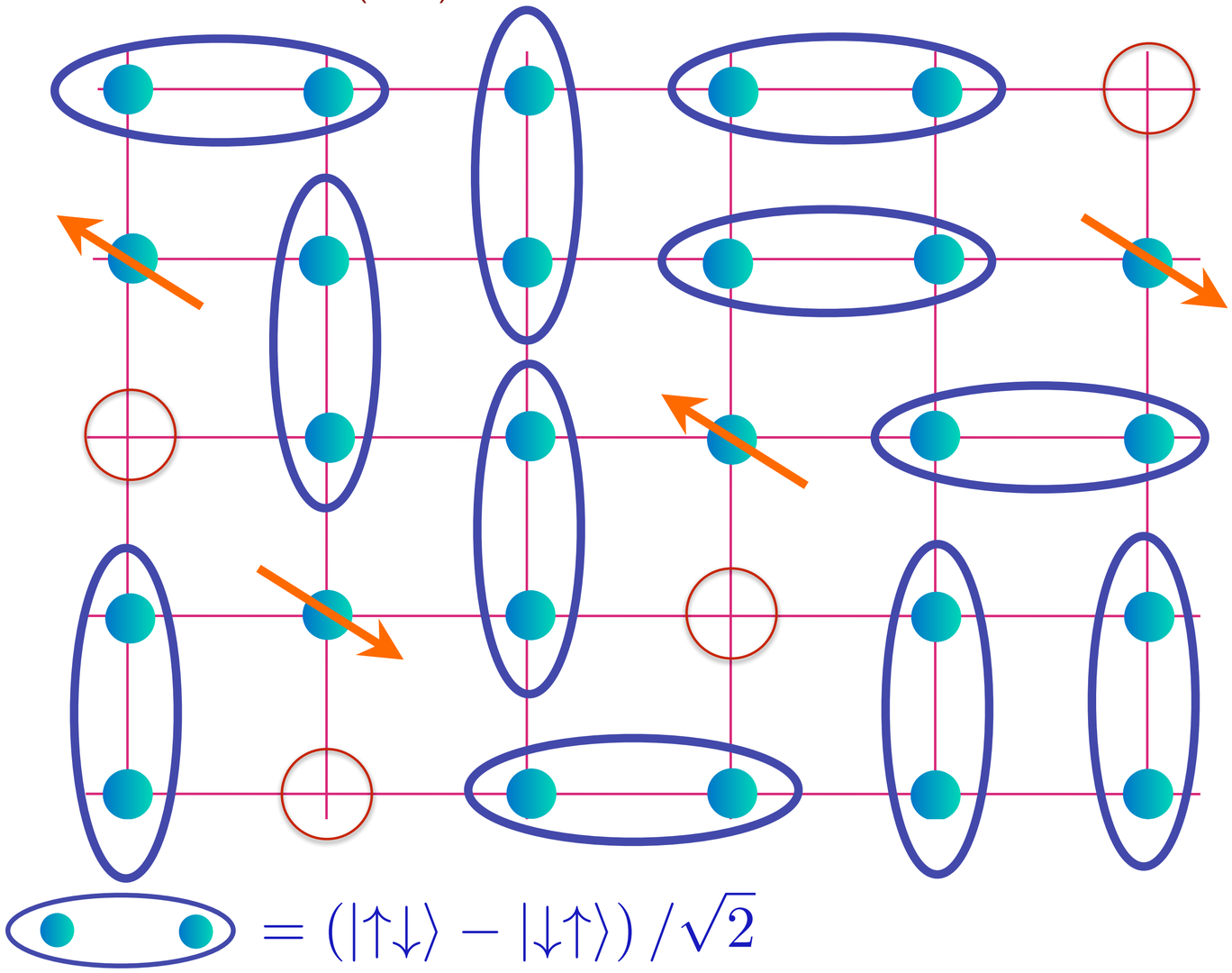

$$= \left(|\uparrow\downarrow\rangle - |\downarrow\uparrow\rangle\right)/\sqrt{2}$$

Spin liquid with density p of spinless, charge +e "holons" and charge 0, spin-1/2 "spinons".

FL* in a ***one-band*** model

S. Sachdev PRB **49**, 6770 (1994); X.-G. Wen and P.A. Lee PRL **76**, 503 (1996)
R. K. Kaul, A. Kolezhuk, M. Levin, S. Sachdev, and T. Senthil, PRB **75**, 235122 (2007)

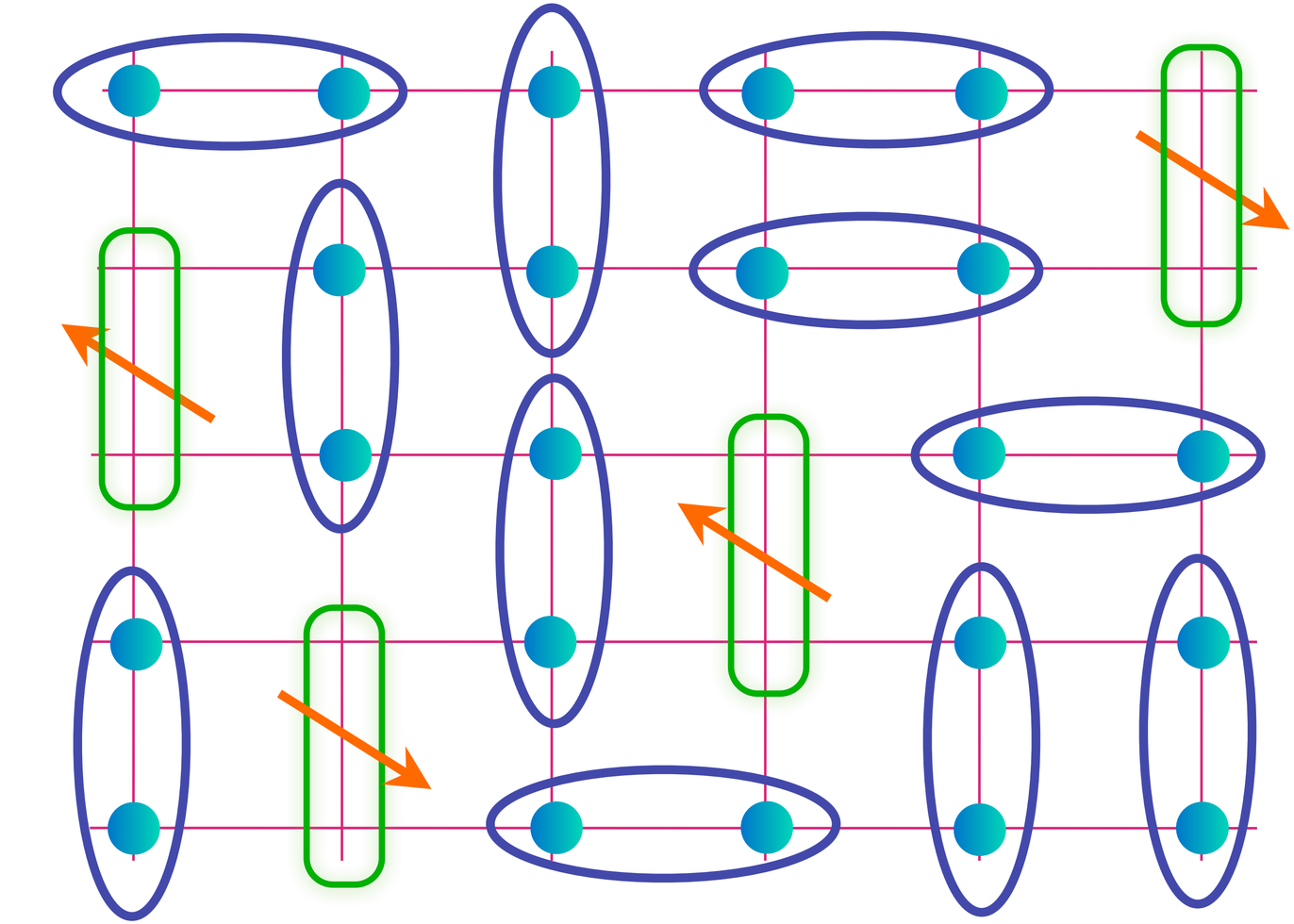

Each green "dimer" is a "bound state" of a vacancy and a free spin

$$= \left(|\uparrow\downarrow\rangle - |\downarrow\uparrow\rangle\right)/\sqrt{2}$$

$$= \left(|\uparrow \circ\rangle + |\circ \uparrow\rangle\right)/\sqrt{2}$$

E. G. Moon and S. Sachdev, PRB **83**, 224508 (2011); M. Punk, A. Allais, and S. Sachdev, PNAS **112**, 9552 (2015)

FL* in a ***one-band*** model

S. Sachdev PRB **49**, 6770 (1994); X.-G. Wen and P.A. Lee PRL **76**, 503 (1996)
R. K. Kaul, A. Kolezhuk, M. Levin, S. Sachdev, and T. Senthil, PRB **75**, 235122 (2007)

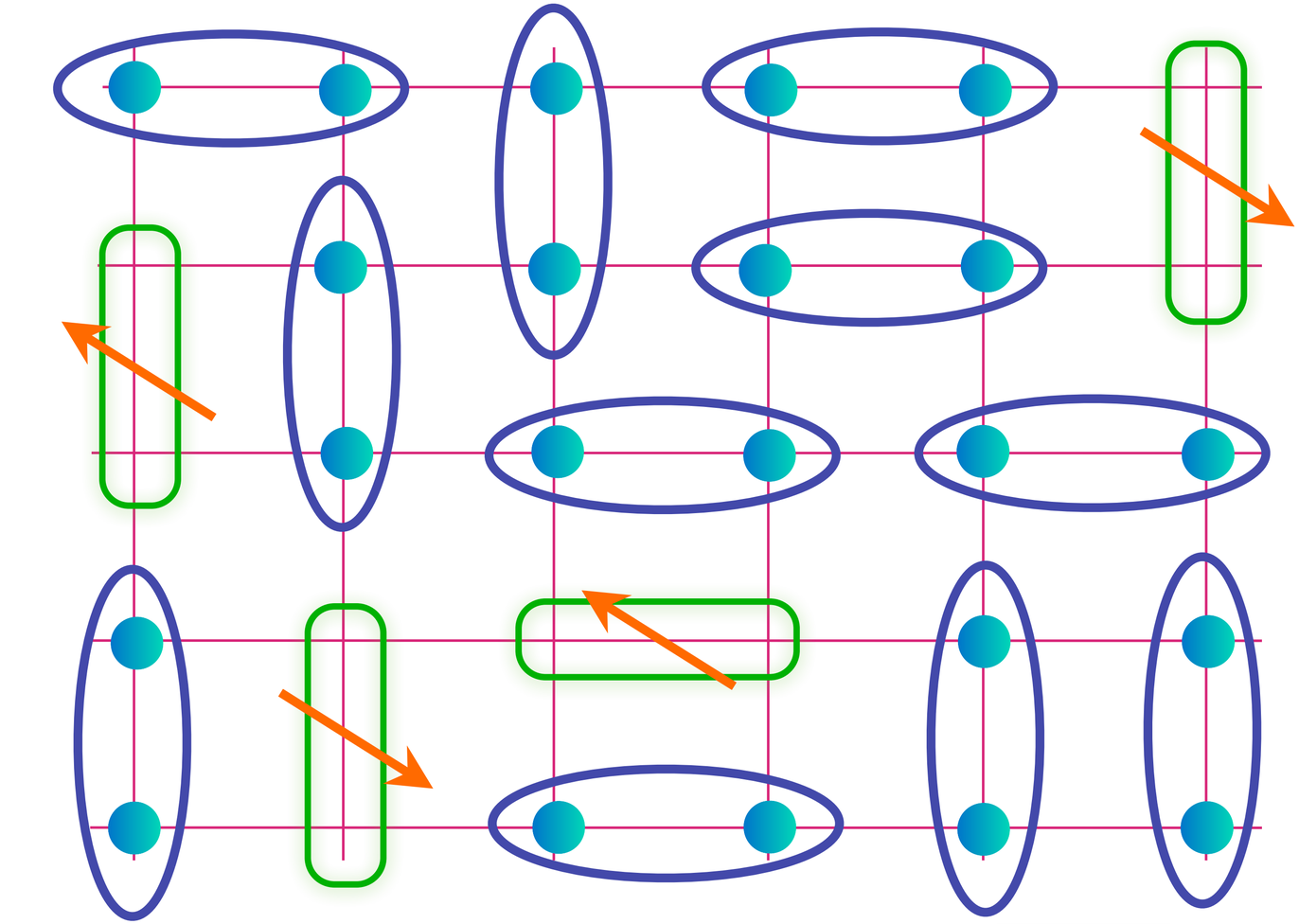

Metal with electron-like quasiparticles on a Fermi surface of size p, and emergent gauge fields

$$= \left(|\uparrow\downarrow\rangle - |\downarrow\uparrow\rangle\right)/\sqrt{2}$$

$$= \left(|\uparrow \circ\rangle + |\circ \uparrow\rangle\right)/\sqrt{2}$$

E. G. Moon and S. Sachdev, PRB **83**, 224508 (2011); M. Punk, A. Allais, and S. Sachdev, PNAS **112**, 9552 (2015)

FL* in a ***one-band*** model

S. Sachdev PRB **49**, 6770 (1994); X.-G. Wen and P.A. Lee PRL **76**, 503 (1996)
R. K. Kaul, A. Kolezhuk, M. Levin, S. Sachdev, and T. Senthil, PRB **75**, 235122 (2007)

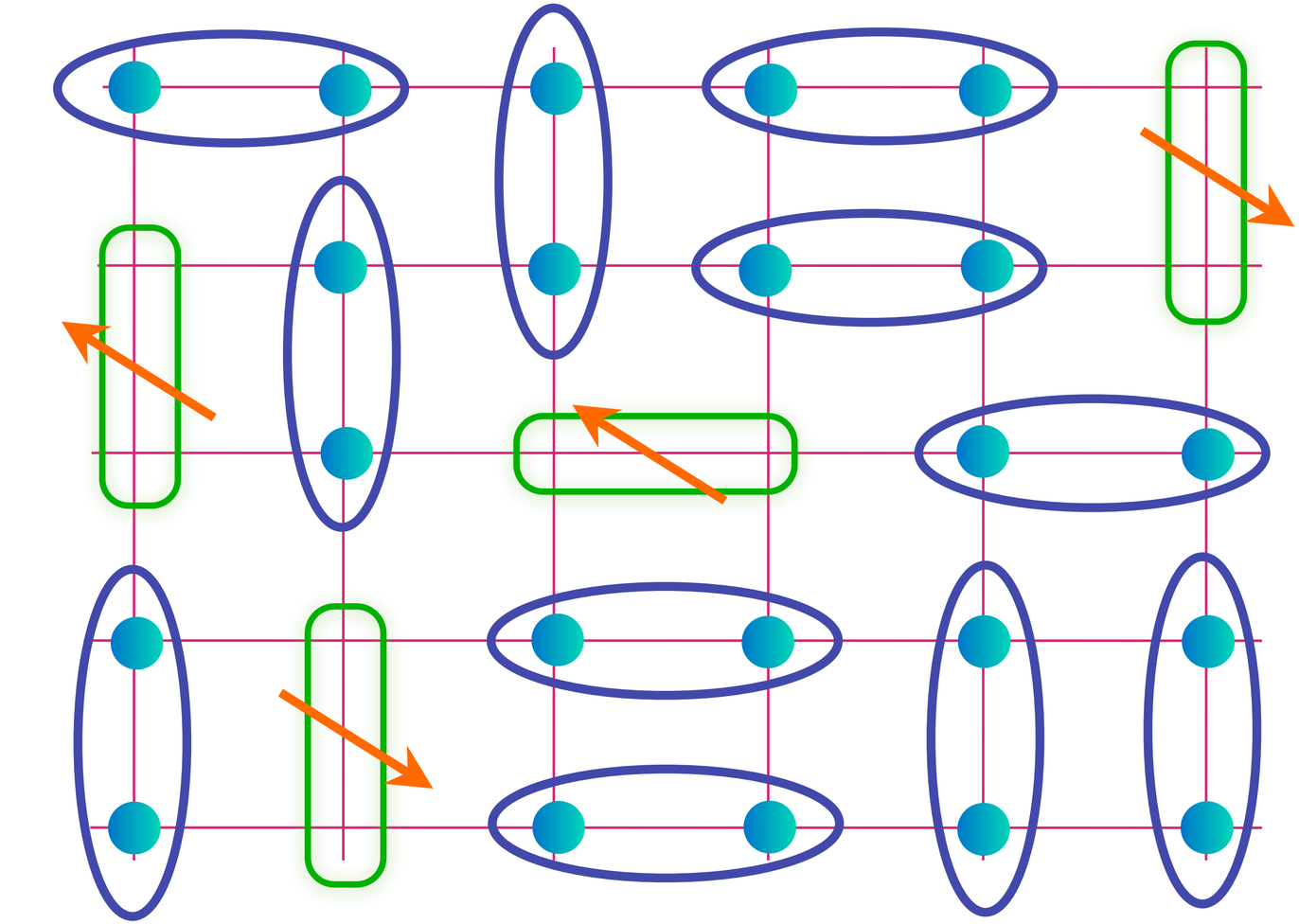

Metal with electron-like quasiparticles on a Fermi surface of size p, and emergent gauge fields

$$= \left(|\uparrow\downarrow\rangle - |\downarrow\uparrow\rangle\right)/\sqrt{2}$$

$$= \left(|\uparrow \circ\rangle + |\circ \uparrow\rangle\right)/\sqrt{2}$$

E. G. Moon and S. Sachdev, PRB **83**, 224508 (2011); M. Punk, A. Allais, and S. Sachdev, PNAS **112**, 9552 (2015)

FL* in a ***one-band*** model

S. Sachdev PRB **49**, 6770 (1994); X.-G. Wen and P.A. Lee PRL **76**, 503 (1996)
R. K. Kaul, A. Kolezhuk, M. Levin, S. Sachdev, and T. Senthil, PRB **75**, 235122 (2007)

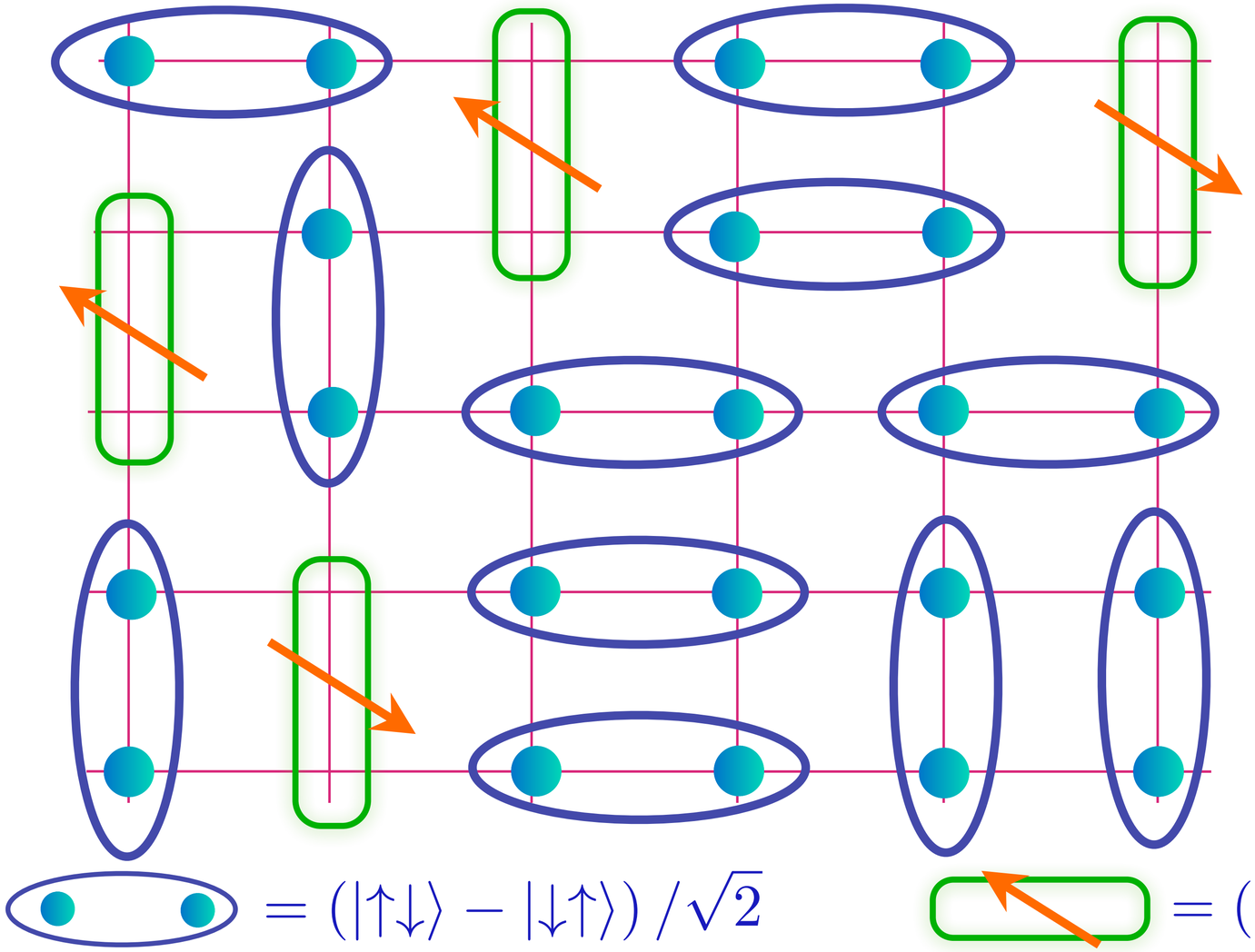

$= \left(|\uparrow\downarrow\rangle - |\downarrow\uparrow\rangle\right)/\sqrt{2}$

$= \left(|\uparrow \circ\rangle + |\circ \uparrow\rangle\right)/\sqrt{2}$

Metal with electron-like quasiparticles on a Fermi surface of size p, and emergent gauge fields

E. G. Moon and S. Sachdev, PRB **83**, 224508 (2011); M. Punk, A. Allais, and S. Sachdev, PNAS **112**, 9552 (2015)

FL* in a ***one-band*** model

S. Sachdev PRB **49**, 6770 (1994); X.-G. Wen and P.A. Lee PRL **76**, 503 (1996)
R. K. Kaul, A. Kolezhuk, M. Levin, S. Sachdev, and T. Senthil, PRB **75**, 235122 (2007)

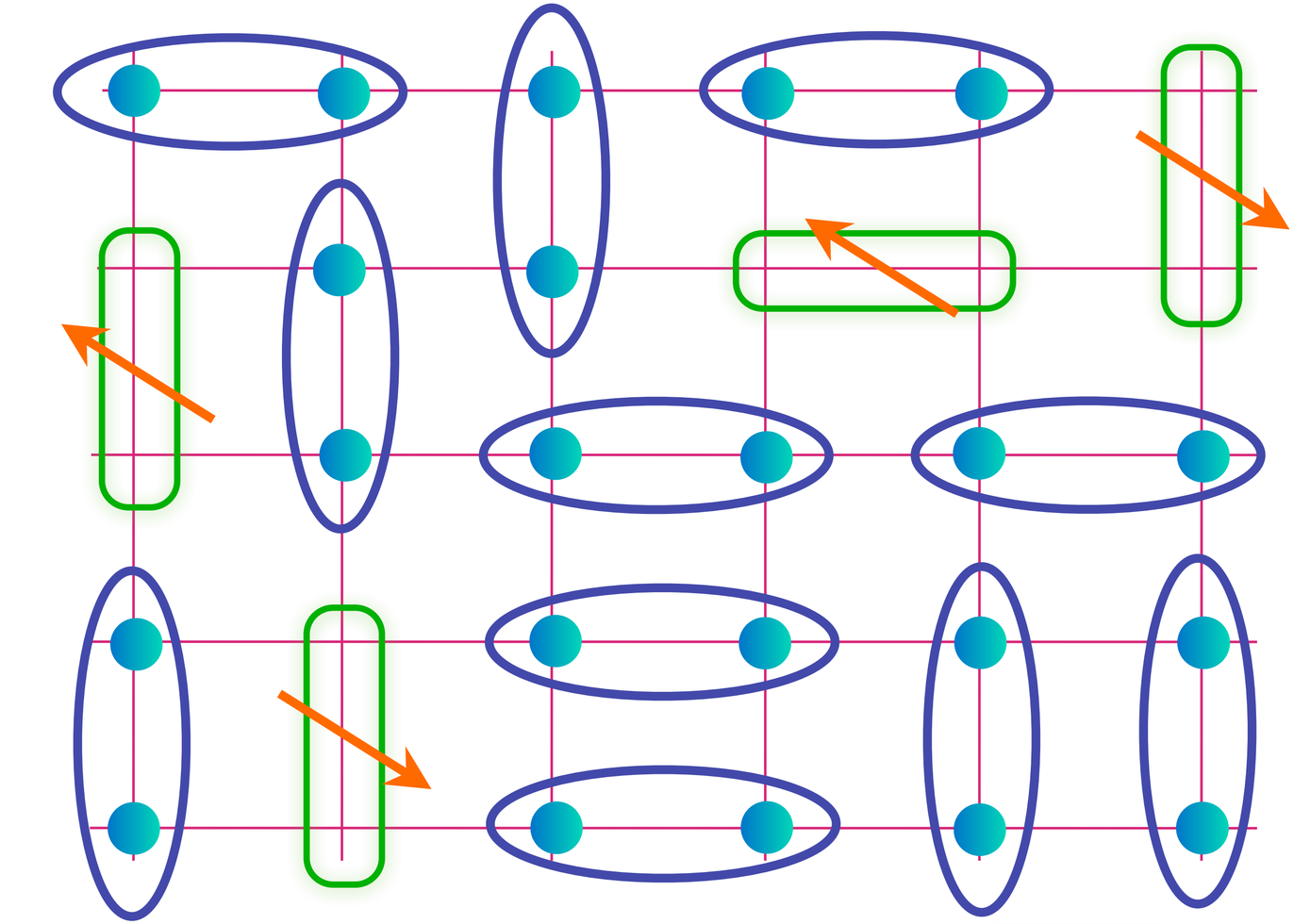

Metal with electron-like quasiparticles on a Fermi surface of size p, and emergent gauge fields

$$= \left(|\uparrow\downarrow\rangle - |\downarrow\uparrow\rangle\right)/\sqrt{2}$$

$$= \left(|\uparrow \circ\rangle + |\circ \uparrow\rangle\right)/\sqrt{2}$$

E. G. Moon and S. Sachdev, PRB **83**, 224508 (2011); M. Punk, A. Allais, and S. Sachdev, PNAS **112**, 9552 (2015)

FL* in a ***one-band*** model

S. Sachdev PRB **49**, 6770 (1994); X.-G. Wen and P.A. Lee PRL **76**, 503 (1996)
R. K. Kaul, A. Kolezhuk, M. Levin, S. Sachdev, and T. Senthil, PRB **75**, 235122 (2007)

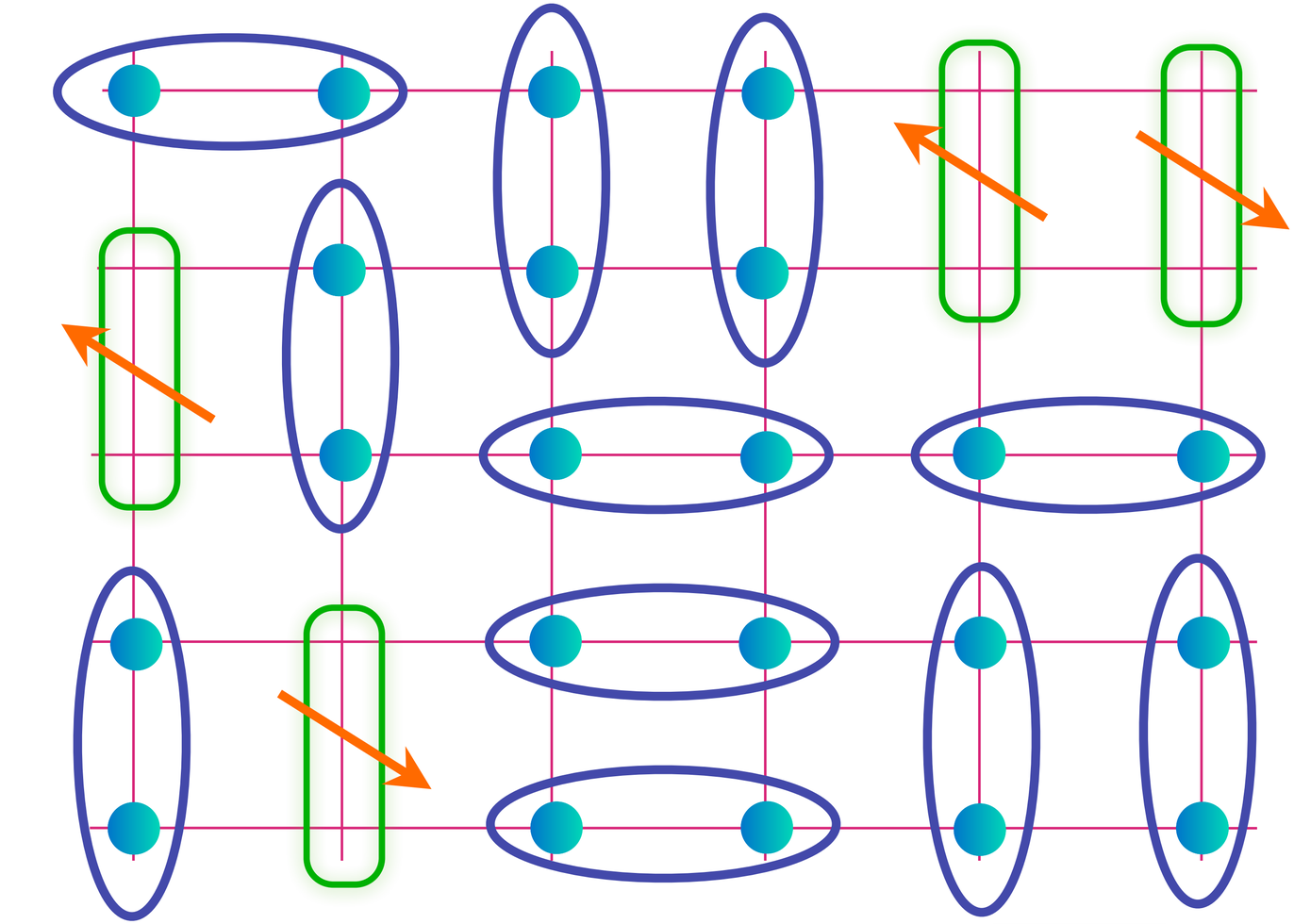

Metal with electron-like quasiparticles on a Fermi surface of size p, and emergent gauge fields

$$= \left(|\uparrow\downarrow\rangle - |\downarrow\uparrow\rangle\right)/\sqrt{2}$$

$$= \left(|\uparrow \circ\rangle + |\circ \uparrow\rangle\right)/\sqrt{2}$$

E. G. Moon and S. Sachdev, PRB **83**, 224508 (2011); M. Punk, A. Allais, and S. Sachdev, PNAS **112**, 9552 (2015)

FL* in a ***one-band*** model

S. Sachdev PRB **49**, 6770 (1994); X.-G. Wen and P.A. Lee PRL **76**, 503 (1996)
R. K. Kaul, A. Kolezhuk, M. Levin, S. Sachdev, and T. Senthil, PRB **75**, 235122 (2007)

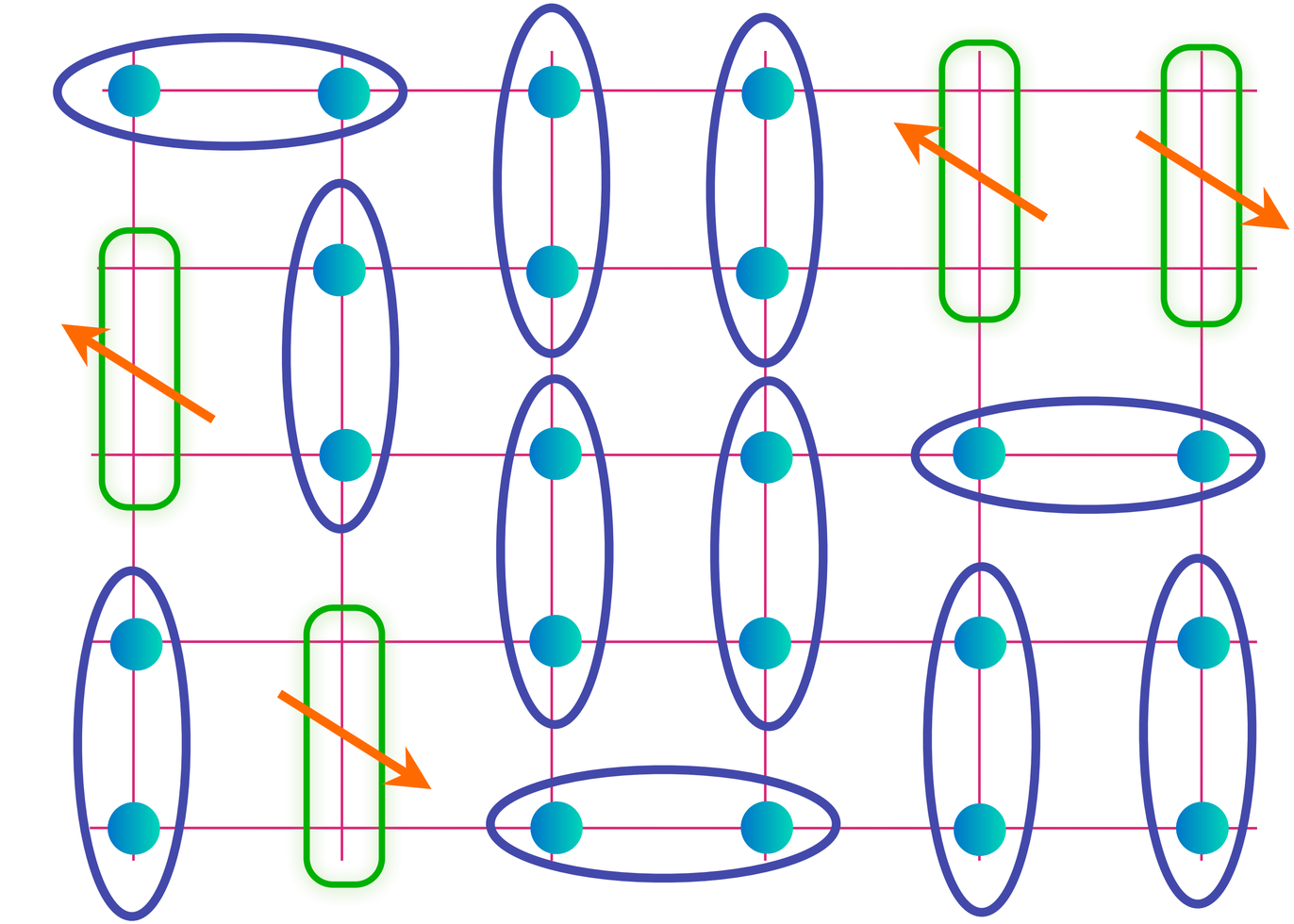

Metal with electron-like quasiparticles on a Fermi surface of size p, and emergent gauge fields

$$= \left(|\uparrow\downarrow\rangle - |\downarrow\uparrow\rangle\right)/\sqrt{2}$$

$$= \left(|\uparrow \circ\rangle + |\circ \uparrow\rangle\right)/\sqrt{2}$$

E. G. Moon and S. Sachdev, PRB **83**, 224508 (2011); M. Punk, A. Allais, and S. Sachdev, PNAS **112**, 9552 (2015)

FL* in a ***one-band*** model

S. Sachdev PRB **49**, 6770 (1994); X.-G. Wen and P.A. Lee PRL **76**, 503 (1996)
R. K. Kaul, A. Kolezhuk, M. Levin, S. Sachdev, and T. Senthil, PRB **75**, 235122 (2007)

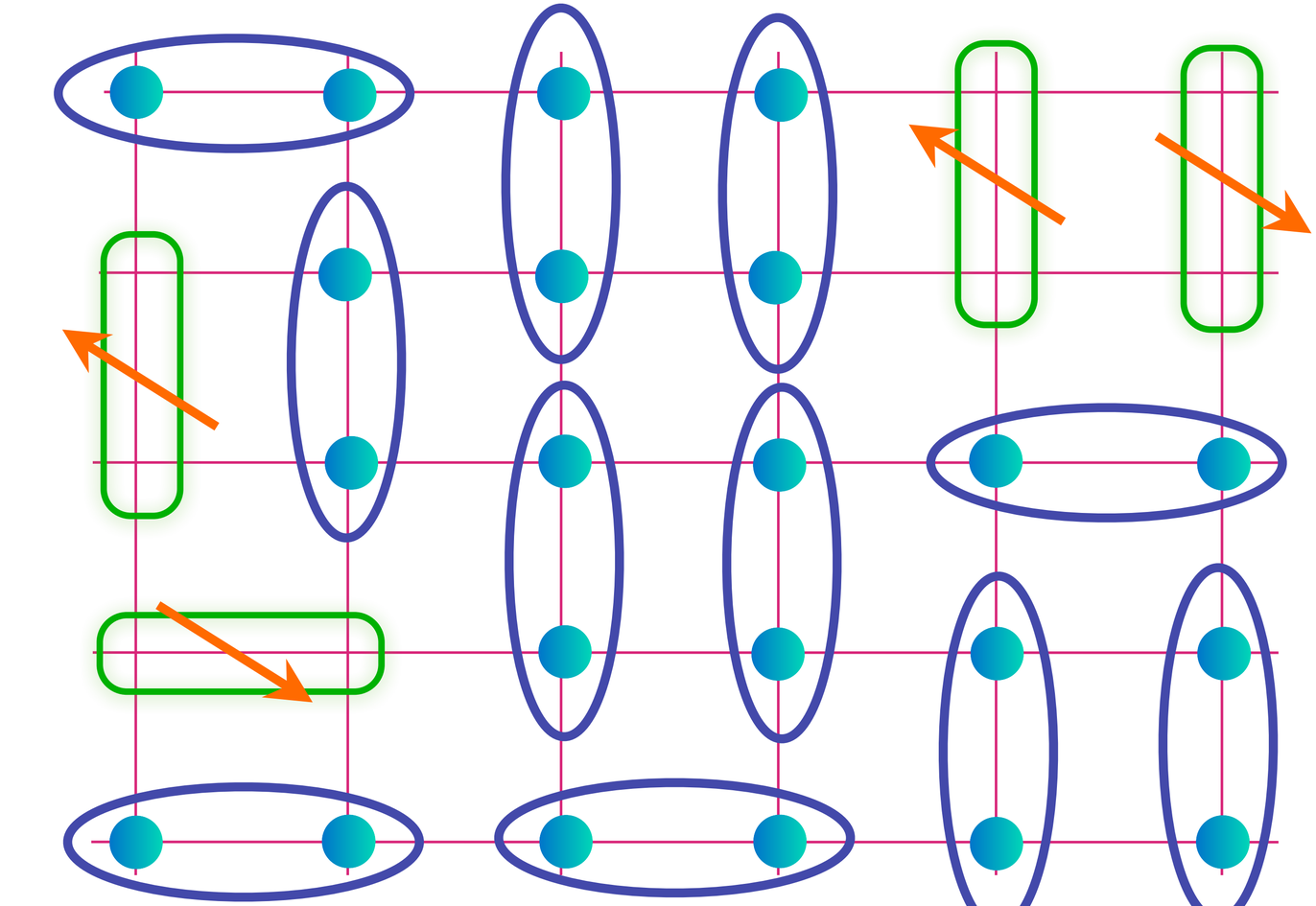

Metal with electron-like quasiparticles on a Fermi surface of size p, and emergent gauge fields

$$= \left(|\uparrow\downarrow\rangle - |\downarrow\uparrow\rangle\right)/\sqrt{2}$$

$$= \left(|\uparrow \circ\rangle + |\circ \uparrow\rangle\right)/\sqrt{2}$$

E. G. Moon and S. Sachdev, PRB **83**, 224508 (2011); M. Punk, A. Allais, and S. Sachdev, PNAS **112**, 9552 (2015)

Ancilla theory of the Hubbard model

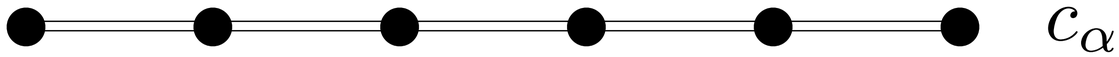

Hubbard model of hole density 1+p

Ancilla theory of the Hubbard model

Free holes of density 1+p

Hubbard model of hole density 1+p

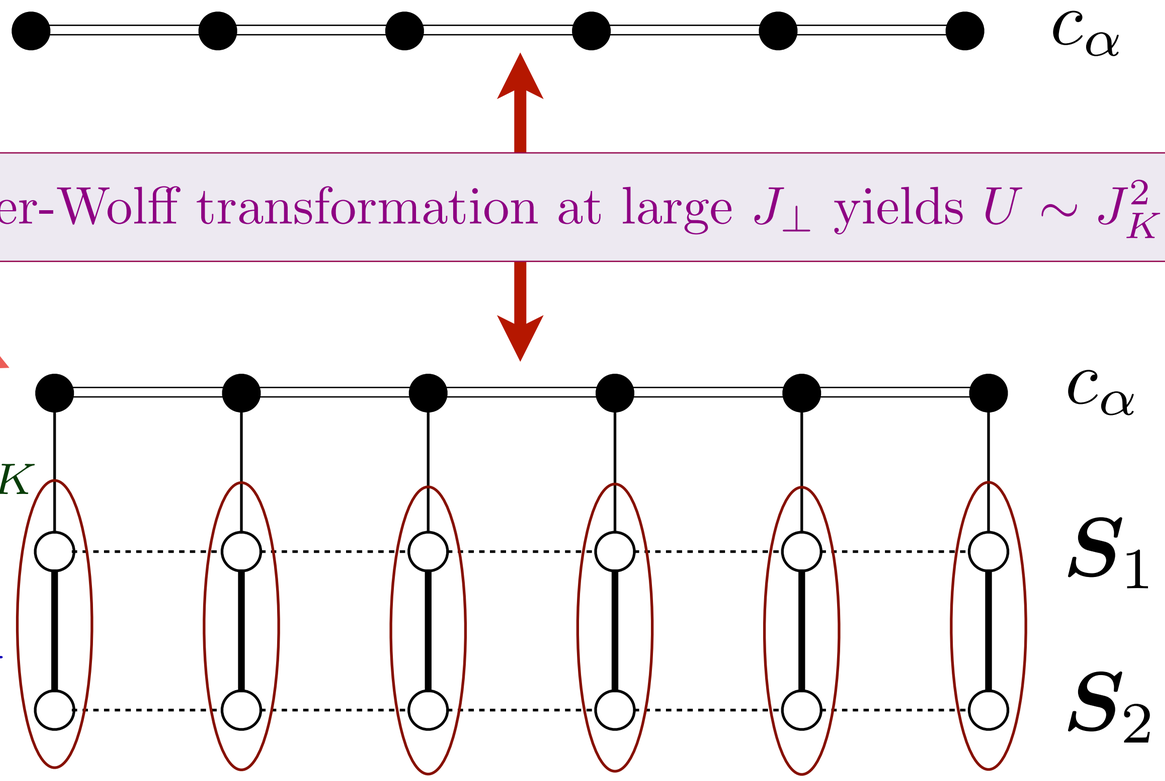

Ancilla qubits

Ya-Hui Zhang and S. S., PRR **2**, 023172 (2020)

A. Nikolaenko, M. Tikhanovskaya, S. S., and Ya-Hui Zhang, PRB **103**, 235138 (2021)

$$\mathcal{H}_{\text{ancilla}} = \sum_{\mathbf{p}} \varepsilon_{\mathbf{p}} c^\dagger_{\mathbf{p}\alpha} c_{\mathbf{p}\alpha} + J_K \sum_i c^\dagger_{i\alpha} \frac{\boldsymbol{\sigma}_{\alpha\alpha'}}{2} c_{i\alpha'} \cdot \boldsymbol{S}_{1i} + J_\perp \sum_i \boldsymbol{S}_{1i} \cdot \boldsymbol{S}_{2i}$$

Ancilla theory of the Hubbard model

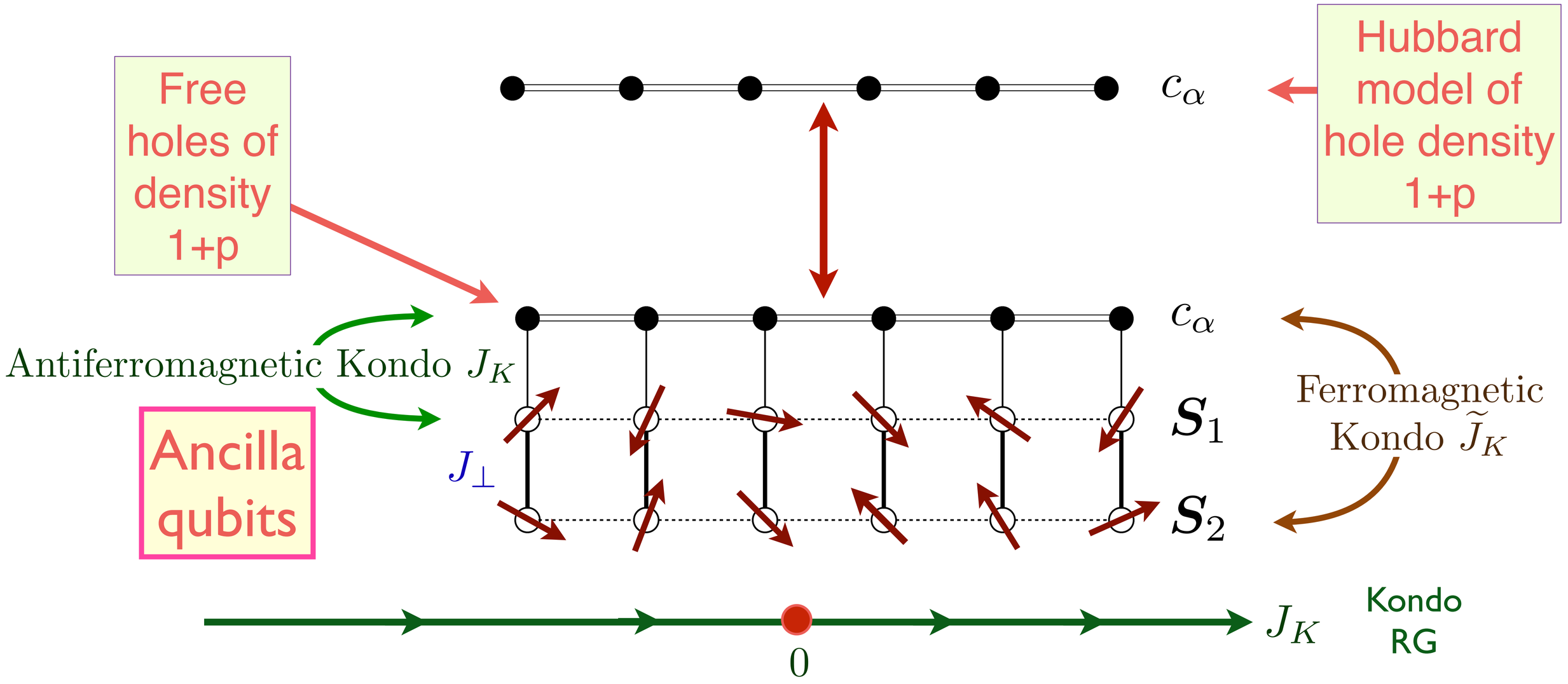

$$\mathcal{H}_{\text{ancilla}} = \sum_{\mathbf{p}} \varepsilon_{\mathbf{p}} c^\dagger_{\mathbf{p}\alpha} c_{\mathbf{p}\alpha} + J_K \sum_i c^\dagger_{i\alpha} \frac{\boldsymbol{\sigma}_{\alpha\alpha'}}{2} c_{i\alpha'} \cdot \boldsymbol{S}_{1i} + J_\perp \sum_i \boldsymbol{S}_{1i} \cdot \boldsymbol{S}_{2i}$$

Ancilla theory of the Hubbard model

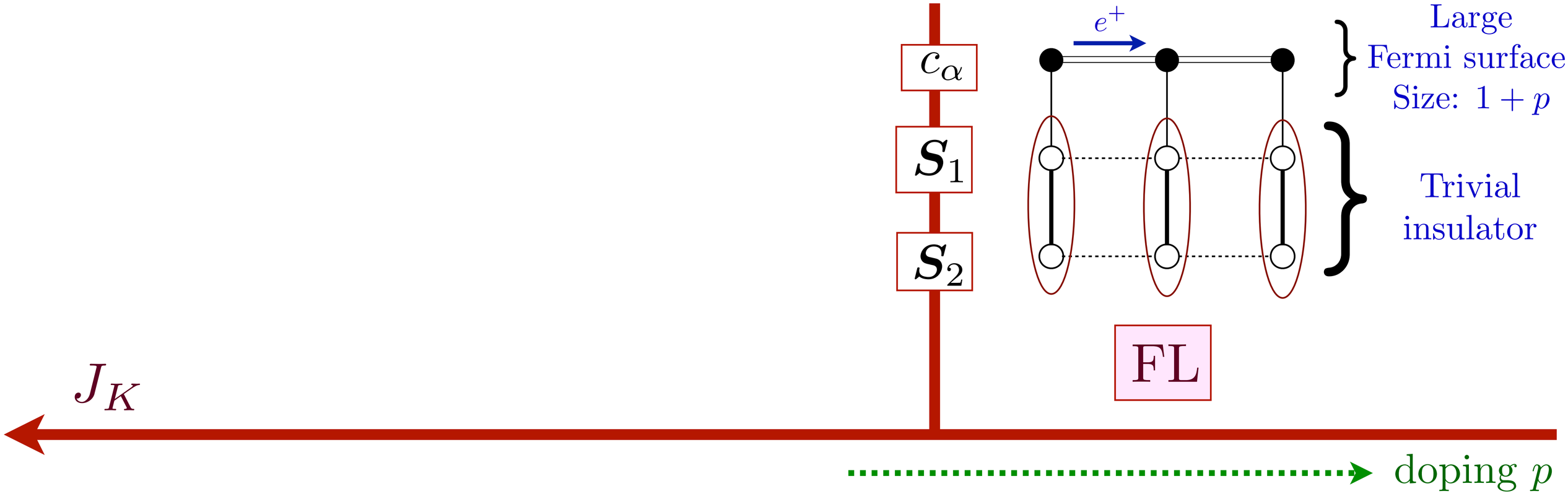

Ancilla theory of the Hubbard model

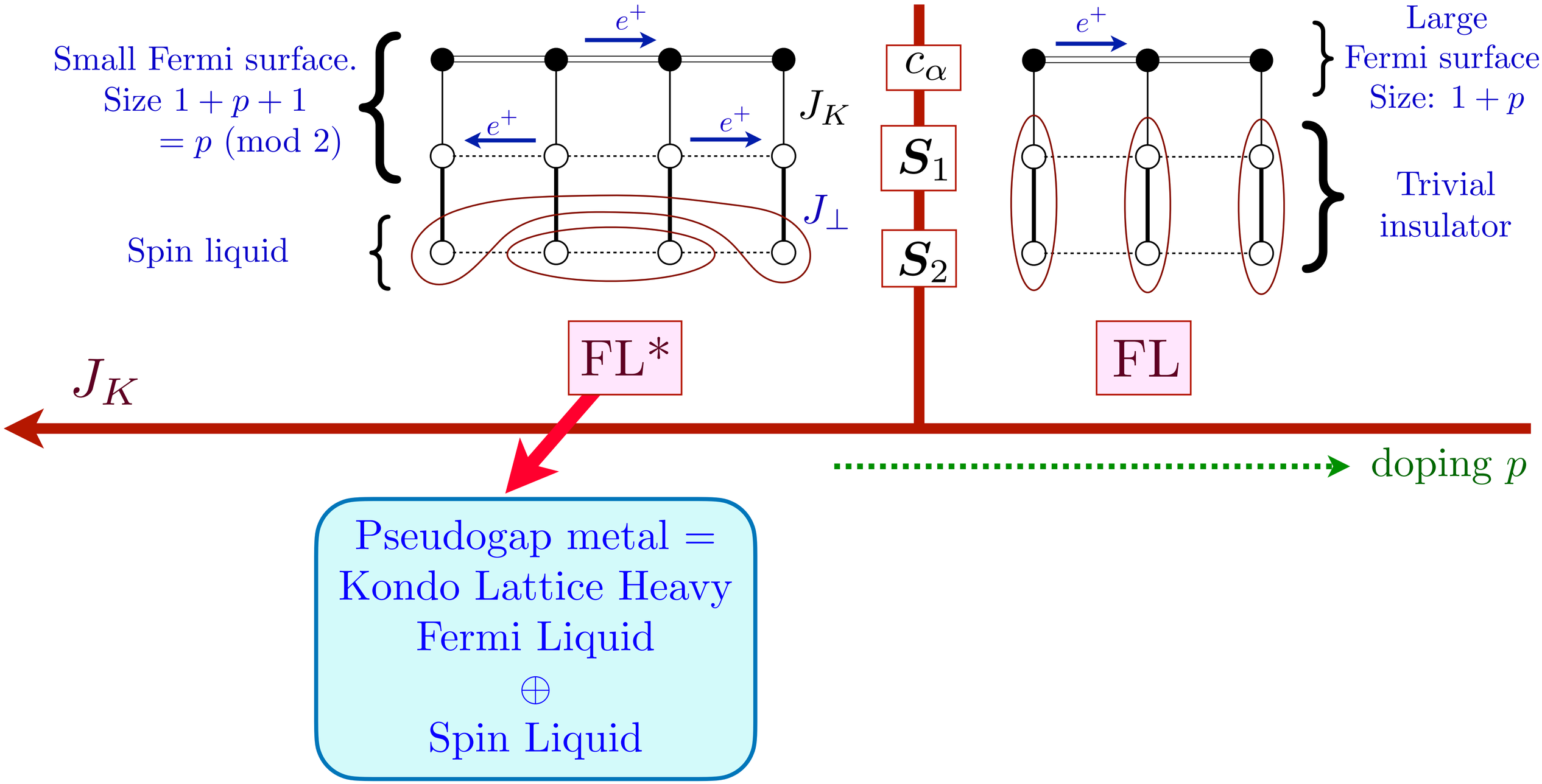

Photoemission at small p

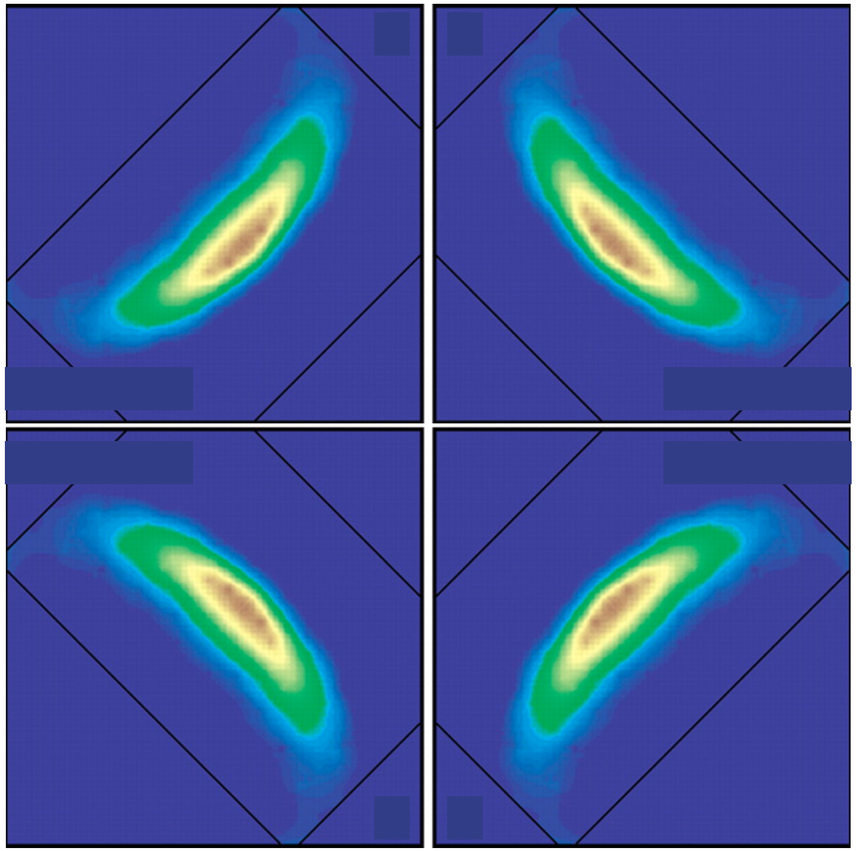

$Ca_{2-x}Na_xCuO_2Cl_2$
at $x = 0.10$

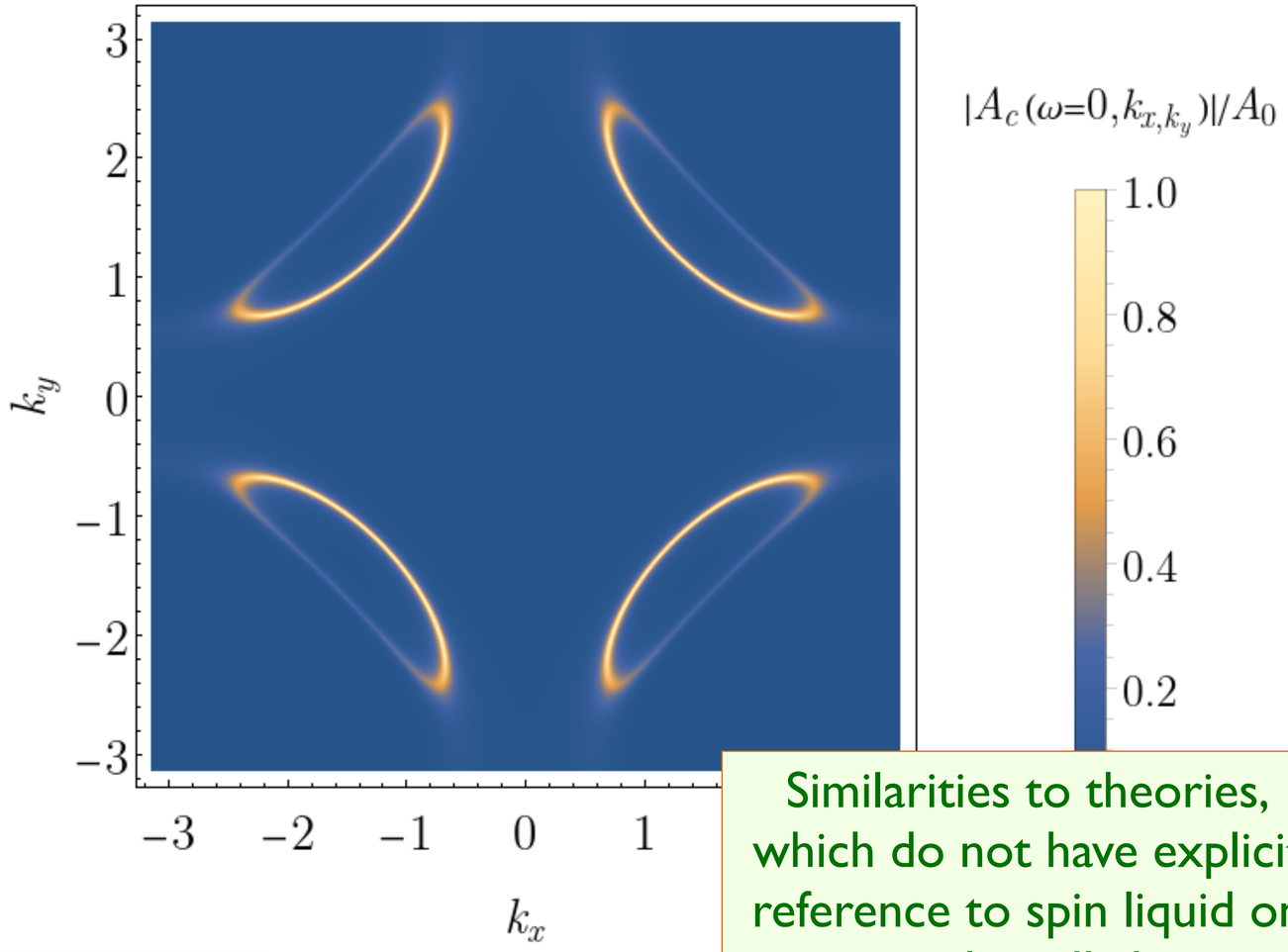

"Fermi arcs"

Similarities to theories, which do not have explicit reference to spin liquid on second ancilla layer

Kai-Yu Yang, T. M. Rice, Fu-Chun Zhang, PRB **73**, 174501 (2006)
S. Sakai, Y. Motome, M. Imada, PRL **102**, 056404 (2009)

Kyle M. Shen, F. Ronning, D. H. Lu, F. Baumberger, N. J. C. Ingle, W. S. Lee, W. Meevasana, Y. Kohsaka, M. Azuma, M. Takano, H. Takagi, Z.-X. Shen, Science **307**, 901 (2005)

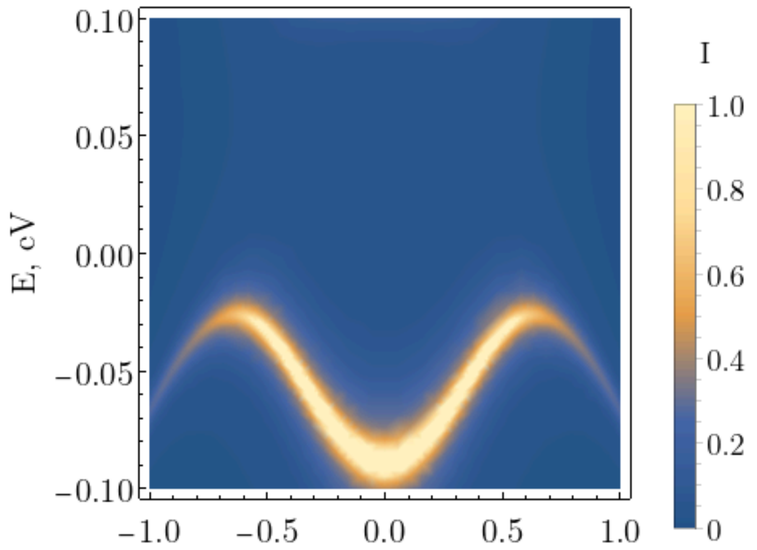

Anti-node

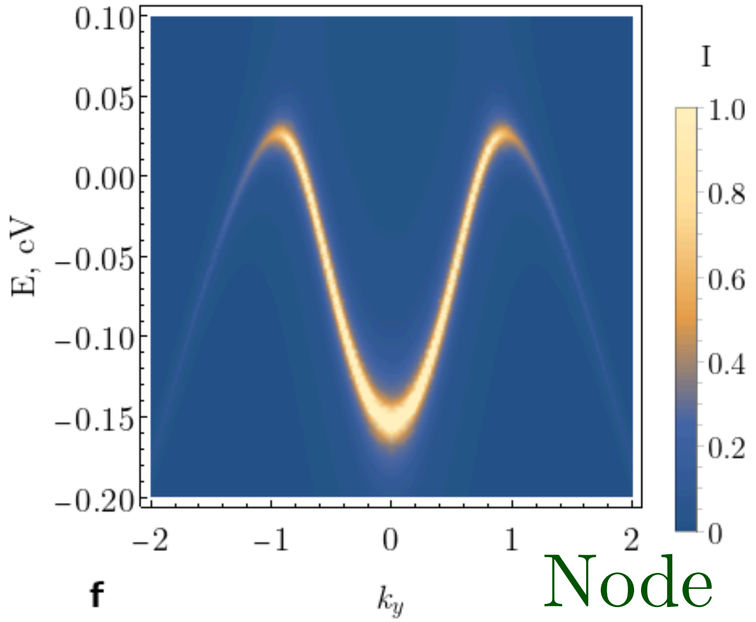

f

Node

FL* in a ***one-band*** model

Second ancilla layer is needed to describe MDC and EDC

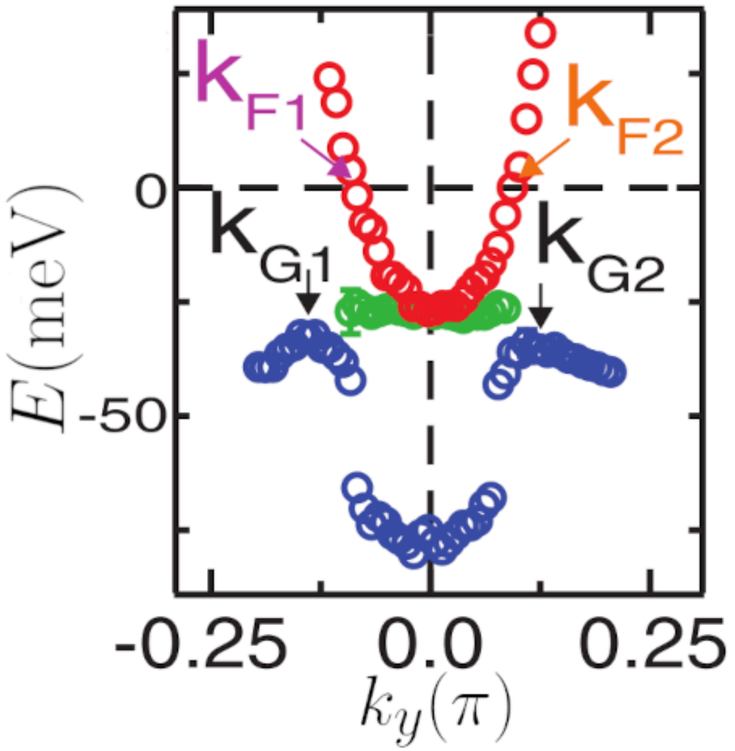

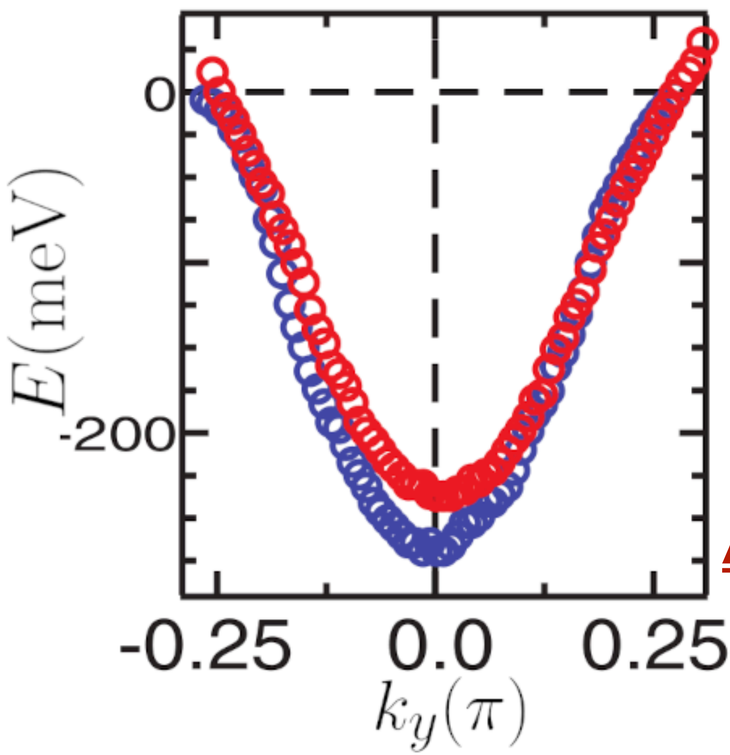

R.-H. He, M. Hashimoto, H. Karapetyan, J. D. Koralek, J. P. Hinton, J. P. Testaud, V. Nathan, Y. Yoshida, H. Yao, K. Tanaka, W. Meevasana, R. G. Moore, D. H. Lu, S. K. Mo, M. Ishikado, H. Eisaki, Z. Hussain, T. P. Devereaux, S. A. Kivelson, J. Orenstein, A. Kapitulnik, and Z.-X. Shen, *Science* **331**, 1579 (2011)

ARPES on Bi2201

Similarities to theories, which do not have explicit reference to spin liquid on second ancilla layer

Kai-Yu Yang, T. M. Rice, Fu-Chun Zhang, PRB **73**, 174501 (2006)
S. Sakai, Y. Motome, M. Imada, PRL **102**, 056404 (2009)

B Keimer *et al. Nature* **518**, 179-186 (2015)

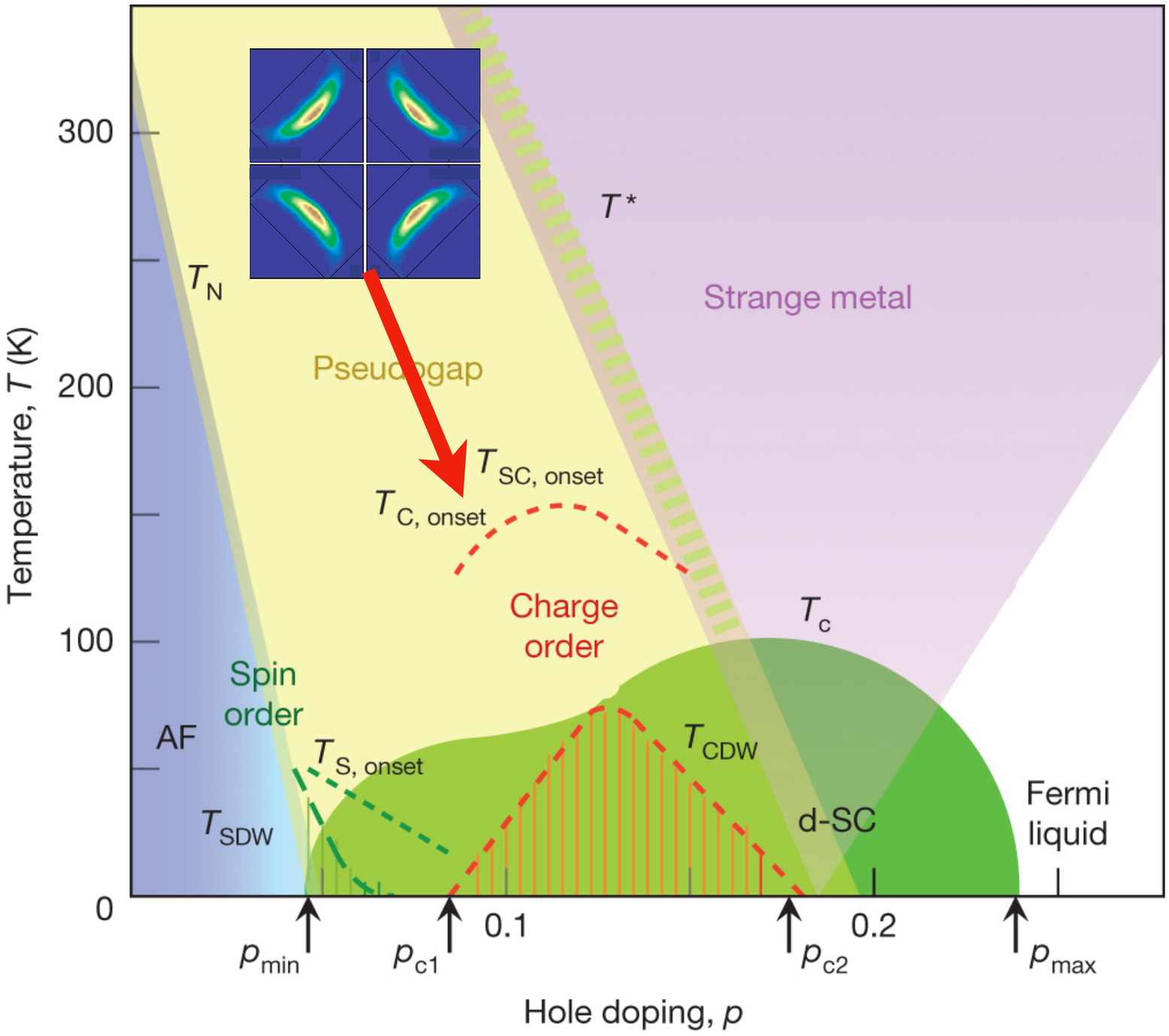

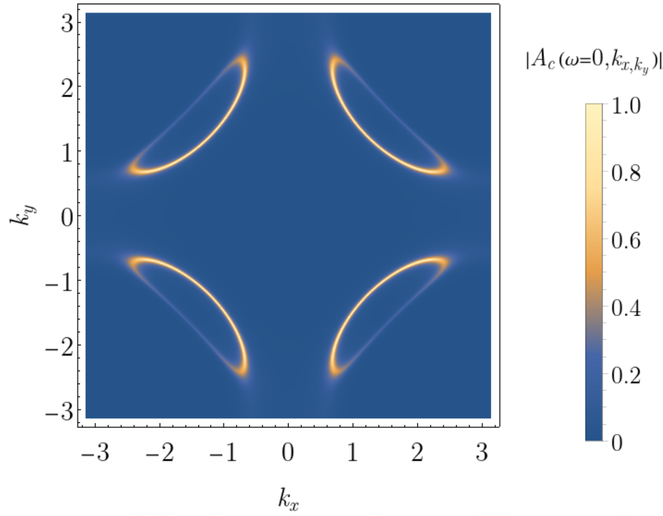

Ya-Hui Zhang and S. Sachdev, PRR **2**, 023172 (2020)

E. Mascot, A. Nikolaenko, M. Tikhanovskaya, Ya-Hui Zhang, D. K. Morr, and S. Sachdev, PRB **105**, 075146 (2022)

Hole pocket Fermi surfaces
of size p with
charge e, spin-1/2 quasiparticles
+
'spectator'
square lattice spin liquid
at half-filling.

B Keimer *et al. Nature* **518**, 179-186 (2015)

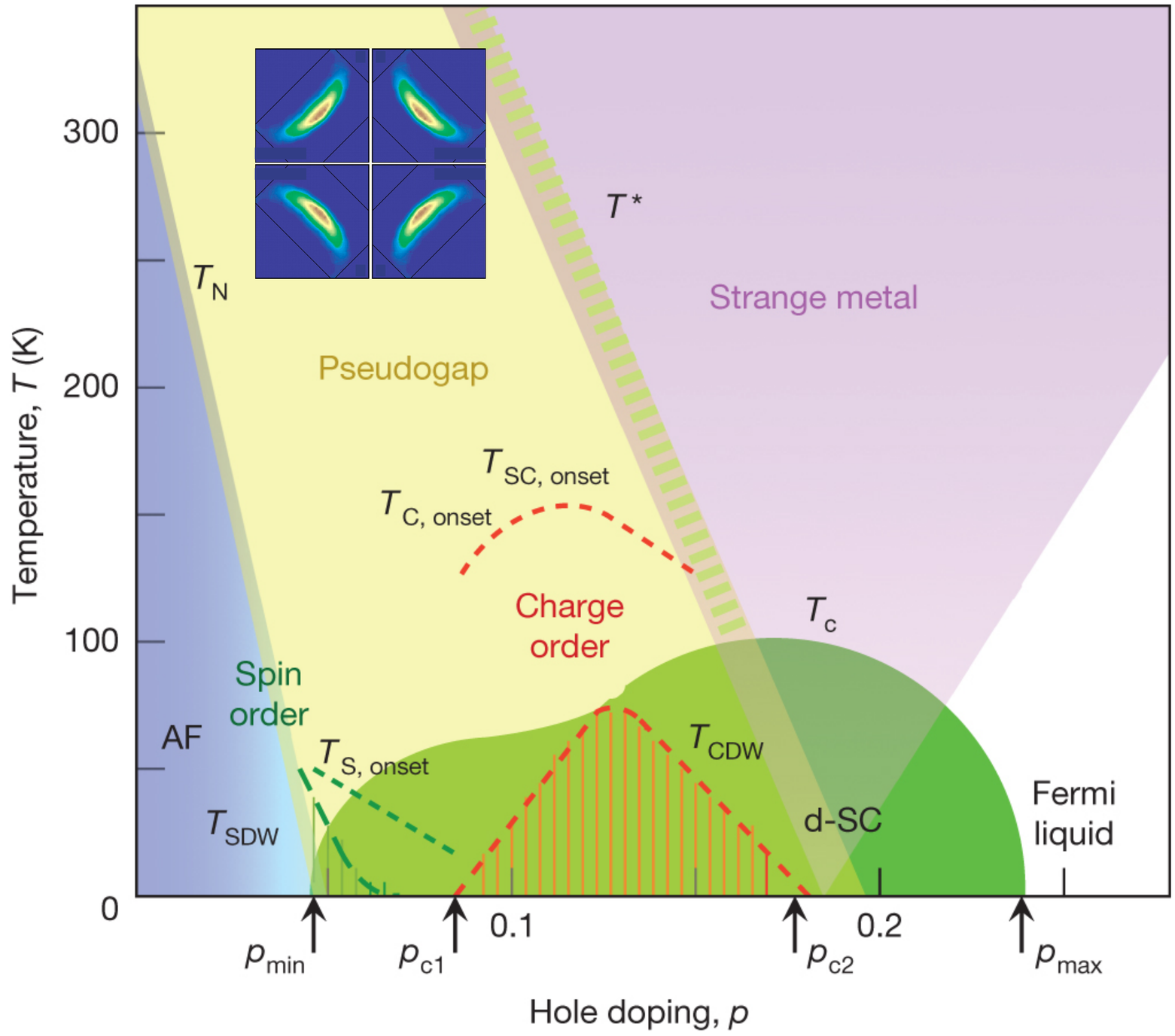

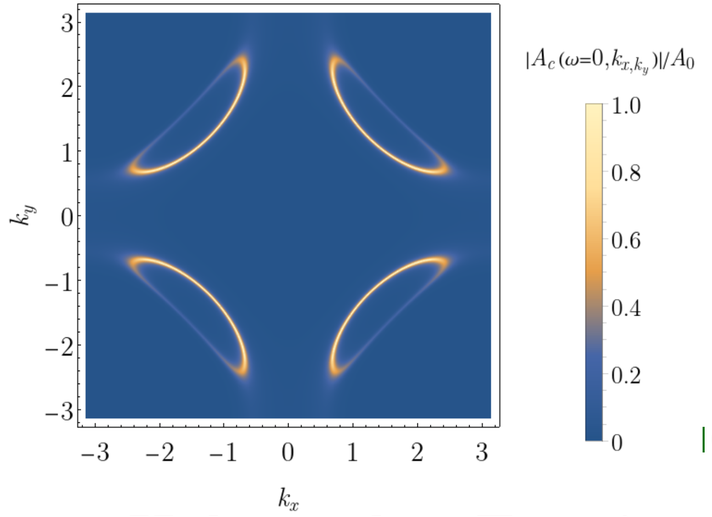

Ya-Hui Zhang and S. Sachdev, PRR **2**, 023172 (2020)

E. Mascot, A. Nikolaenko, M. Tikhanovskaya, Ya-Hui Zhang, D. K. Morr, and S. Sachdev, PRB **105**, 075146 (2022)

Hole pocket Fermi surfaces
of size p with
charge e, spin-1/2 quasiparticles
+
'spectator'
square lattice spin liquid
at half-filling.

But which spin liquid?

Insulating $S=1/2$ antiferromagnet

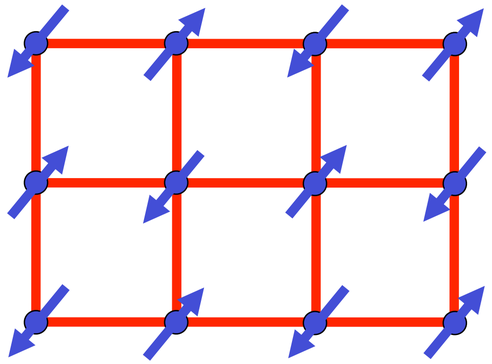

$$H = \sum_{i<j} J_{ij} \boldsymbol{S}_i \cdot \boldsymbol{S}_j$$

Schwinger bosons

$$\boldsymbol{S}_i = \frac{1}{2} b^\dagger_{i\alpha} \boldsymbol{\sigma}_{\alpha\beta} b_{i\beta} \,, \qquad \sum_{\alpha=\uparrow,\downarrow} b^\dagger_{i\alpha} b_{i\alpha} = 1$$

Mean-field spin liquid
with gapped bosonic spinons.

D.P. Arovas and A. Auerbach, PRB **38**, 316 (1988)

Insulating $S=1/2$ antiferromagnet

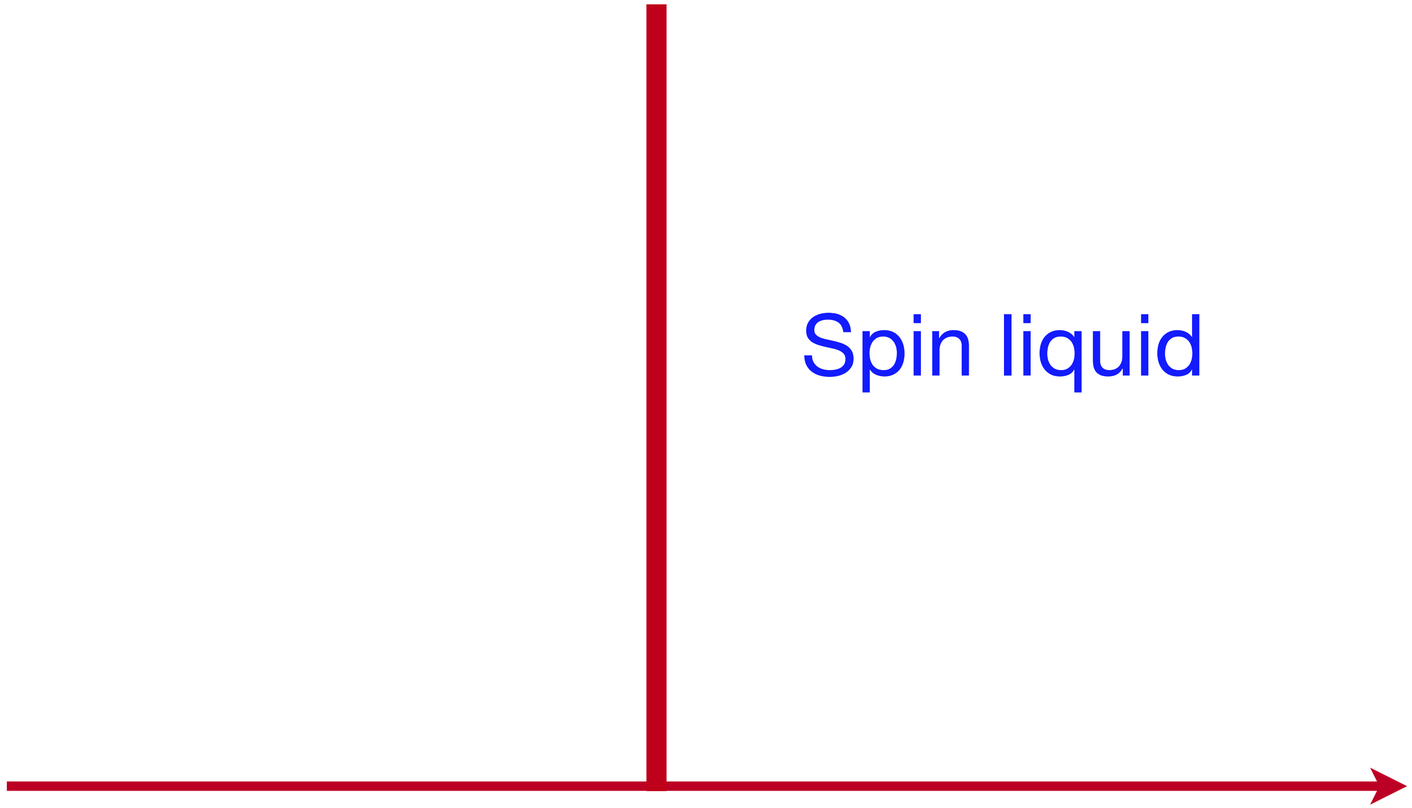

$$H = \sum_{i<j} J_{ij} \boldsymbol{S}_i \cdot \boldsymbol{S}_j$$

Schwinger fermions

$$\boldsymbol{S}_i = \frac{1}{2} f^\dagger_{i\alpha} \boldsymbol{\sigma}_{\alpha\beta} f_{i\beta} \,, \quad \sum_{\alpha=\uparrow,\downarrow} f^\dagger_{i\alpha} f_{i\alpha} = 1$$

π-flux mean-field theory
with gapless spinons at 2 Dirac points.

I. Affleck and J.B. Marston, PRB **37**, 3774 (1988)

Insulating $S=1/2$ antiferromagnet

$$H = \sum_{i<j} J_{ij} \boldsymbol{S}_i \cdot \boldsymbol{S}_j$$

Schwinger bosons

$$\boldsymbol{S}_i = \frac{1}{2} b^\dagger_{i\alpha} \boldsymbol{\sigma}_{\alpha\beta} b_{i\beta} \,, \qquad \sum_{\alpha=\uparrow,\downarrow} b^\dagger_{i\alpha} b_{i\alpha} = 1$$

Mean-field spin liquid
with gapped bosonic spinons.

Low energy $\mathbb{CP}^1$ U(1) gauge theory

$$z_\alpha \sim b_{A\alpha} + \varepsilon_{\alpha\beta} b_{B\beta}$$

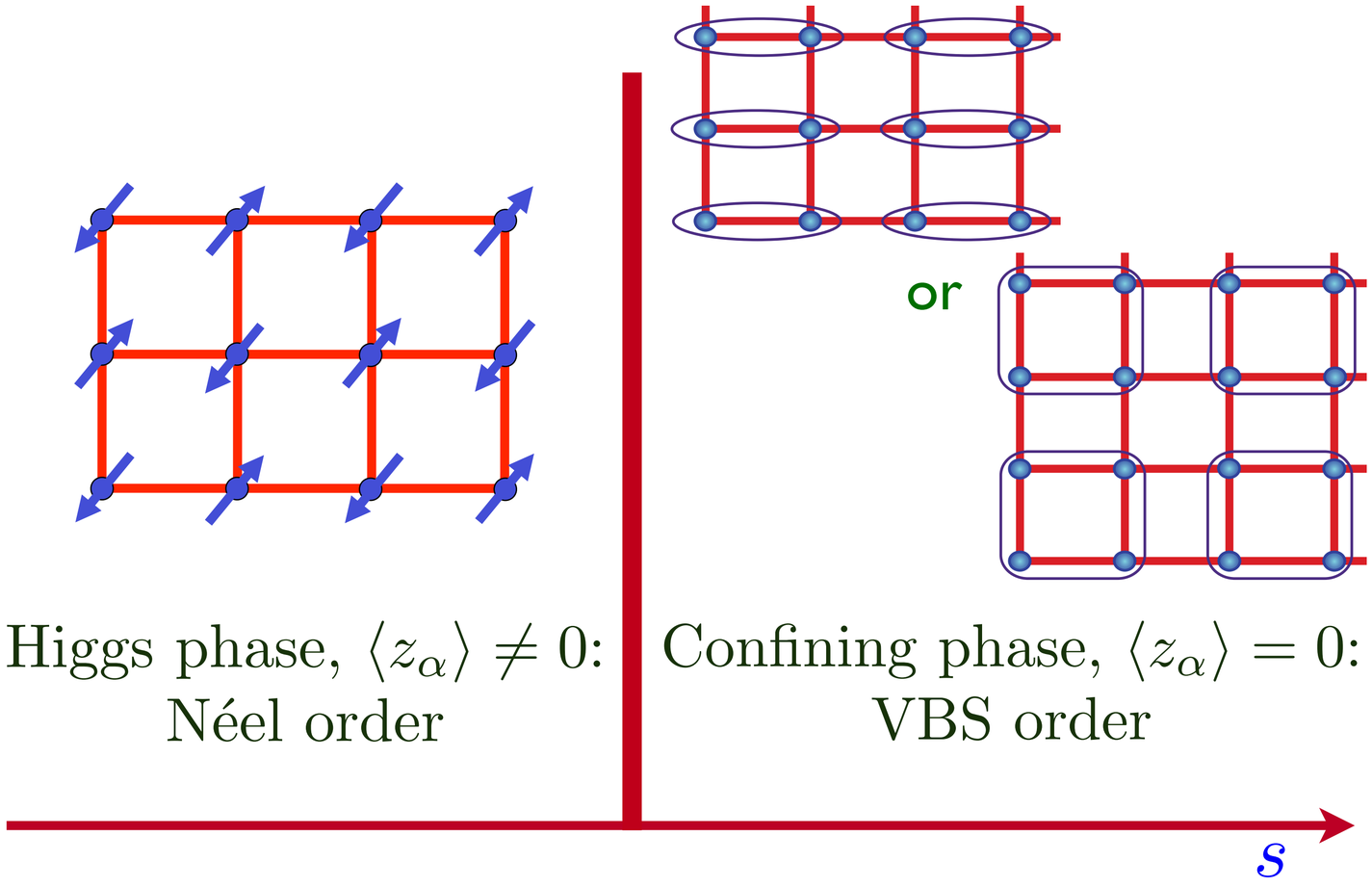

$$\mathcal{L} = |(\partial_\mu - i a_\mu) z_\alpha|^2 + s|z_\alpha|^2 + u|z_\alpha|^4 + \mathcal{L}_{\text{monopole}}$$

N. Read and S. S., PRL **62**, 1694 (1989)

Insulating $S=1/2$ antiferromagnet

$$H = \sum_{i<j} J_{ij} \boldsymbol{S}_i \cdot \boldsymbol{S}_j$$

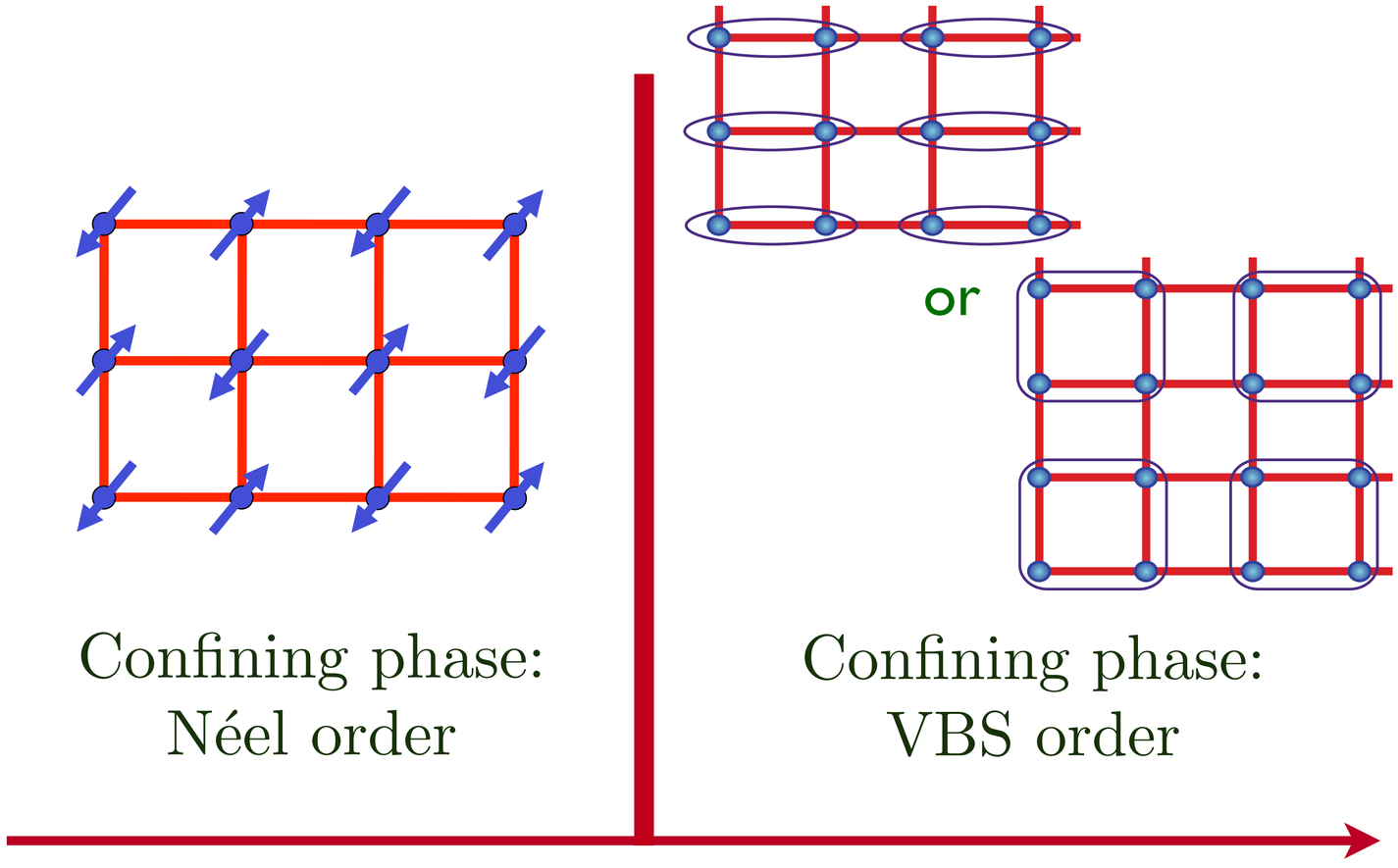

Confining phase:
Néel order

Confining phase:
VBS order

Schwinger fermions

$$\boldsymbol{S}_i = \frac{1}{2} f^\dagger_{i\alpha} \boldsymbol{\sigma}_{\alpha\beta} f_{i\beta} \,, \quad \sum_{\alpha=\uparrow,\downarrow} f^\dagger_{i\alpha} f_{i\alpha} = 1$$

π-flux mean-field theory
with gapless spinons at 2 Dirac points.
Low energy theory of $N_f = 2$
Dirac fermions Ψ_s coupled to
an emergent $\mathrm{SU}(2)_N$ gauge field.
Confining order parameters
are Néel and VBS states,
with a global $\mathrm{SO}(5)_f$ symmetry!

$$\mathcal{L} = i\overline{\Psi}_s \gamma_\mu D_\mu \Psi_s + \ldots$$

A. Tanaka and X. Hu, PRL **95**, 036402 (2005); T. Senthil and M.P.A. Fisher PRB **74**, 064405 (2006); Ying Ran and X.-G. Wen, cond-mat/0609620

Insulating $S=1/2$ antiferromagnet

$$H = \sum_{i<j} J_{ij} \boldsymbol{S}_i \cdot \boldsymbol{S}_j$$

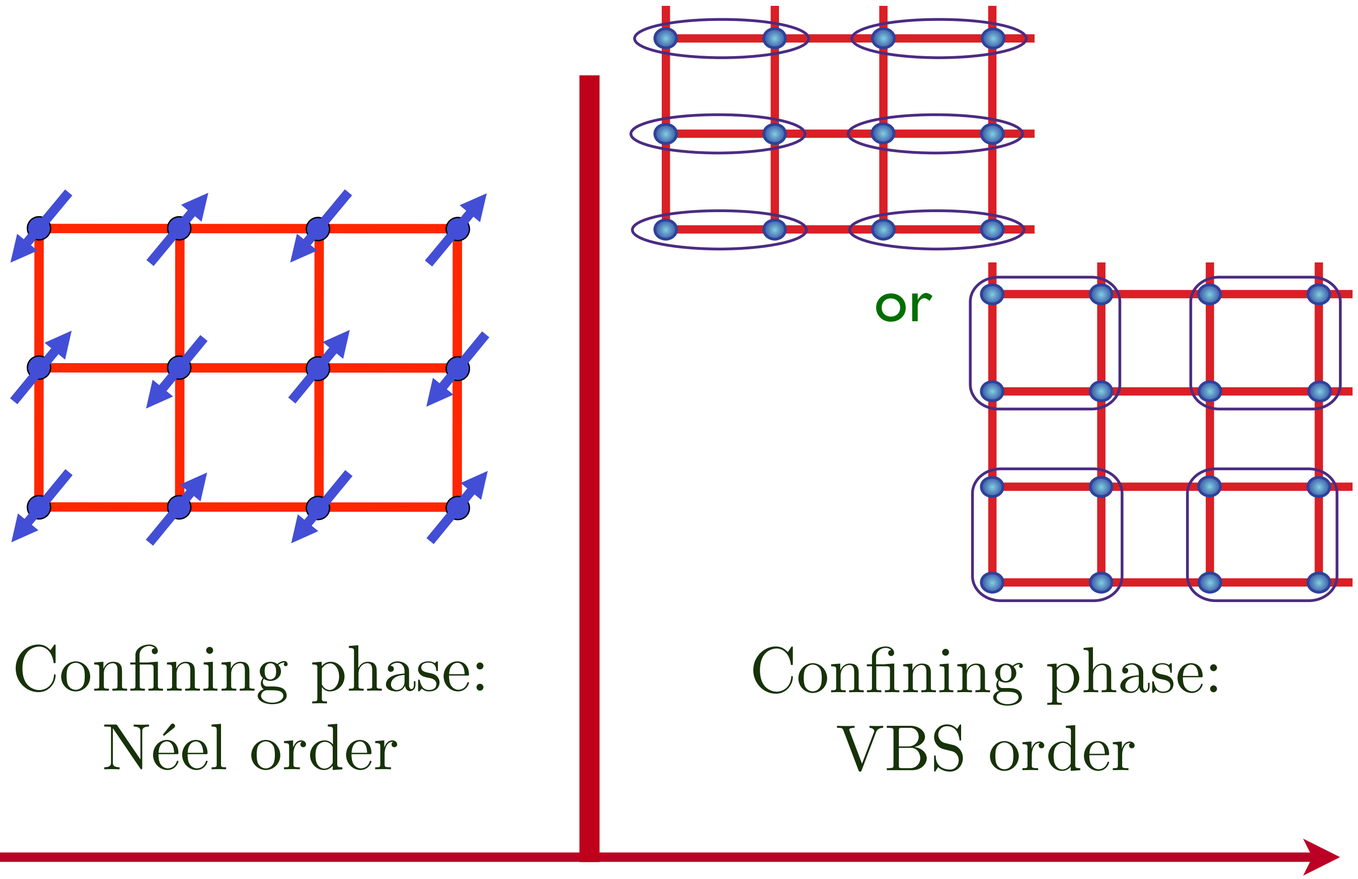

Confining phase:
Néel order

Confining phase:
VBS order

Schwinger fermions

$$\boldsymbol{S}_i = \frac{1}{2} f^\dagger_{i\alpha} \boldsymbol{\sigma}_{\alpha\beta} f_{i\beta} \,, \quad \sum_{\alpha=\uparrow,\downarrow} f^\dagger_{i\alpha} f_{i\alpha} = 1$$

π-flux mean-field theory
with gapless spinons at 2 Dirac points.
Low energy theory of $N_f = 2$
Dirac fermions Ψ_s coupled to
an emergent $\mathrm{SU}(2)_N$ gauge field.
Confining order parameters
are Néel and VBS states,
with a global $\mathrm{SO}(5)_f$ symmetry!

$$\mathcal{L} = i\overline{\Psi}_s \gamma_\mu D_\mu \Psi_s + \ldots$$

Dual to $\mathbb{CP}^1$ U(1) gauge theory.

A. Tanaka and X. Hu, PRL **95**, 036402 (2005); T. Senthil and M.P.A. Fisher PRB **74**, 064405 (2006); Ying Ran and X.-G. Wen, cond-mat/0609620
C. Wang, A. Nahum, M. A. Metlitski, C. Xu, and T. Senthil, Physical Review X **7**, 031051 (2017)

$$H = J_{1x} \sum_{\langle i,j \rangle_x} \mathbf{S_i} \cdot \mathbf{S_j} + J_{1y} \sum_{\langle i,j \rangle_y} \mathbf{S_i} \cdot \mathbf{S_j} + J_2 \sum_{\langle\langle i,j \rangle\rangle} \mathbf{S_i} \cdot \mathbf{S_j}.$$

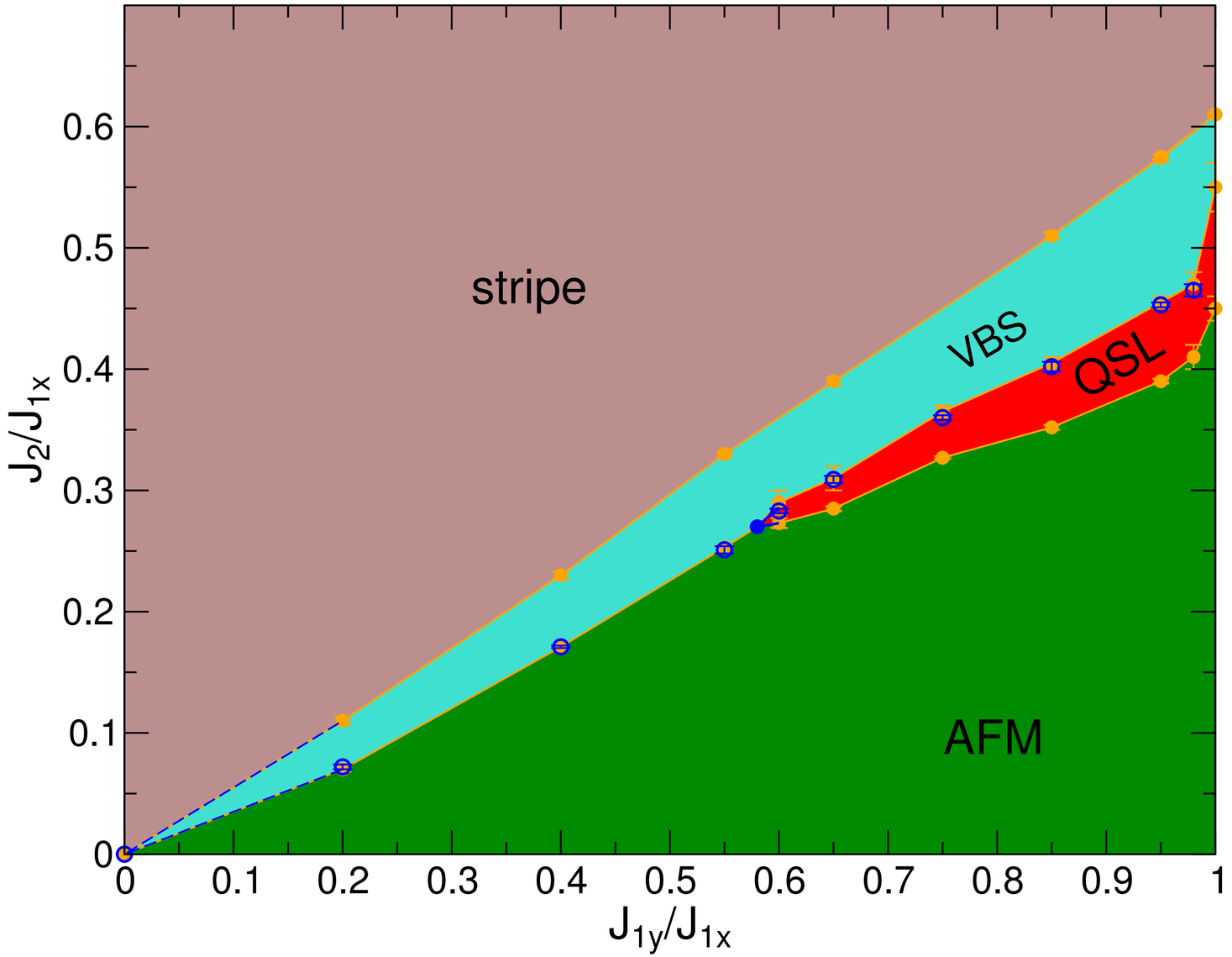

Wen-Yuan Liu,
Shou-Shu Gong,
Wei-Qiang Chen,
and Zheng-Cheng Gu,
arXiv:2212.00707

High Temperature Superconductivity in a Lightly Doped Quantum Spin Liquid

Hong-Chen Jiang[1,*] and Steven A. Kivelson[2]

We have performed density-matrix renormalization group studies of a square lattice t-J model with small hole doping, $\delta \ll 1$, on long four and six-leg cylinders. We include frustration in the form of a second-neighbor exchange coupling, $J_2 = J_1/2$, such that the undoped ($\delta = 0$) "parent" state is a quantum spin liquid. In contrast to the relatively short range superconducting (SC) correlations that have been observed in recent studies of the six-leg cylinder in the absence of frustration, we find power-law SC correlations with a Luttinger exponent, $K_{SC} \approx 1$, consistent with a strongly diverging SC susceptibility, $\chi \sim T^{-(2-K_{SC})}$ as the temperature $T \to 0$. The spin-spin correlations—as in the undoped state—fall exponentially suggesting that the SC "pairing" correlations evolve smoothly from the insulating parent state.

DOI: 10.1103/PhysRevLett.127.097002

Superconducting valence bond fluid in lightly doped 8-leg *t-J* cylinders
Hong-Chen Jiang, Steven A. Kivelson, and Dung-Hai Lee, arXiv:2303.11633

Superconductivity in doped quantum paramagnets has been a subject of long theoretical inquiry. In this work we report a density matrix renormalization group study of lightly doped t-J models on the square lattice (doped hole densities $\delta = 1/12$ and $1/8$) with parameters for which previous studies have suggested that the undoped system in 2D is either a quantum spin liquid or a valence bond crystal. Our studies are performed on cylinders with width up to 8. Ground-state correlations are found to be nearly identical for the "doped quantum spin liquid" and "doped valence bond crystal". Upon increasing the cylinder width from 4 to 8, we observed a significant strengthening of the quasi-long-range superconducting correlations, and a dramatic suppression of any "competing" charge-density-wave order. Extrapolating from the observed behavior of the width 8 cylinders, we speculate that the system has a nodeless d-wave superconducting ground-state in the 2D limit.

B Keimer *et al. Nature* **518**, 179-186 (2015)

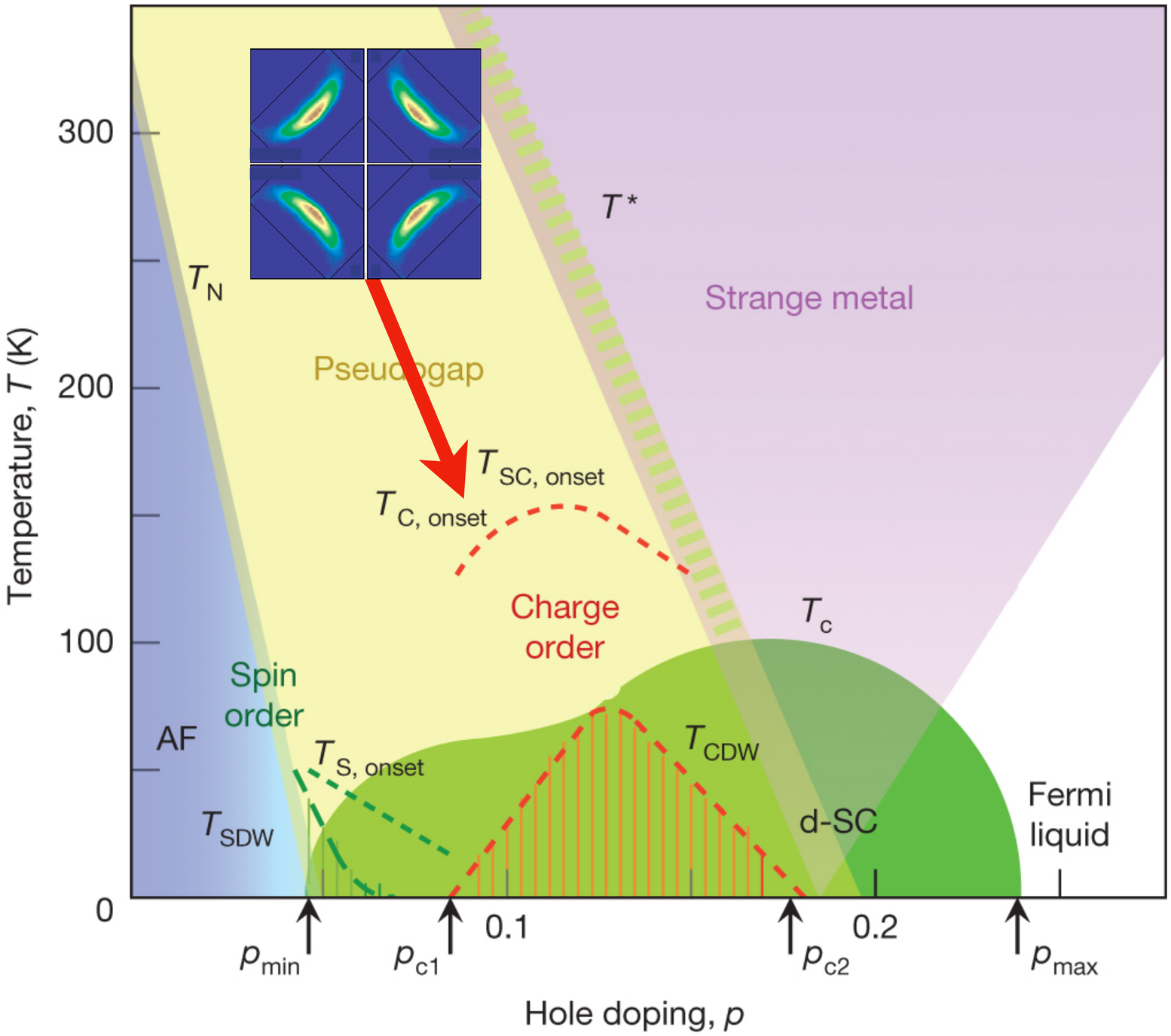

A theory for the confinement
of fractionalized excitations
in the
Arovas-Auerbach-Affleck-Marston
π-flux spin liquid
(which is dual to the
$\mathbb{CP}^1$ spin liquid)
from
electrically charged excitations.

Ancilla theory of the Hubbard model

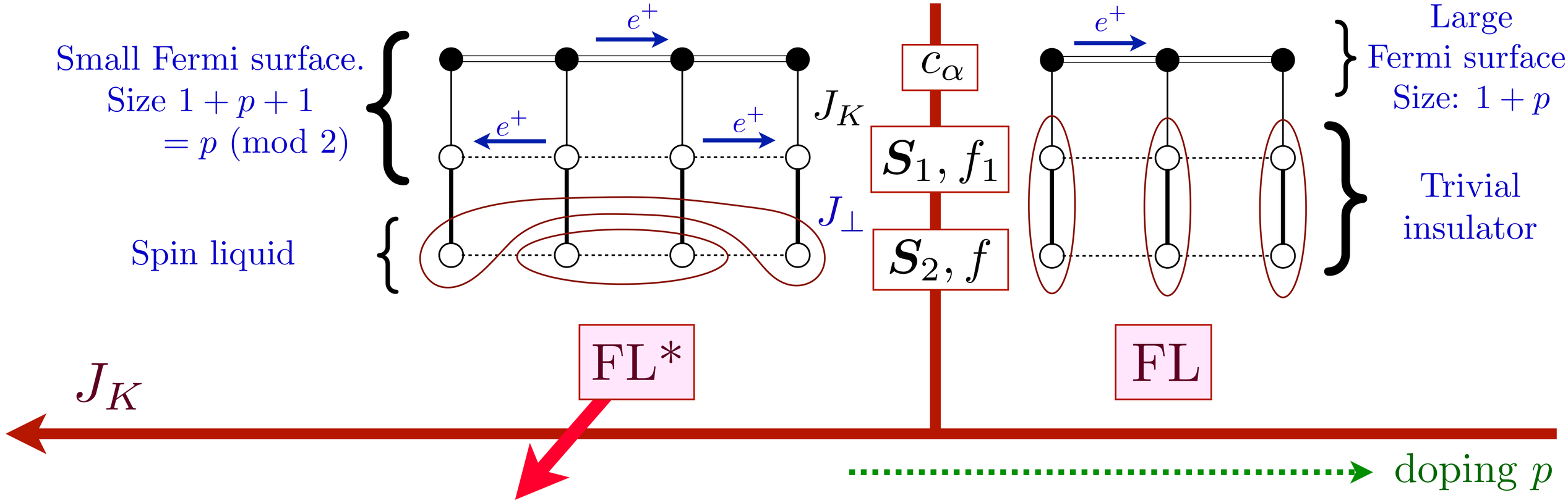

Pseudogap metal: $\left\langle c^\dagger_\alpha f_{1\alpha} \right\rangle \neq 0$

f_α form π-flux spin liquid with $\mathrm{SU}(2)_N$ gauge field

Charge e, $\mathrm{SU}(2)_N$ fundamental, Higgs boson $B \sim \begin{pmatrix} f^\dagger_{1\alpha} f_\alpha \\ \varepsilon_{\alpha\beta} f^\dagger_{1\alpha} f^\dagger_\beta \end{pmatrix}$

Boson with same quantum numbers in X.-G. Wen and P.A. Lee, PRL **76**, 503 (1996)

Confinement of SU(2)$_N$ gauge theory by charge fluctuations

- Begin with the π-flux spin liquid in the fermionic spinon description.

$$H_f = iJ \sum_{\langle ij \rangle} e_{ij} \left(f^\dagger_{i\alpha} f_{j\alpha} - f^\dagger_{j\alpha} f_{i\alpha} \right)$$

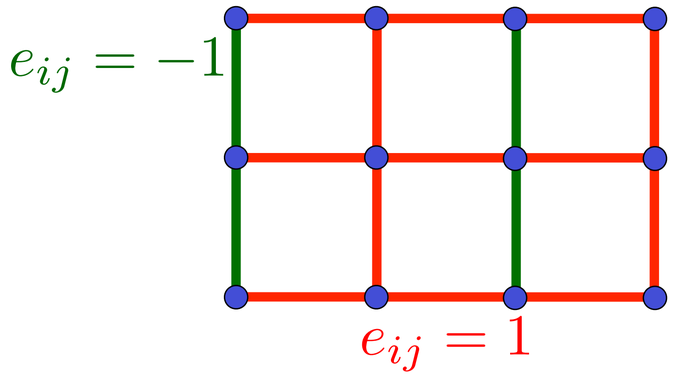

Confinement of SU(2)$_N$ gauge theory by charge fluctuations

- Begin with the π-flux spin liquid in the fermionic spinon description.

$$H_f = iJ \sum_{\langle ij \rangle} e_{ij} \left(f^\dagger_{i\alpha} f_{j\alpha} - f^\dagger_{j\alpha} f_{i\alpha} \right) = iJ \sum_{\langle ij \rangle} e_{ij} \left(\Psi^\dagger_i U_{ij} \Psi_j - \Psi^\dagger_j U_{ji} \Psi_i \right); \quad \Psi_i = \begin{pmatrix} f_{i\uparrow} \\ f^\dagger_{i\downarrow} \end{pmatrix}$$

H_f is invariant under SU(2) rotations in spin and SU(2)$_N$ rotations in Nambu space; U_{ij} is the SU(2)$_N$ gauge field.

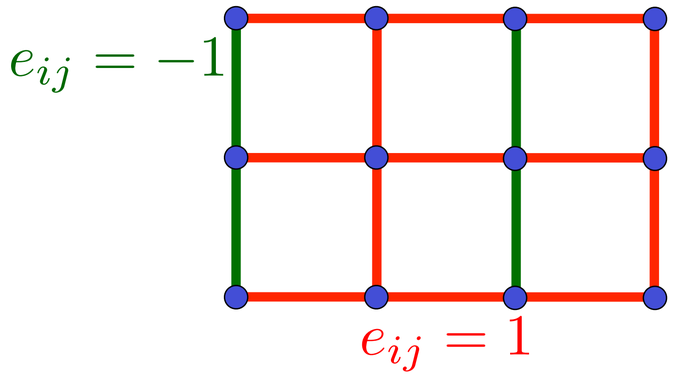

Confinement of $SU(2)_N$ gauge theory by charge fluctuations

- Begin with the π-flux spin liquid in the fermionic spinon description.

$$H_f = iJ \sum_{\langle ij \rangle} e_{ij} \left(f^\dagger_{i\alpha} f_{j\alpha} - f^\dagger_{j\alpha} f_{i\alpha} \right) = iJ \sum_{\langle ij \rangle} e_{ij} \left(\Psi^\dagger_i U_{ij} \Psi_j - \Psi^\dagger_j U_{ji} \Psi_i \right); \quad \Psi_i = \begin{pmatrix} f_{i\uparrow} \\ f^\dagger_{i\downarrow} \end{pmatrix}$$

H_f is invariant under SU(2) rotations in spin and $SU(2)_N$ rotations in Nambu space; U_{ij} is the $SU(2)_N$ gauge field.

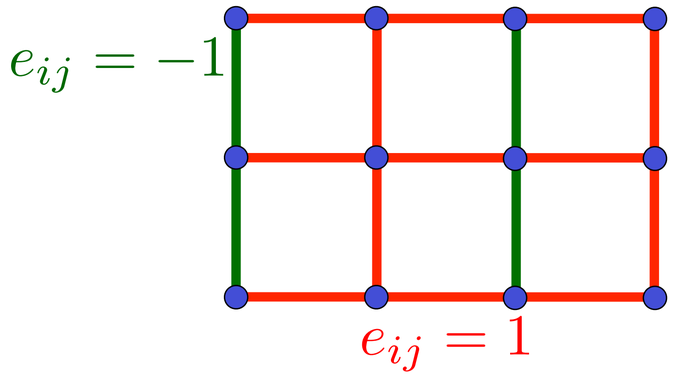

- The nearest-neighbor effective Hamiltonian for charge e, $SU(2)_N$ fundamental boson B_i is constrained by the fact that the composite of B_i and Ψ_i is an electron:

$$H_B = r \sum_i B^\dagger_i B_i + iw \sum_{\langle ij \rangle} e_{ij} \left(B^\dagger_i U_{ij} B_j - B^\dagger_j U_{ji} B_i \right) + \ldots$$

Confinement of SU(2)$_N$ gauge theory by charge fluctuations

$$\mathcal{L}(B) = H_B + \frac{u}{2}\sum_{\boldsymbol{i}} \rho_{\boldsymbol{i}}^2 + V_1 \sum_{\boldsymbol{i}} \rho_{\boldsymbol{i}} \left(\rho_{\boldsymbol{i}+\hat{\boldsymbol{x}}} + \rho_{\boldsymbol{i}+\hat{\boldsymbol{y}}}\right) + g\sum_{\langle \boldsymbol{ij}\rangle} |\Delta_{\boldsymbol{ij}}|^2 + J_1 \sum_{\langle \boldsymbol{ij}\rangle} Q_{\boldsymbol{ij}}^2 + K_1 \sum_{\langle \boldsymbol{ij}\rangle} J_{\boldsymbol{ij}}^2 .$$

site charge density: $\left\langle c_{\boldsymbol{i}\alpha}^\dagger c_{\boldsymbol{i}\alpha} \right\rangle \sim \rho_{\boldsymbol{i}} = B_{\boldsymbol{i}}^\dagger B_{\boldsymbol{i}}$

bond density: $\left\langle c_{\boldsymbol{i}\alpha}^\dagger c_{\boldsymbol{j}\alpha} + c_{\boldsymbol{j}\alpha}^\dagger c_{\boldsymbol{i}\alpha} \right\rangle \sim Q_{\boldsymbol{ij}} = Q_{\boldsymbol{ji}} = \mathrm{Im}\left(B_{\boldsymbol{i}}^\dagger e_{\boldsymbol{ij}} U_{\boldsymbol{ij}} B_{\boldsymbol{j}}\right)$

bond current: $i\left\langle c_{\boldsymbol{i}\alpha}^\dagger c_{\boldsymbol{j}\alpha} - c_{\boldsymbol{j}\alpha}^\dagger c_{\boldsymbol{i}\alpha} \right\rangle \sim J_{\boldsymbol{ij}} = -J_{\boldsymbol{ji}} = \mathrm{Re}\left(B_{\boldsymbol{i}}^\dagger e_{\boldsymbol{ij}} U_{\boldsymbol{ij}} B_{\boldsymbol{j}}\right)$

Pairing: $\langle \varepsilon_{\alpha\beta} c_{i\alpha} c_{j\beta} \rangle \sim \Delta_{\boldsymbol{ij}} = \Delta_{\boldsymbol{ji}} = \varepsilon_{ab} B_{a\boldsymbol{i}} e_{\boldsymbol{ij}} U_{\boldsymbol{ij}} B_{b\boldsymbol{j}}$.

Confinement of SU(2)$_N$ gauge theory by charge fluctuations

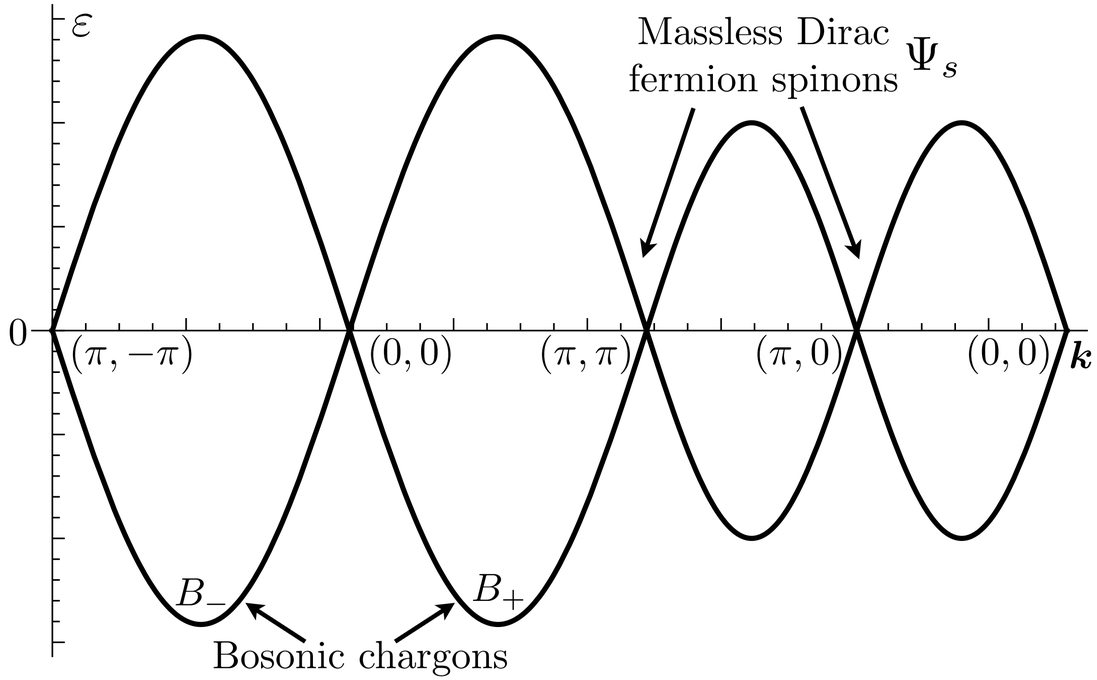

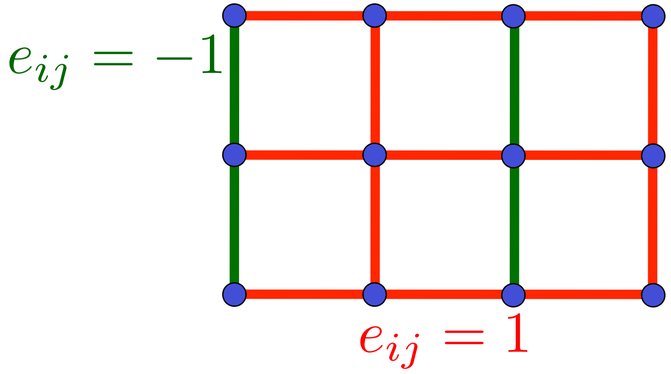

Confinement of $SU(2)_N$ gauge theory by charge fluctuations

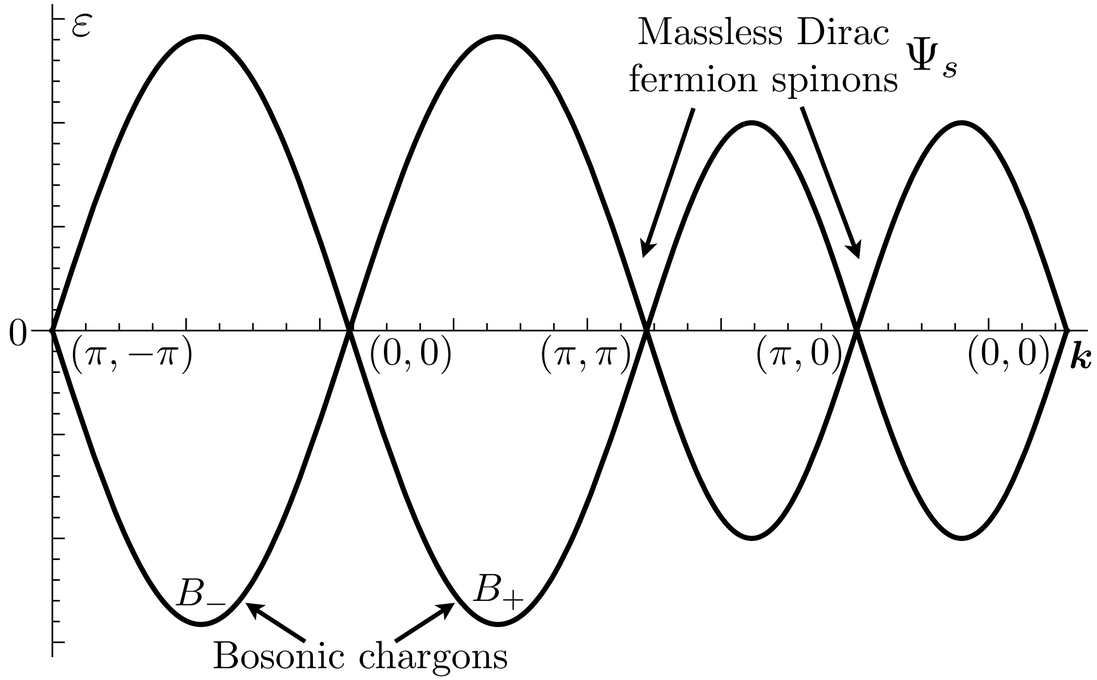

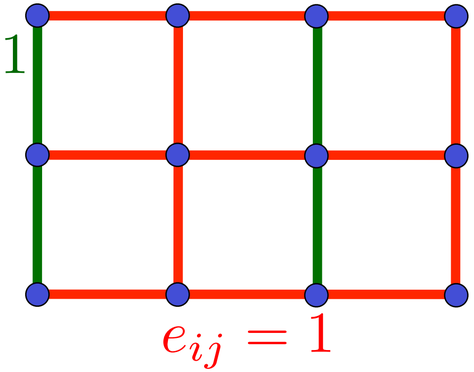

$SU(2)_N$ gauge-invariant and SU(2) spin invariant order parameters of Higgs phases:

$$x\text{-CDW}: \quad \rho_{(\pi,0)} = B^*_{a+}B_{a+} - B^*_{a-}B_{a-}$$

$$y\text{-CDW}: \quad \rho_{(0,\pi)} = B^*_{a+}B_{a-} + B^*_{a-}B_{a+}$$

$$d\text{-density wave}: \quad D = i\left(B^*_{a+}B_{a-} - B^*_{a-}B_{a+}\right)$$

$$d\text{-wave superconductor}: \quad \Delta = \varepsilon_{ab}B_{a+}B_{b-}$$

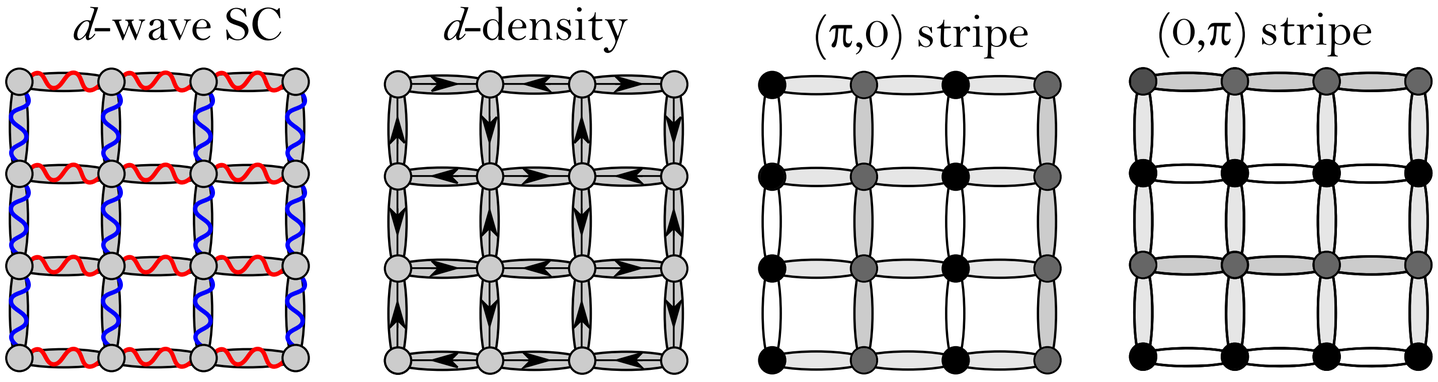

The $\mathcal{O}(B^2_{a\pm})$ terms in the energy have a $SO(5)_b$ rotation symmetry between these orders.

Confinement of SU(2)$_N$ gauge theory by charge fluctuations

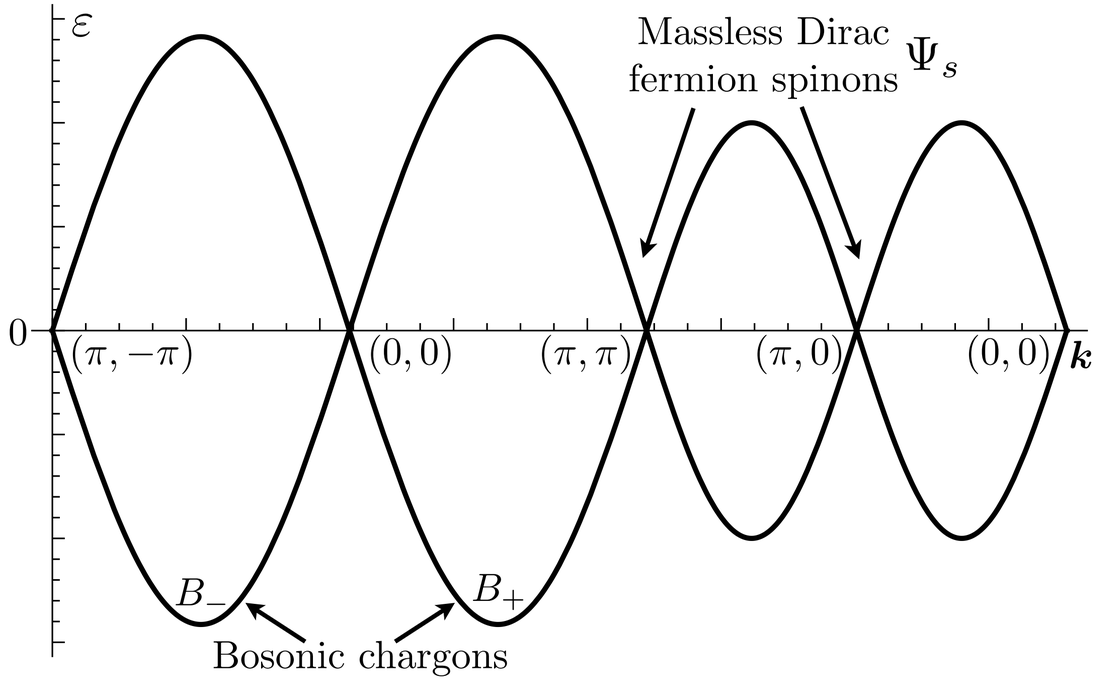

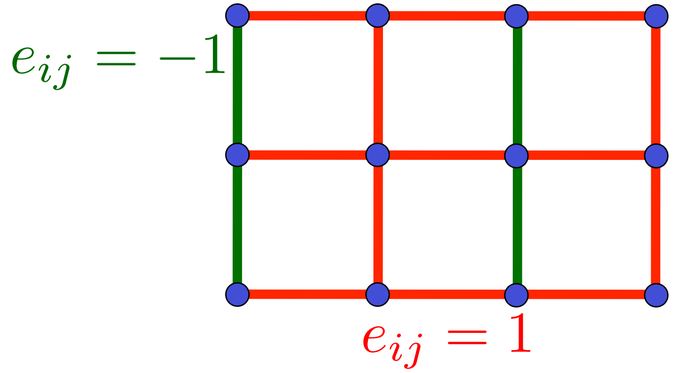

The B_{av}
($a \to \mathrm{SU}(2)_N$ gauge, $v \to$ valley)
are the "square roots" of
conventional
d-wave superconductor,
charge density wave,
pair density wave
...

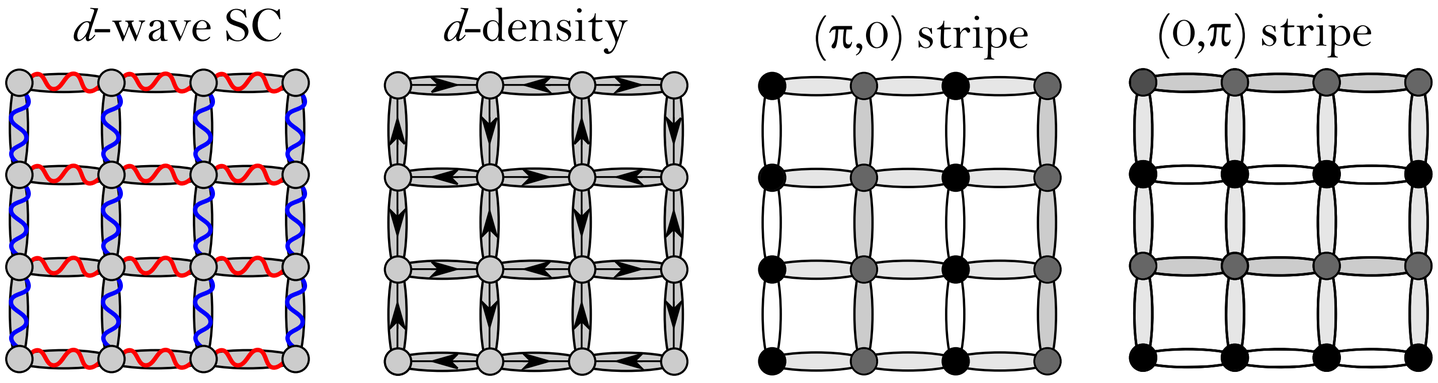

Confinement of $SU(2)_N$ gauge theory by charge fluctuations

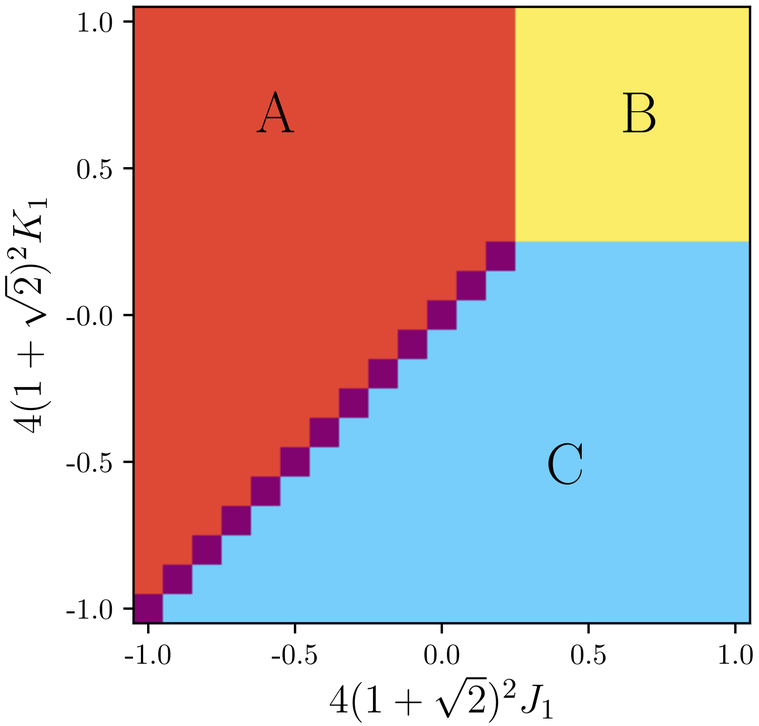

$$\langle B \rangle \neq 0$$

Phase B
d-wave SC

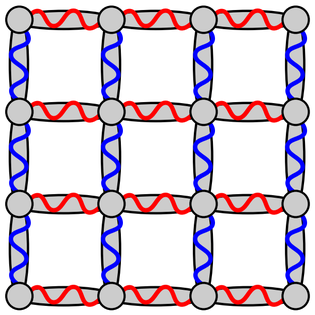

Phase C
d-density

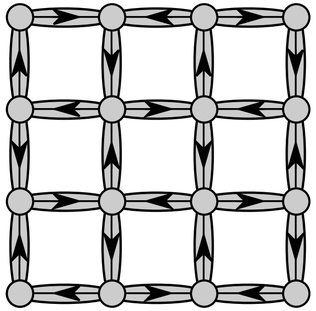

Phase A
(π,0) stripe

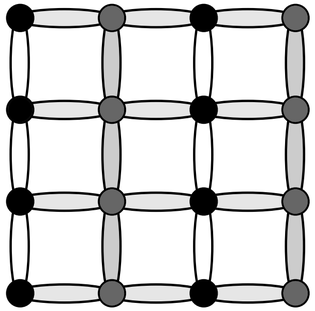

Phase A
(0,π) stripe

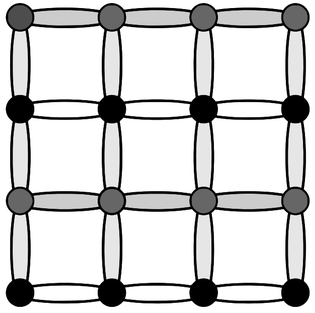

Global phase diagram of $SU(2)_N$ gauge theory

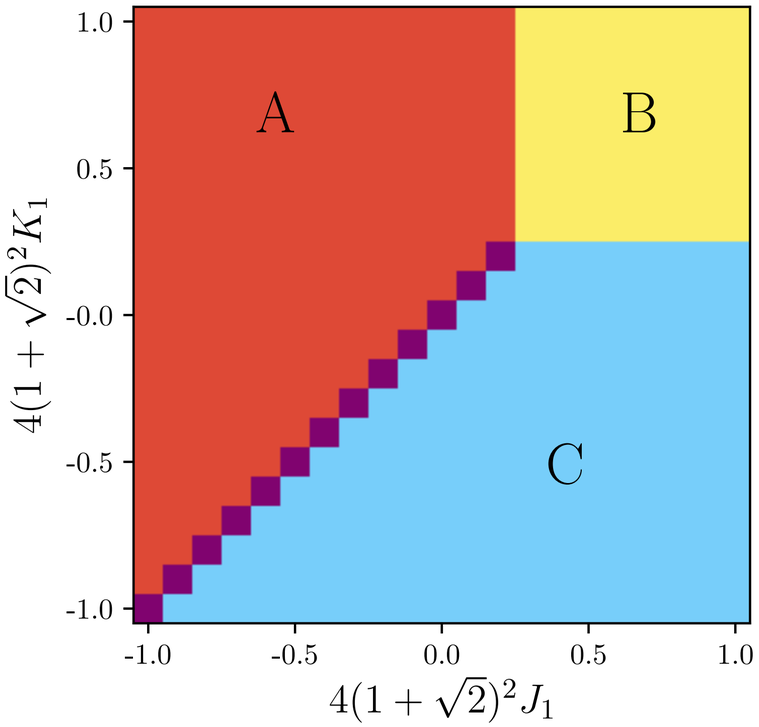

$\langle B \rangle \neq 0$

$\mathrm{SO}(5)_b$

$\langle B \rangle = 0$

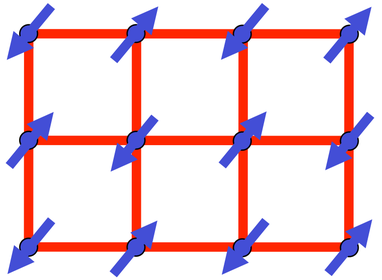

Confining phase:
Néel order

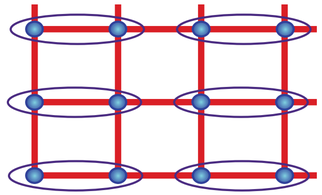

$\mathrm{SO}(5)_f$

or

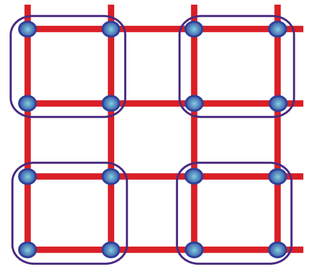

Confining phase:
VBS order

s

r

Phase B
d-wave SC

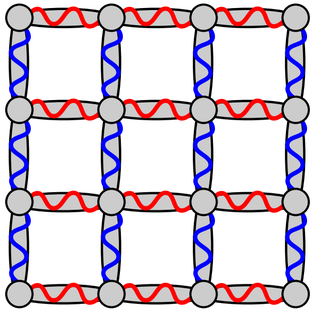

Phase C
d-density

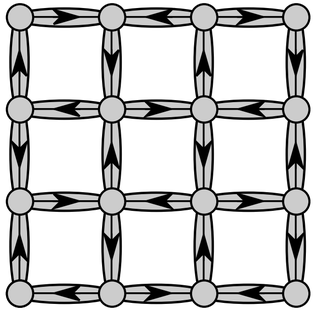

Phase A
(π,0) stripe

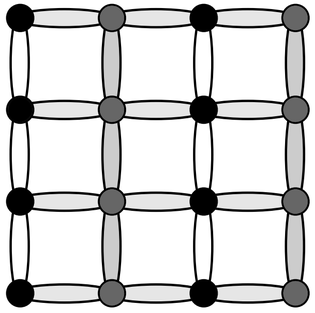

Phase A
(0,π) stripe

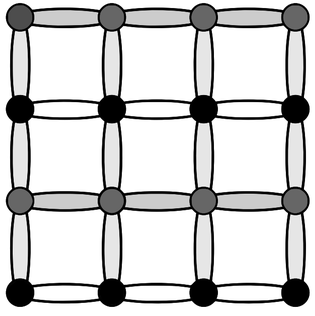

Global phase diagram of $SU(2)_N$ gauge theory

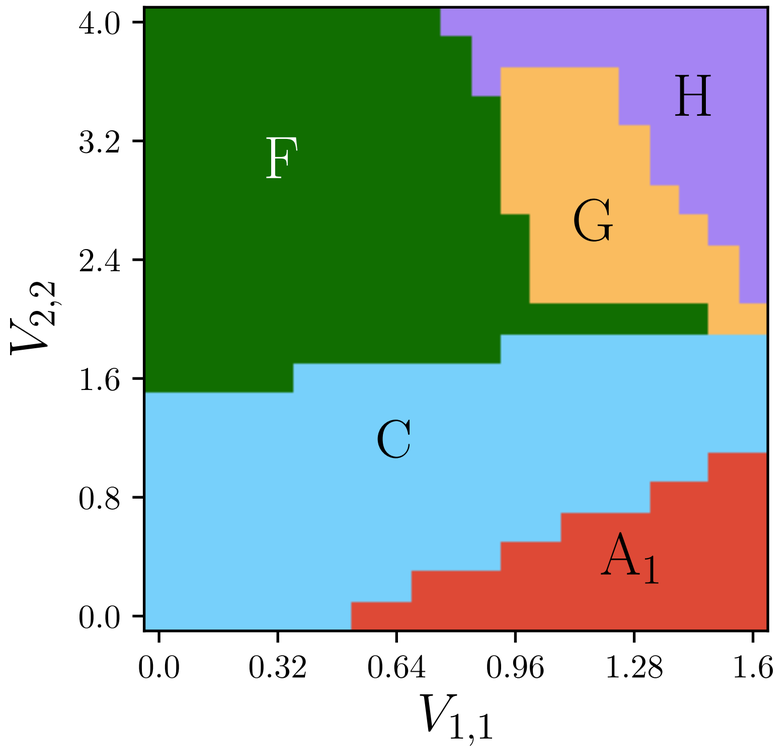

$\langle B \rangle \neq 0$

Including further-neighbor couplings in B

$\langle B \rangle = 0$

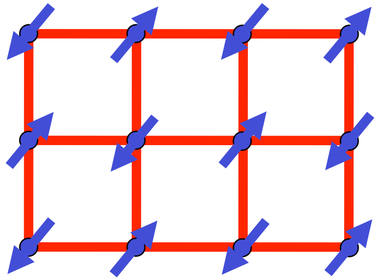

Confining phase: Néel order

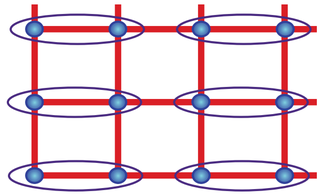

$SO(5)_f$

or

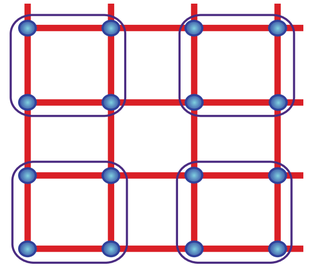

Confining phase: VBS order

s

r

Phase B
d-wave SC

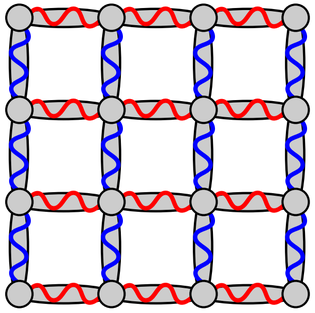

Phase C
d-density

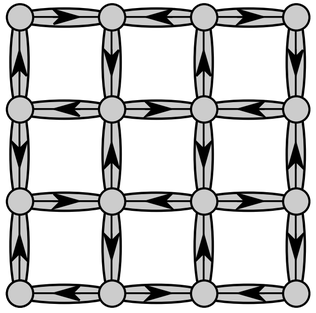

Phase A
(π,0) stripe

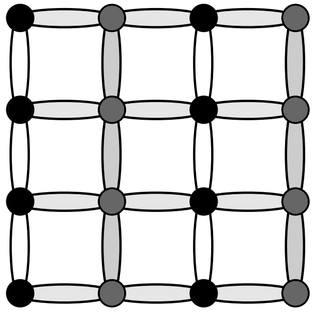

Phase A
(0,π) stripe

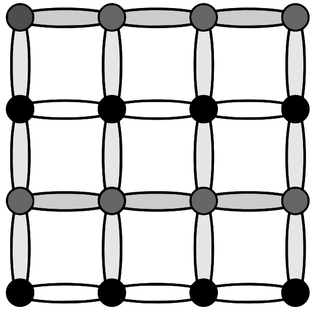

Phase F
Period 4 bond centered stripe + d-density

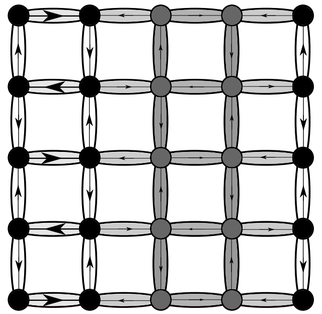

Phase G
Period 4 site centered stripe + d-density

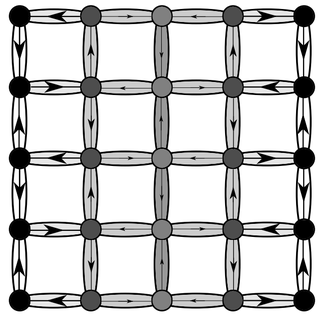

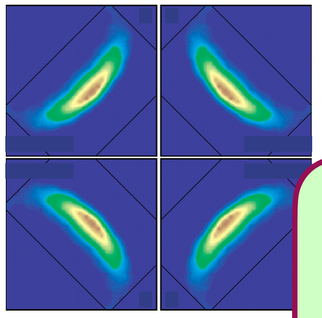

Pseudogap Metal (FL*)
with hole pocket Fermi surfaces
and underlying π-flux spin liquid

T

p

$\mathbb{B}$

Metal with
(π, π) SDW
(Néel) order.

$\mathbb{A}$

d-wave superconductivity.
Charge order.

Strange
Metal.

$\mathbb{C}$

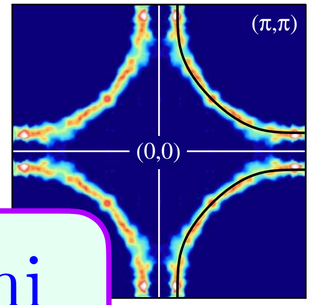

Fermi
Liquid.
FL

Arrow $\mathbb{A}$

Condensation of B
in $SU(2)_N$ gauge theory.

Arrow $\mathbb{B}$

Condensation of z_α in dual $\mathbb{CP}^1$
U(1) gauge theory.

Arrow $\mathbb{C}$

$SU(2)_s \times U(1)_a$ gauge theory
in ancilla model
with Higgs field $H_{\alpha a} \sim c^\dagger_\alpha f_{1a}$

Can the underlying spin liquid help understand experimental observations of spin dynamics ?

Spin fluctuations associated with the collapse of the pseudogap in a cuprate superconductor

Received: 7 January 2022

Accepted: 6 October 2022

Published online: 17 November 2022

Check for updates

M. Zhu[1] ✉, D. J. Voneshen[2,3], S. Raymond[4], O. J. Lipscombe[1], C. C. Tam[1,5] & S. M. Hayden[1] ✉

Theories of the origin of superconductivity in cuprates depend on an understanding of their normal state, which exhibits various competing orders. Transport and thermodynamic measurements on $La_{2-x}Sr_xCuO_4$ show signatures of a quantum critical point and the associated fluctuations, including a peak in the electronic specific heat versus doping, near the doping p^* where the pseudogap collapses. The fundamental nature of these quantum fluctuations is unclear. Here we use inelastic neutron scattering to show that, close to the superconducting critical temperature and near p^*, there are very-low-energy collective spin excitations with characteristic energies of ~5 meV. Cooling and applying a magnetic field creates a mixed state with a stronger magnetic response below 10 meV. We conclude that the low-energy spin fluctuations are due to the collapse of the pseudogap combined with an underlying tendency to magnetic order. We show that the large specific heat near p^* can be understood in terms of collective spin fluctuations. The spin fluctuations we measure exist across the superconducting phase diagram and may be related to the strange metal behaviour observed in overdoped cuprates.

Can the underlying spin liquid help understand experimental observations of spin dynamics ?

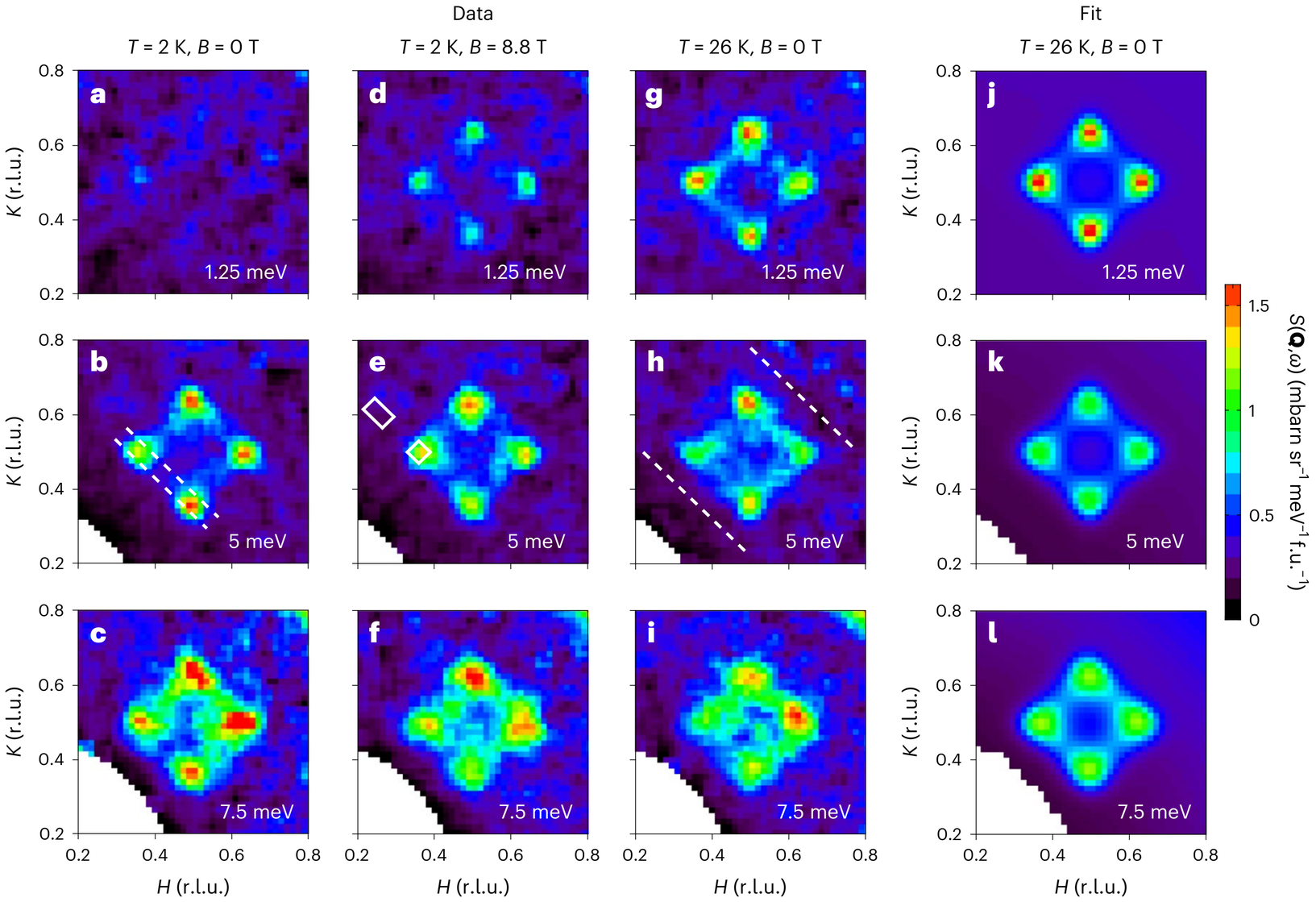

Fig. 2 | Wavevector-dependent maps of low-energy spin fluctuations in $La_{2-x}Sr_xCuO_4$ ($x = 0.22$). a–i, Constant-energy maps of $S(\mathbf{Q}, \omega)$ measured at $T = 2$ K, $B = 0$ T (**a**–**c**); $T = 2$ K, $B = 8.8$ T (**d**–**f**); $T = 26$ K (T_c), $B = 0$ T (**g**–**i**). We label reciprocal space as $\mathbf{Q} = H\mathbf{a}^* + K\mathbf{b}^* + L\mathbf{c}^*$. L is integrated over the range $|L| \leq 1$. White dashed lines in **b** show the range of integration used to produce Fig. 3. The white boxes in **e** define the integration ranges for the signal and background used to produce Fig. 4a,b. **j**–**l**, The result of a global fit of equation (1) including correction of a magnetic form factor and a $|\mathbf{Q}|^2$ background. Data shown in Figs. 2–4 were collected on LET.

Can the underlying spin liquid help understand experimental observations of spin dynamics ?

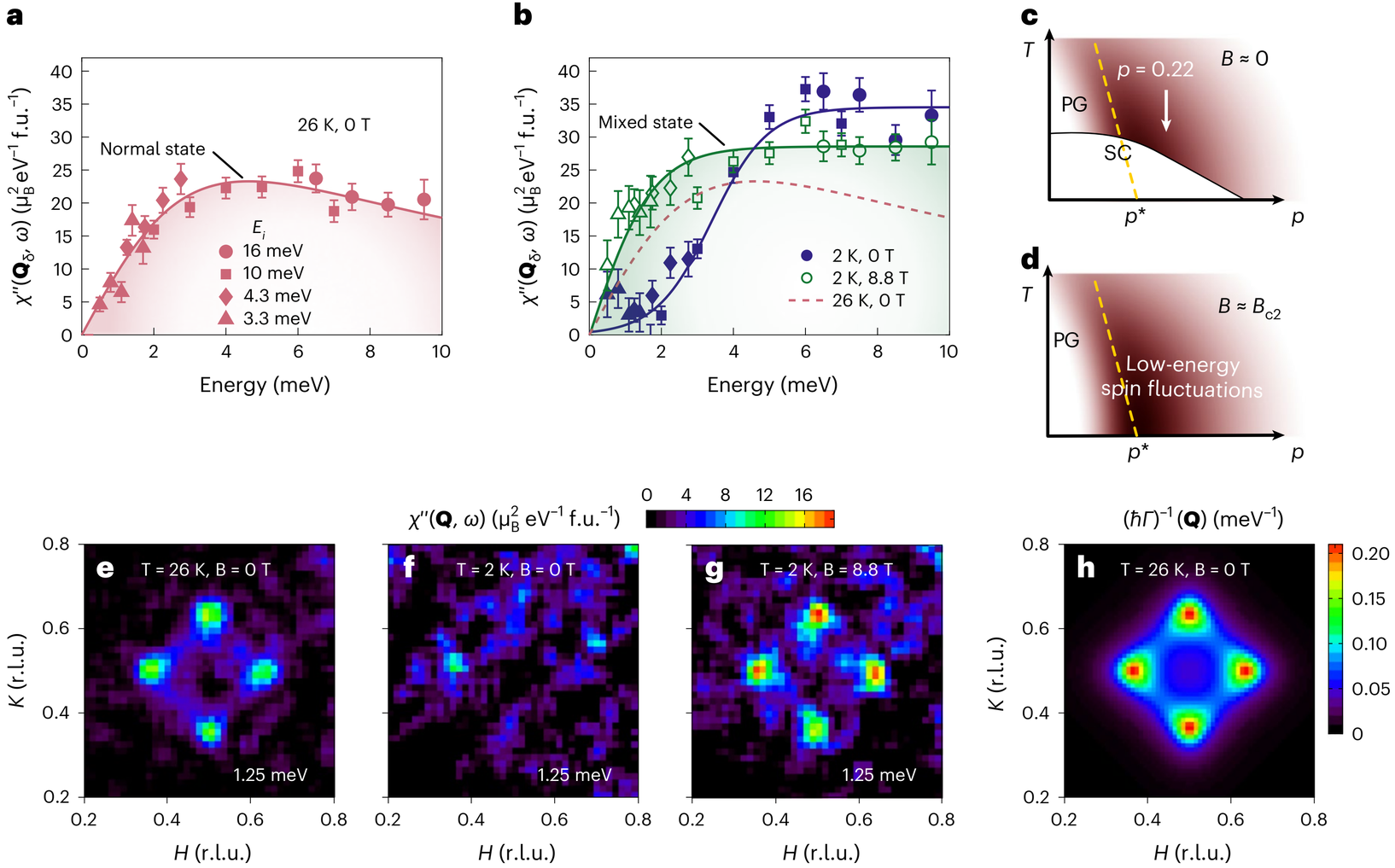

Fig. 4 | Magnetic excitations with a low-energy scale in the normal and mixed states of LSCO (p = 0.22). Energy dependence of the magnetic response $\chi''(\mathbf{Q}_\delta, \omega)$. **a**, Normal state ($T$ = 26 K, B = 0, filled symbols and pink shading) showing the low-energy scale. **b**, Increased response in the mixed state (T = 2 K, B = 8.8 T, open symbols and green shading) and suppression at low energy in the superconducting state (T = 2 K, B = 0, blue filled symbols). The solid line in **a** is a fit of $\chi''(\mathbf{Q}_\delta, \omega)/\omega$ to a Lorentzian response. Solid lines in **b** are guides to the eye. Symbols indicate incident energy E_i. Error bars are determined from Poisson counting statistics. **c**,**d**, Schematics illustrating the magnitude (red shading) of $\chi''(\mathbf{Q}_\delta, \hbar\omega \approx 1\,\text{meV})$ in the normal state (**c**) and its enhancement under an applied magnetic field (**d**). **e**–**g**, Maps of low-energy $\chi''(\mathbf{Q}, \omega)$ at $T \approx T_c$ (**e**) and at T = 2 K with B = 0 (**f**) and 8.8 T (**g**). **h**, Wavevector dependence of the relaxation parameter $\Gamma^{-1}(\mathbf{Q})$ in the normal state, obtained from a global fit.

Can the underlying spin liquid help understand experimental observations of spin dynamics ?

Dispersion, damping, and intensity of spin excitations in the monolayer $(Bi,Pb)_2(Sr,La)_2CuO_{6+\delta}$ cuprate superconductor family

Y. Y. Peng,[1,*] E. W. Huang,[2,3] R. Fumagalli,[1] M. Minola,[4] Y. Wang,[3,5] X. Sun,[6] Y. Ding,[6] K. Kummer,[7] X. J. Zhou,[6] N. B. Brookes,[7] B. Moritz,[3] L. Braicovich,[7] T. P. Devereaux,[3] and G. Ghiringhelli[1,8,†]

[1]*Dipartimento di Fisica, Politecnico di Milano, Piazza Leonardo da Vinci 32, I-20133 Milano, Italy*

[2]*Department of Physics, Stanford University, Stanford, California 94305, USA*

[3]*Stanford Institute for Materials and Energy Sciences, SLAC National Accelerator Laboratory and Stanford University, Menlo Park, California 94025, USA*

[4]*Max-Planck-Institut für Festkörperforschung, Heisenbergstraße 1, D-70569 Stuttgart, Germany*

[5]*Department of Physics, Harvard University, Cambridge, Massachusetts 02138, USA*

[6]*Beijing National Laboratory for Condensed Matter Physics, Institute of Physics, Chinese Academy of Sciences, Beijing 100190, China*

[7]*ESRF, The European Synchrotron, CS 40220, F-38043 Grenoble Cedex, France*

[8]*CNR-SPIN, Politecnico di Milano, Piazza Leonardo da Vinci 32, I-20133 Milano, Italy*

(Received 5 August 2018; revised manuscript received 24 September 2018; published 10 October 2018)

Using Cu-L_3 edge resonant inelastic x-ray scattering (RIXS) we measured the dispersion and damping of spin excitations (magnons and paramagnons) in the high-T_c superconductor $(Bi,Pb)_2(Sr,La)_2CuO_{6+\delta}$ (Bi2201), for a large doping range across the phase diagram ($0.03 \lesssim p \lesssim 0.21$). Selected measurements with full polarization analysis unambiguously demonstrate the spin-flip character of these excitations, even in the overdoped sample. We find that the undamped frequencies increase slightly with doping for all accessible momenta, while the damping grows rapidly, faster in the $(0, 0) \rightarrow (0.5, 0.5)$ nodal direction than in the $(0, 0) \rightarrow (0.5, 0)$ antinodal direction. We compare the experimental results to numerically exact determinant quantum Monte Carlo (DQMC) calculations that provide the spin dynamical structure factor $S(\mathbf{Q}, \omega)$ of the three-band Hubbard model. The theory reproduces well the momentum and doping dependence of the dispersions and spectral weights of magnetic excitations. These results provide compelling evidence that paramagnons, although increasingly damped, persist across the superconducting dome of the cuprate phase diagram; this implies that long-range antiferromagnetic correlations are quickly washed away, while short-range magnetic interactions are little affected by doping.

DOI: 10.1103/PhysRevB.98.144507

Can the underlying spin liquid help understand experimental observations of spin dynamics ?

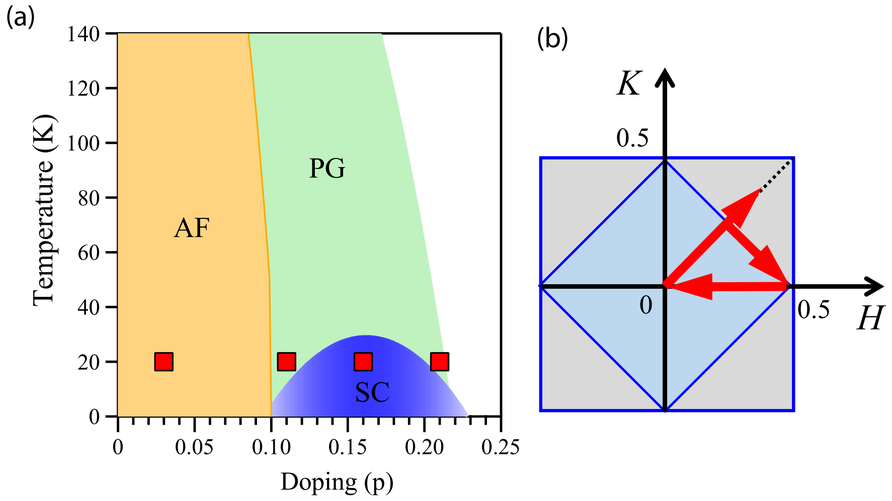

FIG. 1. (a) Schematic temperature-doping phase diagram of $(Bi,Pb)_2(Sr,La)_2CuO_{6+\delta}$. It shows the antiferromagnetic (AF), superconducting (SC), and the pseudogap (PG) regions. Here we study four doping levels as indicated by the solid red squares. (b) 2D reciprocal lattice for the pseudotetragonal structure and the first Brillouin zones (structural in light grey, magnetic in light blue). Coordinates H and K are in r.l.u.. The path followed for the measurements is indicated by the red arrows, starting at (0.25,0.25) and ending around (0.30,0.30) via (0.5,0) and (0,0).

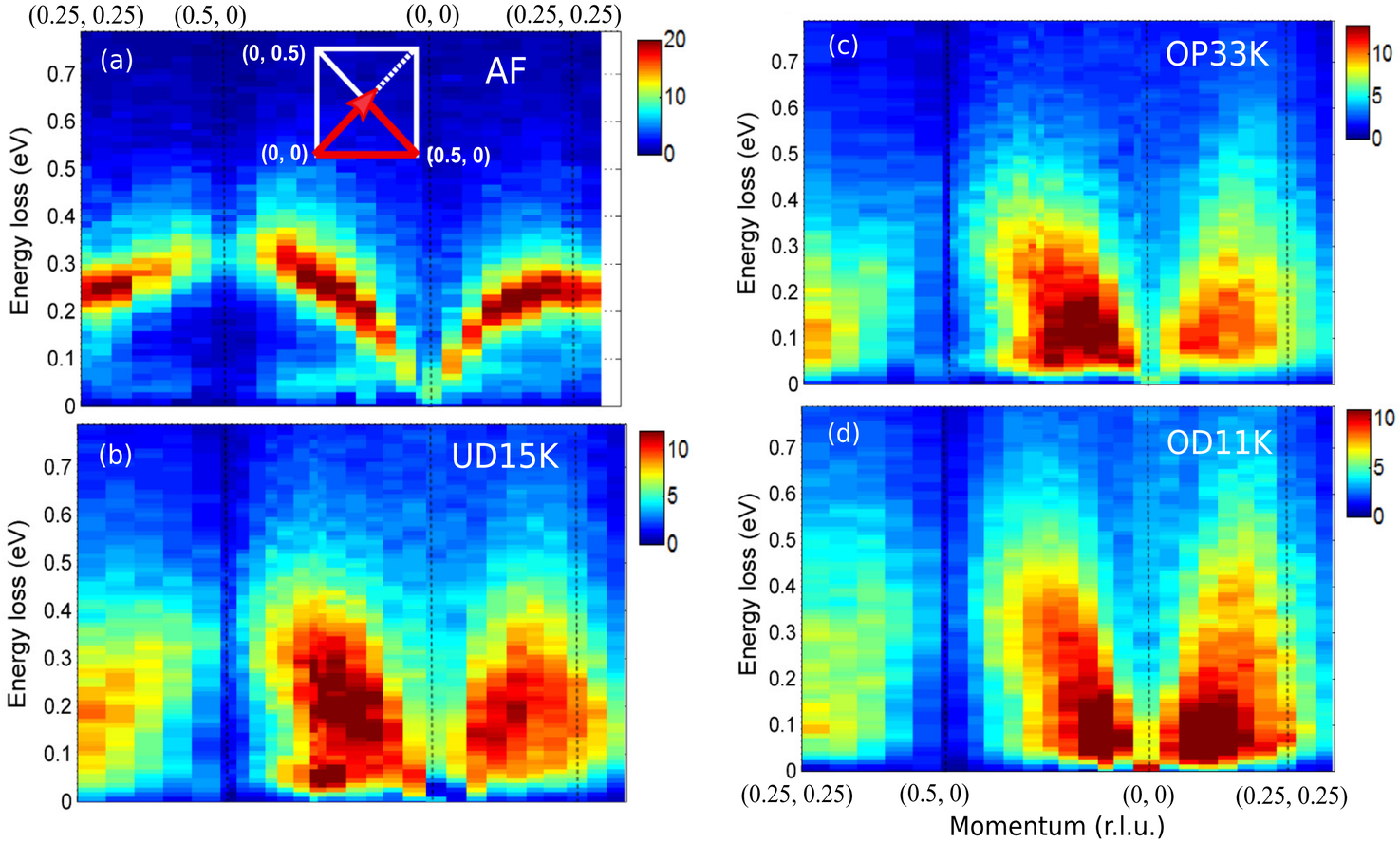

FIG. 2. Energy/momentum intensity maps of RIXS spectra for (a) AF ($p \simeq 0.03$), (b) UD15K ($p \simeq 0.11$), (c) OP33K ($p \simeq 0.16$), and (d) OD11K ($p \simeq 0.21$) along the high-symmetry momentum trajectory indicated in Fig. 1(b) and in the inset of (a). The intensity is in unit of photons/s/eV. Data were taken with π-polarized incident light at 20 K. Elastic peaks were subtracted for a better visualization of the low energy features.